UNIVERSITÀ DEGLI STUDI FIRENZE

DOTTORATO DI RICERCA IN
Scienze Agrarie e Ambientali

CICLO XXXII

COORDINATORE Prof. Giacomo Pietramellara

COMPLEMENTARY RESEARCHES and BIOTECHNOLOGICAL INNOVATIVE APPROACHES TOWARDS THE ENVIRONMENTALLY-FRIENDLY CONTROL OF BACTERIAL DISEASES of PLANTS

Patologia vegetale AGR/12

Dottorando
Dott. Silvia Calamai

(firma)

Tutore
Prof. Stefania Tegli

(firma)

Co-Tutore
Prof. Stefano Biricolti

(firma)

Coordinatore
Prof. Giacomo Pietramellara

(firma)

Anni 2017/2020

Alla mia famiglia

TABLE OF CONTENTS

Summary

Objectives: The control and the management of phytopathogenic bacteria is going to get definitely more arduous in the next future, considering both the increasing threat from invasive alien species and increasing European legislation concerning restriction of copper use to control phytopathogenic bacteria. This thesis aims to respond to the urgent need for innovation in plant protection, using a complementary research approach to detect potential targets among new pathogenicity and virulence determinants of Gram-negative and Gram-positive phytopathogenic bacteria. As a model, *Pseudomonas savastanoi* pv. *nerii* (*Psn23*) and *Curtobacterium flaccumfaciens* pv. *flaccumfaciens* (*Cff*) have been selected for Gram-negative and Gram-positive phytopathogenic bacteria, respectively.

Methods and results: The role played in the plant pathogenic bacterium *Psn23* by the membrane protein *Psn*MATE on IAA efflux and homeostasis, as well as the consequences of these *Psn*MATE - mediated processes on the different stages of plant infection, has been evaluated. To this purpose, in *silico* analysis of *Psn*MATE protein has been conducted, to detect those amino acids supposed to be involved in substrate and ions bounding. Accordingly, several mutants have been produced and then phenotypical characterized (*i.e*. gene expression, pathogenicity tests, and evaluation of IAA production by Salkowski assay and HPLC-FLD). The mutant tested have showed different phenotype compared to wild type, when inoculated on Oleander plants, as well as different extracellular efflux level of IAA (IAA-free and IAA-Lys). Obtained results has allowed to detect for the first time a new model for IAA biosynthesis and efflux, which is regulated by the paired activity of *matE* and IAA-related genes.

The phenotypic characteristic (*i.e*. pathogenicity, arsenic resistance, and plasmid profile) of *C. flaccumfaciens* strains isolated from different annual crops in Iran have been evaluated, and the phylogenetic position of the *C. flaccumfaciens* strains having different geographical origins has been analysed, in comparison to members of *Curtobacterium* spp., also with the aid of molecular fingerprint such as those obtained by rep-PCR. The results revealed that the strain causing wilt disease on dry beans are distributed into two phylogenetic lineages, yellow-pigmented and red-/orange pigmented strains, and no-pathogenic strains do not form a separate phylogenetic group. Despite no differences between pathogenic and non-pathogenic strains in their plasmid contents, the results show that those strains pathogenic on dry bean are resistant to arsenic compounds. The Phenotype MicroArray analysis combined with traditional microbiological plate have been conducted in order to further investigated the putatively correlation between metal resistance and the differential

virulence on bean. Obtained results have confirmed that all the strain virulent on bean are resistant to arsenic compounds, except for Cff type strain which shows a moderate tolerance. Thus, the genome of three strain, both virulent and no virulent on beans, has been sequenced and the comparative genomes analysis has been conducted to detect the genetic determinants of arsenic resistance. For the first time a putative *arsRBC* of *Cff* P990 strain has been identified, whereas arsenic resistant mechanism of Cff type strain, which are moderately tolerant to arsenic compounds, has yet to be elucidated. Furthermore, the genomes comparative analysis has allowed to detect a genome island (GIs) involved in virulence of *Cff*, which has been acquired from other plant pathogenic bacteria by horizontal gene transfer (HGT) events.

Conclusion: The complementary research approach adopted has allowed to detect a potential virulence determinant of *Psn23*, which have never been studied before, and thus to detect a new model for IAA biosynthesis and transport outside the bacterial membrane. The IAA genes and MATE protein are widely diffuse in *P. syringae* complex, hence studies on MATE proteins can be considered pivotal to provide information essential for the development of innovative control molecules and strategies against these bacteria. In addition, phenotypic and genotypic characterization of *C. flaccumfaciens* and *Cff* strains have been allowed to provide interesting information concerning virulence/metal resistance correlation, as well as putatively virulence and pathogenicity determinants. Therefore, the obtained results on *Cff*, which has been definitely less investigated until now, will afford to develop innovative control methods for this pathogen.

Chapter 1

Introduction

1.1 Copper in plant protection: risks and regulatory frameworks

Copper is an oligo-element essential for life, that participate in cellular physiology process (La Torre *et al*. 2018). The first copped-based antimicrobial compound used in agriculture was Bordeaux mixture (*i.e*. copper sulfate pentahydrate and lime mixture), which was discovered in 1885 by the French scientist Pierre-Marie Alexis Millardet. Since that time, there was a rapid development of copper-based antimicrobial compounds which revolutionized the twentieth century agriculture in general, and crop protection in particular (Lamichhane *et al.,* 2018) Consequently, many thousands of tons of copper compounds were, and are still now, used annually in agricultural practices worldwide.

Massive use of copper-based bactericide and fungicides to control plant disease lead to copper accumulation in the soil. Following application, copper which is no absorbed by plant tissues reaches the soil where it is accumulated and it is leached into surface and deep waters (La Torre *et al*. 2018). Moreover, this heavy metal cannot be degraded and its removal from soils is limited. Thus, copper can persist as contaminant and causes bioaccumulation and toxicity (Komarek *et al*., 2010; Mackie *et al*., 2012).

The copper concentrations in soil show significant variations among and within countries, which depend by both natural conditions (*e.g*. climate and geology) and anthropogenic activities (Ballabio *et al*., 2018). For example, Cu has higher phytotoxicity in acid soils with a low cation exchange capacity than in slightly alkaline conditions (Fan *et al.,* 2012). On the contrary of sandy soils, fine texture soils with high concentrations of organic matter, carbonates, clay, and oxides can have a higher holding capacity for Cu (Lamichhane *et al.,*2018). Moreover, absorption and precipitation and complexation reactions are influenced by pH (La Torre *et al*. 2018). Copper bioavailability as well as its toxicity greatly increases the soil pH decreases below 5.5 (Fan *et al.,* 2012).

The agricultural soils have higher Cu concentrations compared to forested lands, further indicating the link between Cu accumulation in topsoil and agricultural practices (Ballabio *et al*., 2018). Soil contamination by copper following repeated fungicides applications has been reported in vineyards in Italy, south France, southwest Germany (Ballabio *et al*., 2018). Similarly, contamination by copper occurs in soils where this element is used as broad fungicide and antimicrobial compound on olives and fruit trees, as well as on horticultural crops (Ballabio *et al*., 2018).

High uptake of copper ions by plant at any time may lead to damage, also known as phytotoxicity (Lamichhane *et al.,*2018). In plant, excess copper adversely effects the

metabolic activity of roots and absorption of nutrients, thus having negative effects on crop yield and quality (La Torre *et al*. 2018).

Additionally, copper is potentially toxic to the soil biota, including an extremely diverse array of micro- and macroorganisms (Lamichhane *et al.*,2018) Microorganisms are generally more sensitive to copper than other organisms in soil biocoenosis (Giller *et al.*, 1998). High copper concentrations can lead to reduce metabolic activity of microorganism, modifying both the size of microbial biomass and soil processes (Giller *et al.*, 1998, Kunito *et al.*, 2001). Potential negative effects also have been observed on many macro-organisms, including earthworm population and nematodes (Van Zwieten *et al*, 200; Jaworska and Gorczyca et al., 2002).

High copper level into the soils may cause the contamination of surface and subsurface water (Fernandez Calvino *et al.,* 2009). Copper can interfere with aquatic organisms, such us sediment dwellers, algae, invertebrate and fish (La Torre *et al*. 2018). Heavy metals can be easily transferred to animals and humans if enter the food chain, causing toxic reaction in case of elevated intake (Lamichhane *et al.*,2018). Furthermore, despite antibiotics are forbidden in Europe in plant protection, copper-contaminated soils show a higher percentage of antibiotic resistant bacteria in comparison to those not contaminated (Knapp *et al.*, 2010). This phenomenon can be explained on the basis of cross-resistance mechanisms related to the presence of genes for copper and antibiotics resistance located on the same plasmids (Baker *et al.*, 2006, Hu *et al.*, 2016). Therefore, copper-contaminated soils have to be considered a dangerous reservoir of genes for antibiotic resistance, easily transmitted to pathogenic bacteria infecting animals and humans, with a dramatic impact on their health.

In summary, soils contaminated by copper following application of copper-based plant protection products and other agricultural practices represent a risk for a wide range of organisms and for the environment. For all these reasons, use of copper compounds in organic production were limited by the European Commission Regulation 473/2002/EC. Copper use is allowed up to 6Kg/ha/year, as specified in Regulation 889/2008/EC, detailing the rules for the implementation of Council Regulation 834/2007/EC on organic production (Lamichhane *et al.*,2018). Active substance copper compounds were approved as bactericide and fungicides by Commission Directive 2009/37/EC but the approval period was limited to 7 years (La Torre *et al*. 2018). In 2014, with commission Implementing Regulation (EU) 85/2014, the expiry of the approval period was postponed to 31 January 2018, and than to 31 January 2019 (Commission Implementing Regulation (EU) 2018/1981) (La Torre *et al*. 2018). Therefore, pursuant to above-mentioned Regulation, the approval of copper

compounds, as well as of candidates for its substitution, is confirmed until 31 December 2025, under the conditions set out in Annex I and II. In addition, the use of copper-based plant protection products was restricted to a maximum application rate of 28 kg/ha of copper over a period of 7 years (*i.e*. on average 4 kg/ha/year)

Heavy metals can be easily transferred to animals and humans if enter the food chain, causing toxic reaction in case of elevated intake (Lamichhane *et al.*,2018). Furthermore, despite antibiotics are forbidden in Europe in plant protection, copper-contaminated soils show a higher percentage of antibiotic resistant bacteria in comparison to those not contaminated (Knapp *et al.*, 2010). This phenomenon can be explained on the basis of cross-resistance mechanisms related to the presence of genes for copper and antibiotics resistance located on the same plasmids (Baker *et al.*, 2006, Hu *et al.,* 2016). Therefore, copper-contaminated soils have to be considered a dangerous reservoir of genes for antibiotic resistance, easily transmitted to pathogenic bacteria infecting animals and humans, with a dramatic impact on their health.

Heavy metals can be easily transferred to animals and humans if enter the food chain, causing toxic reaction in case of elevated intake (Lamichhane *et al.*,2018). Furthermore, despite antibiotics are forbidden in Europe in plant protection, copper-contaminated soils show a higher percentage of antibiotic resistant bacteria in comparison to those not contaminated (Knapp *et al.*, 2010). This phenomenon can be explained on the basis of cross-resistance mechanisms related to the presence of genes for copper and antibiotics resistance located on the same plasmids (Baker *et al.*, 2006, Hu *et al.,* 2016). Therefore, copper-contaminated soils have to be considered a dangerous reservoir of genes for antibiotic resistance, easily transmitted to pathogenic bacteria infecting animals and humans, with a dramatic impact on their health.

Heavy metals can be easily transferred to animals and humans if enter the food chain, causing toxic reaction in case of elevated intake (Lamichhane *et al.*,2018). Furthermore, despite antibiotics are forbidden in Europe in plant protection, copper-contaminated soils show a higher percentage of antibiotic resistant bacteria in comparison to those not contaminated (Knapp *et al.*, 2010). This phenomenon can be explained on the basis of cross-resistance mechanisms related to the presence of genes for copper and antibiotics resistance located on the same plasmids (Baker *et al.*, 2006, Hu *et al.,* 2016). Therefore, copper-contaminated soils have to be considered a dangerous reservoir of genes for antibiotic resistance, easily transmitted to pathogenic bacteria infecting animals and humans, with a dramatic impact on their health.

Heavy metals can be easily transferred to animals and humans if enter the food chain, causing toxic reaction in case of elevated intake (Lamichhane *et al.*,2018). Furthermore, despite antibiotics are forbidden in Europe in plant protection, copper-contaminated soils show a higher percentage of antibiotic resistant bacteria in comparison to those not contaminated (Knapp *et al.*, 2010). This phenomenon can be explained on the basis of cross-resistance mechanisms related to the presence of genes for copper and antibiotics resistance located on the same plasmids (Baker *et al.*, 2006, Hu *et al.*, 2016). Therefore, copper-contaminated soils have to be considered a dangerous reservoir of genes for antibiotic resistance, easily transmitted to pathogenic bacteria infecting animals and humans, with a dramatic impact on their health.

Heavy metals can be easily transferred to animals and humans if enter the food chain, causing toxic reaction in case of elevated intake (Lamichhane *et al.*,2018). Furthermore, despite antibiotics are forbidden in Europe in plant protection, copper-contaminated soils show a higher percentage of antibiotic resistant bacteria in comparison to those not contaminated (Knapp *et al.*, 2010). This phenomenon can be explained on the basis of cross-resistance mechanisms related to the presence of genes for copper and antibiotics resistance located on the same plasmids (Baker *et al.*, 2006, Hu *et al.*, 2016). Therefore, copper-contaminated soils have to be considered a dangerous reservoir of genes for antibiotic resistance, easily transmitted to pathogenic bacteria infecting animals and humans, with a dramatic impact on their health.

Copper is still necessary at the present, especially in organic farming to contain plant diseases (La Torre *et al*. 2018). Although different approaches have been studied, no substance have yet been identified to entirely replace copper in plant protection (La Torre *et al*. 2018). Therefore, research efforts in this direction must continue in order to develop strategies to decrease copper load into the topsoil, and to search realistic and efficient alternative strategies.

1.2 Global threat to agriculture from invasive species.

For millennia, the natural barriers of oceans, mountains, rivers and deserts provided the isolation essential for unique species and ecosystems to evolve (IUNC, 2000). In just a few hundred years these barriers have been rendered ineffective by major global forces that combined to help alien species travel vast distances to new habitats and become alien invasive species (IUNC, 2000). Invasive alien species (IAS) are non-native species whose

introduction and/or spread outside their natural past or present ranges pose a risk to biodiversity (IEEP, 2009). Despite of humans have transported and traded plant and animal species for millennia, only in the last 50 years have witnessed an unprecedented acceleration in the importance and value of merchandise trade. (Hulme et al., 2009). With increased globalization and connectedness via world trade, the threat from invasive species arriving to countries in which they were previously absent was increased (Paini *et al*., 2016).

Invasive alien species (IAS) have led and continue to lead to a wide range of ecological and socio-economic (Braat *et.al,* 2008). IAS, together with habitat destruction, have been a major cause of extinction of native species throughout the world in the past few hundred years (Braat *el at*., 2008). Additionally, it has been suggested that 80% of endangered species worldwide could suffer losses due to competition with or predation by IAS (Pimentel *et. al.,* 2005). Moreover, the introduction of IAS between continents, regions and nations has often had significant impacts on the structure and functioning of the recipient ecosystems (Braat *et al.,* 2008). Economic impacts can be divided into two main categories, i.e. costs of damage and costs of control measures (IEEP, 2009). Information on the cost of damage is the most common cost item for negative impacts on agricultural, forestry and fisheries sectors resulting from invasions of non-native pests, such as plant diseases (fungi and bacteria), insects and fouling organisms (marine, freshwater and terrestrial invertebrates) (IEEP, 2009).

In Europe the accidental introduction of the grape pest *Phylloxera*, *Daktulosphaira vitifolia* (Fitch) in 1862 on infested vines imported from the US resulted in significant impacts to the viticulture industry (MacLeod *et al*. 2010 Ormsby et al., 2017). Moreover, *Dryocosmus kuriphilus Yasumatsu*, one of the most dangerous pests attacking chestnut trees (*Castanea* spp.), is native of China and it was recorder for the first time in Pidmont and pest quickly spread throughout the Italian peninsula (Quacchia *et al.,* 2008; Brussino *et al.*, 2002). Furthermore, considerable number of bacteria species were introduced in EPPO area. For instance, *Erwinia amylovora* (Mazzucchi *et al.,* 1994), several *Pseudomonas syringe* pathovars (Fouts *et al*., 2002) and in recent times *Xylella Fastidiosa* (Saponari *et al.*,2014) have spread in Italy, causing production losses.

In this frame Member State provides a set of measures to be taken across the EU in relation to invasive alien species. The EU Regulation 1143/2014 on invasive alien species (the IAS Regulation) envisages three distinct types of measures, which follow an internationally agreed hierarchical approach to combatting IAS. At first, several robust measures aimed at preventing the introduction of IAS (e.g. restrictions on keeping,

importing, selling). Then, Member States must put in place a surveillance system to detect the presence of IAS as early as possible and take rapid eradication measures to prevent them from establishing. When species are already widely spread in the territory, concerted management action is needed to prevent them from spreading any further and to minimize the harm they cause. Global goals in the management of threats from invasive alien species should include making best use of existing regulatory frameworks with emphasis on developing more effective instruments that are directly linked to legal or regulatory authority, investing more into global research initiatives, and targeting existing tools and resources more effectively. (Ormsby et al., 2017).

1.3 *Curtobacterium flaccumfaciens* pv. *flaccumfaciens*

Curtobacterium flaccumfaciens pv. *flaccumfaciens (Cff)* is the causal agent of bacterial wilt in dry beans worldwide (Chase *et al.,* 2016). The pathogen is responsible for severe yield losses and seed quality reduction (Osdaghi *et al*, 2015a) on *Phaseolus* spp. and other leguminous plants. The disease was first identified from South Dakota (USA) in 1926 on *Phaseolus vulgaris* (Hedges,1926). Since then, the pathogen has rapidly spread to several geographic regions, and currently bacterial wilt disease has been reported from Mexico (Yerkes and Crispin, 1956), Australia (Wood and Easdown, 1990), Brazil (Maringoni and Rosa, 1997), Canada (Hsieh *et al*., 2002), Turkey (Bastas *et al*., 2014), South America and Tunisia (EPPO, 2011). *Cff* is included in the A2 quarantine list of the European and Mediterranean Plant Protection Organization (EPPO, 2011). Nevertheless, during the past decade *Cff* has been reported in a few bean fields of south-eastern Spain (Gonzalez *et al.,* 2005) and on soybean samples from Germany (Sammer and Reiher, 2012), where it recently eradicated.

Based on the color of their colony, different phenotypic variants of *Cff* are described worldwide (Harveson and Vidaver, 2008), and the aggressiveness of these colony variants often differs from one to another (Osdaghi *et al.,* 2015). While the yellow and orange variants are the most common phenotypes isolated from areas affected by the disease (Conner *et al.*, 2008), there are several other colony variants of the pathogen. For example, the purple variant was reported on beans from western Nebraska (Schuster *et al.,* 1968) and Canada (Huang *e*t al., 2006). Likewise, the pink variant of the pathogen was described on soy-bean from Brazil (Soares *et al.,* 2013), and on common bean from western Nebraska (Harveson and Vidaver, 2008). Recently, the red variant was isolated in Iran (Osdaghi et al., 2016).

Host range of the pathogen varies among *Phaseolus* sp. (Hedges, 1926; Schuster and Sayre, 1967), *Vigna* sp. (EPPO, 2011, Wood and Easdown, 1990), *Glycine max* (Sammer and Reiher, 2012), *Pisum sativum* (EPPO, 2011), *Lupinus polyphyllus* Lindl (Schuster and Sayre 1967), *Amaranthus retroflexus* L., *Chenopodium album* L. (Schuster 1959), *Cicer arietinum* L., *Vicia faba* L., *Vicia villosa* Roth. and *Lens culinaris* Medik (Osdaghi *et al*. 2015). Although leaves and stems of wheat (*Triticum aestivum*) were shown to be colonized by *Cff*, no leaf chlorosis/necrosis or wilting symptoms are reported on wheat to date (Silva Júnior *et al.*, 2012). Moreover, epiphytic *C. flaccumfaciens* strains isolated from symptomless solanaceous vegetables are pathogenic on leguminous but not on solanaceous plants (Osdaghi et al., 2018). Epiphytic and endophytic survival has greater impact on a source of inoculum because bacteria can be protected inside the plant tissue (Gonçalves *et al*., 2017).

Initial disease symptoms in the field consist of leaf wilting, during the period of warm, dry weather or moisture stress, followed by a recovery as the temperature drops in the evening (Harveson *et al*., 2015). Wilting becomes permanent during the following days as a result of bacterial plugging of the vessels when the water supply is cut off and then the leaves turn brown and then drop (EPPO, 2011). Infected plants can exhibit field symptoms consisting of interveinal, necrotic lesions surrounded by bright yellow borders (Harveson *et al.*, 2013) (Figure 1). Young *Phaseolus* plants, when they are 5-7 cm tall, are particularly susceptible, and usually killed (EPPO, 2011). Symptoms on older plants are less pronounced as the disease generally develops and progress more slowly (Harveson *et al.*, 2015).

Initial infection occurs when the pathogen enters the vascular system through either infected seed or through wounds on leaves or stems (Harveson *et al.*, 2015). After initial infection, secondary spread of bean wilt occurs similarly to common bacterial and halo blights (Harveson *et al.*, 2015). If plants survive to produce mature seed, infection and systemic spread enable the pathogen to move through the vascular system into developing pods and seed embryos (Harveson *et al.*, 2015). Detection of pathogen on infected seeds is relatively easy when present signs on their surface such as pigmentation or discoloration (EPPO, 2011). Unfortunately, *Cff*-infected seeds are very often asymptomatic and appear healthy (Harveson *et al.*, 2015). Therefore, due to the seedborne nature of *Cff*, infected seeds represent the major source of inoculum and means for dispersal, both long and short distances (Zaumeyer and Thomas, 1957). Infected seeds also provide an excellent mechanism of survival for *Cff*, both internally and on the external seed surfaces (Harveson *et al.*, 2015). Longevity outside the host is a major challenge to plant pathogenic bacteria

since most of them, including *Cff*, do not form spores or resistance structure (Gonçalves *et al*., 2018). *Cff* survived for up to 240 days in crop debris of common bean kept on the soil surface, but the survival period decreased to 30 days when debris are incorporated at a depth of 20 cm (Silva Júnior *et al*. 2012). In recent research about the survival capacity of *Cff* in the soil, the bacteria survived under controlled conditions for a period between 2 to 16 days, being influenced by soil type, *Cff* strains, moisture, and incubation temperature of the samples (Silva Júnior *et al*. 2012; Gonçalves *et al*., 2018). Therefore, more attention in the management of bacterial wilt in common bean cultivations is pivotal to minimize the risk of primary inoculum (Gonçalves *et al*., 2018).

Figure 1: Marginal necrotic and yellow symptoms associated with common bacteria wilt, caused by *Curtobacterium flaccumfaciens* pv. *flaccumfaciens.*

Accordingly, the management of bacterial wilt and of *Cff* is essentially based on using seeds with high sanitary quality and crop rotation with non-host species for *Cff* (Gonçalves *et al*., 2017). In addition, breeding for resistance in order to develop resistant cultivars is highly recommended (Silva Júnior *et a*l., 2012 II; Urrea and Harveson, 2014), although such an approach is time-consuming and resource-intensive (Osdaghi *et al.*, 2015). However, in some areas cultivated with common bean in the USA, where bacterial wilt was not detected for almost 25 years, the disease recurred, even with the adoption of recommended management measures (Harveson *et al.* 2011). Overall, it is essential to significantly increase the studies concerning *Cff* both for the development of innovative strategies for *Cff*-disease control and to prevent the introduction of the pathogen into a new area.

1.4 Multidrug-resistance efflux pumps in bacteria: not just for resistance

Intrinsic resistance to certain antimicrobial agents is conferred by basal levels of efflux ability (Piddock, 2006). Efflux pumps transport several compounds which can be associated with the resistance to multiple antibiotics and antimicrobials (*i.e.* multidrug resistance, MDR) (Piddock, 2006). The mechanism of resistance to tetracycline in *Escherichia coli* was the first to be correlated with efflux pumps in 1980 (Mc Murry *et al.*,1980). Nowadays it is well known that MDR pumps constitute the most ubiquitous type of resistance element, present in all organisms (Martinez *et al.*,2009).

Currently, six families of bacterial drug efflux pumps have been identified that contribute to the efflux pathway (Du *et al.*, 2018). One of these, the ATP-binding cassette (ABC), directly utilizes ATP as energy source to drive transport (Piddock, 2006). The other five groups are secondary active transporters. These are the major facilitator superfamily (MFS), the multidrug and toxin extrusion (MATE) family, the small multidrug resistance (SMR) family, the resistance-nodulation-cell division (NRD) superfamily and proteobacterial antimicrobial compound efflux (PACE) family (Du *et al.*, 2018).

Different studies have demonstrated that MDR pumps are capable of extruding not only antibiotics but also antiseptics, heavy metals, solvents and detergents, among other toxic molecules (Martinez *et al.*, 2009). For this reason, bacteria carrying MDR pumps not occurred only to environments with a high antibiotics load (Martinez *et al.*,2009). Soil and plants incorporate the organism with largest number of MDR pumps. (Konstantinidis *et al.*, 2004). The use of antibiotics for the therapy human infection is quite recent compared to efflux pumps selection, which are ancient and highly conserved determinants. These characteristics further support the paramount role of the efflux pumps to bacterial physiology, and likely their secondary role to antibiotics resistance. (Blanco *et al.*, 2016).
It has been found that MDR efflux pumps might have a relevant role in plant-pathogen interaction, during all stages of infection (Martinez *et al.*,2009). Mutants of *Erwinia amylovora* impaired in their AcrAB efflux pump exhibited reduced virulence (Burse *et al.*, 2004). Similarly, the ability of *Pseudomonas syringae* pv. *tomato* DC3000 to resist the action of flavonoids produced by the host depends from a functional mexAB-oprM efflux pump plays essential roles in (Vargas *et al.*, 2011).

In conclusion, bacterial efflux pumps are relevant elements for the physiology of microorganism in natural ecosystem and in bacteria/plant interaction, in addition to be antibiotic resistance determinants.

1.4.1 *The MATE transporters and their hypothetic role in Pseudomonas savastanoi pv. nerii*

The MATE transporters can be categorized into NorM, DinF (DNA-demage-inducible protein F) and eukaryotic subfamilies on the basis of their amino acid sequence similarity (Du *et al.,* 2018). MATE homologs share about 40% sequence similarity, suggesting an overall conserved structure and transport function (He *et al.,* 2010). Members of NorM and DinF subfamilies can use either the Na^+ or H^+ electrochemical gradient to extrude polyaromatic and cationic drugs (Lu *et al.,* 2013). To date, the X-ray structures of the Na^+-dependent NorM transporters from *Vibrio cholera*e (NorM-VC) (He *et al.,* 2010) and *Neisseria gonorrhoeae* (NorM-NG) (Lu *et al.,* 2013), as well as the H^+-dependent DinF transporters from *Pyrococcus furiosus* (PfMATE) (Tanaka *et al.,* 2013) and *Bacillus halodurans* (DinF-BH) (Lu *et al.,* 2013 b) have been reported (Du *et al.,* 2018).

Their crystal structures share a similar protein fold, comprising 12 membrane-spanning segments (TM1-TM12). Nevertheless, the NorM and DinF proteins show a different arrangement of cation- and substrate-binding sites, suggesting a remarkable diversity among MATE transporters on their mechanistic and operational features (Radchenko *et al.,* 2015). MATE transporters have a V-shaped central cavity open to the extracellular space, which is composed by amino-terminal and carboxyterminal domains related by pseudo-twofold symmetry. (Du *et al.,* 2018). These structures probably show a mechanism transport identify by outward open state in which the central cavity is situated about halfway through the membrane bilayer (Figure 2).

In the central cavity of NorM-NG pump, near the membrane-periplasm interface, a drug binding site has been identified (Lu *et al.,* 2013). The mechanism of substrate transport needs ionic and hydrogen bonding. (Jin *et al*., 2014). NorM-VC interaction with the substrate is largely mediated by Na^+ and H^+ gradients, and an aspartate has been identified to be involved in proton coupling (Jin *et al*., 2014). The substrate and cation can bind the protein simultaneously, interacting with distinct subsets of amino acids. (Steed *et al*., 2013). Therefore, the protein conformational changes may indirectly mediate the coupling between the fluxes of ions and drugs (Du *et al.,* 2018). The antiport mechanism proposed shows that high affinity for monovalent cations is reached by the outward-facing conformation state (He *et al.,* 2010). After binding of cations, the structure undergoes an outward-facing to inward-facing conformational change that is more favourable to substrate binding (He 2010). Then, the outward-facing conformation could be restored by cation release and/or substrate

binding, and into the outer leaflet of the lipid bilayer and/or extracellular space the substrate is thus released (He *et al.*, 2010; Lu *et al.*, 2013; Du *et al.*, 2018) (Figure 3).

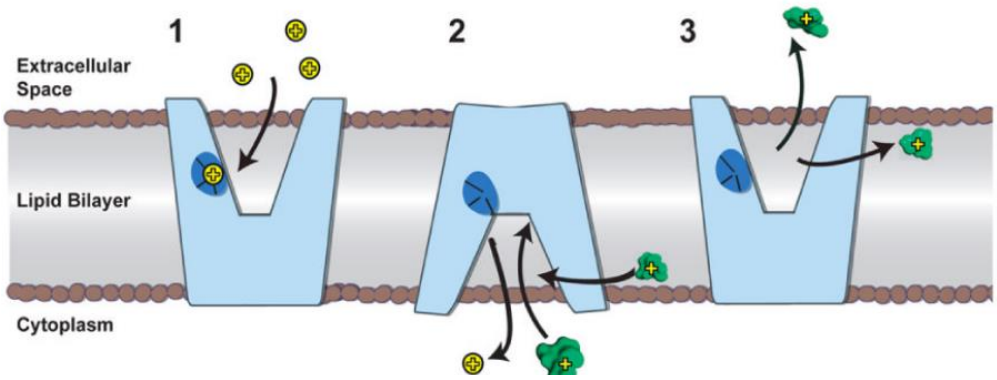

Figure 2: The cation-binding site of NorM-VC and mechanism of transport (He *at al*., 2010).

For the DinF subfamily members pfMATE, the drug-binding site is dominated by polar amino acid and is forming exclusively within the amino-terminal domain (Tanaka *et al.*, 2014). For another DinF subfamily, DinF-BH, substrates interaction are largely mediated by hydrophobic amino-acid within the central cavity (Lu *et al.*, 2013b). Evidence indicates that residue D40 in DifN- BH makes charge-charge interaction with cationic substrate, and H^+ directly compete with this interaction (Lu *et al.*, 2013b). As shows in Figure 3, the resulting extracellular-facing protonated transporter then switches to the intracellular facing and protonated state (Lu *et al.*, 2013b). Then the drug binding, which directly compete for D40, triggers deprotonation of the transporter and the intracellular-facing can return to the extracellular-facing, starting another transport cycle (Lu *et al.*, 2013b).

Recently, by *in silico* analysis the gene matE of *Pseudomonas savastanoi* pv. *nerii* (*Psn*) was found located into a specific genomic region including the genes *iaaM* and *iaaH*, for the biosynthesis of indole-3-acetic acid (IAA) using tryptophan (Trp) as precursor (Comai *et al.*, 1982; Sekine *et al.*, 1988) as well as the gene *iaaL* coding for the homonym enzyme, able to convert IAA into IAA–lysine (IAA–Lys), supposed to be a less biologically active compound (Fett *et al.*, 1987; Glass *et al*., 1986) . Preliminary studies revealed that in *Psn* the *matE/iaaL* operon could be also crucial for simultaneous regulation of intracellular IAA levels as well as for their differential modulation during the various stages of infection (Cerboneschi *et al*., 2016). In particular, several evidences suggest the MATE protein having a role in the secretion/transport of IAA, such as already demonstrated for the Mte1 protein of *Tricoloma vaccinum* (Krauss *et al.*, 2015). Therefore, here the MATE putative protein of

Psn will be investigate and evaluated as a potential target for the development of innovative anti-infective inhibitors, making bacteria more sensitive to a range of xenobiotic compounds for the “green control” of this pathogen.

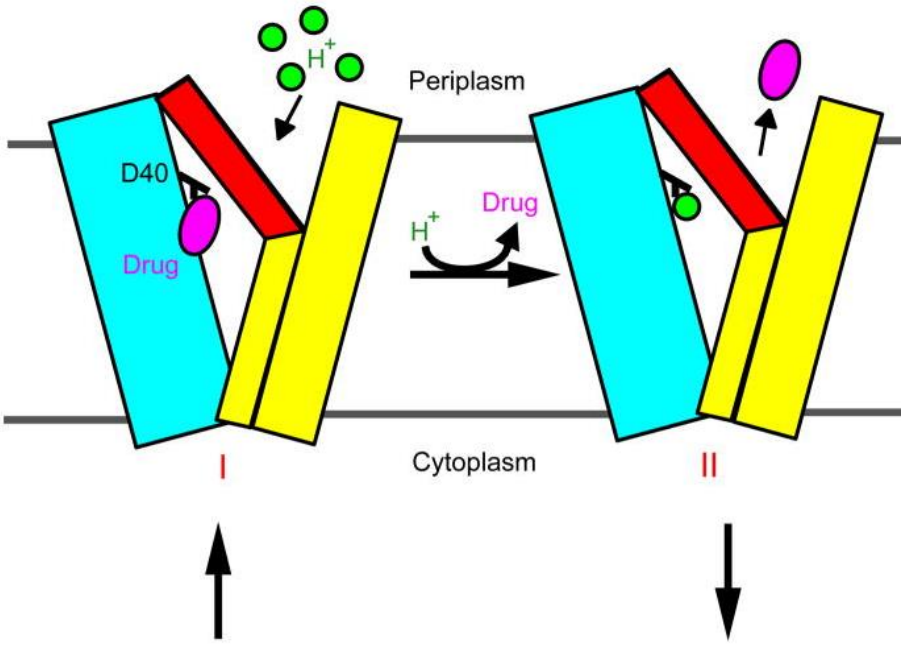

Figure 3: Proposed transport mechanism for DinF-BH (Le et al., 2013)

1.5 References

- **Baker-Austin C.,** Wright M.S., Stepanauskas R., McArthur J.V. (2006). Co-selection of antibiotic and metal resistance. *TRENDS in Microbiology* Vol.14 No.4
- **Ballabio C.,** Panagos P., Lugato E., Huang J.H., Orgiazzi A., Jones A., Fernández-Ugalde O., Borrelli P., Montanarella L. (2018) Copper distribution in European topsoils: An assessment based on LUCAS soil survey. Science of the Total Environment 636, 282–298.
- **Bastas K. K**., Sahin F. (2017). Evaluation of seed borne bacterial pathogens on common bean cultivars grown in central Anatolia region, Turkey. European Journal of Plant Pathology, 147:239–253.
- **Blanco P.,** Hernando-Amado S., Reales-Calderon J.A., Corona F., Lira F., Alcalde-Rico M., Bernardini A., Sanchez M.B., Martinez J.L. (2016). Bacterial Multidrug Efflux Pumps: Much More Than Antibiotic Resistance Determinants. Microorganisms, 4, 14.
- **Braat** L. & Brink P. (2008). Cost of Policy Inaction (COPI): The case of not meeting the 2010 biodiversity target, a study for the European Commission.
- **Brussino G**., Bosio G., Baudino M., Giordano R., Ramello F., Melika G. (2002). Pericoloso insetto esotico per il castagno europeo. L'Informatore Agrario 37:59–61.
- **BurseA.,** Weingart H., Ullrich M.S. (2004). NorM, an *Erwinia amylovora* multidrug efflux pump involved in in vitro competition with other epiphytic bacteria. Applied and Environmental Microbiology, 70, 693–703.
- **Chase A.B**., Arevalo P., Polz M.F., Berlemont R. and Martiny J.B.H. (2016). Evidence for Ecological Flexibility in the Cosmopolitan Genus *Curtobacterium*. Frontiers in Microbiology, 7:1874.
- **Conner R.L.,** Balasubramanian P., Erickson R.S., Huang H.C., Mundel H.H. (2008). Bacterial wilt resistance in kidney beans. Canadian Journal of Plant Science, 88, 1109e1113.
- **Du D.,** Wang-Kan X., Neuberger A., van Veen H.W., Pos K.M., Piddock L.J.V.2 and Luisi B.F. (2018). Multidrug efflux pumps: structure, function and regulation. REVIEWS|MICROBIOLOGY, volume 16.
- **EPPO**. (1994) *Curtobacterium Flaccumfaciens* pv. *flaccumfaciens*. Field Inspection and Seed-Testing Methods. Bulletin OEPP/EPPO 24:329–331
- **Fan J.,** He Z., Ma L.Q., Nogueira T.A.R., Wang Y., Liang Z., Stoffella P.J. (2012). Calcium water treatment residue reduces copper phytotoxicity in contaminated sandy soils. Journal of Hazardous Materials 199–200, 375–382.
- **Fernández-Calviño**, D., Rodríguez-Suárez, J.A., López-Periago, E., Arias-Estévez, M., Simal-Gándara, J., (2008). Copper content of soils and river sediments in a winegrowing area, and its distribution among soil or sediment components. Geoderma 145 (1-2),91–97.
- **Fouts D.E.,** Abramovitch R.B., Alfano J.R., Baldo A.M., Buell C.R., Cartinhour S. (2002). Genomewide identification of *Pseudomonas syringae* pv. *tomato* DC3000 promoters controlled by the *HrpL* alternative sigma factor. Proceedings of the National Academy of Science, 99(4):2275–80.
- **Giller K.E.,** Witter E., Mcgrath S.P. (1998). Toxicity of heavy metals to microorganisms and microbial processes in agricultural soils: a review. Soil Biology and Biochemistry 30:1389–1414.
- **Gonçalves R.M.,** Schipanski C.A, Koguishi L., Soman J.M., Sakate R.K., Silva T.A.F., Maringoni A.C. (2017). Alternative hosts of *Curtobacterium flaccumfaciens* pv. *flaccumfaciens*, causal agent of bean bacterial wilt. European Journal of Plant Pathology, 148:357–365.
- **Gonzalez A.J.,** Tello J.C., Rodicio M.R. (2005). Bacterial wilt of beans (*Phaseolus vulgaris*) caused by Curtobacterium flaccumfaciens in Southeastern Spain. Plant Disease. 89 (12), 1,361.3.

- **Harveson R.M. (2013)**. The multicolored bacterium. APSnet features.
- **Harveson R.M.,** Schwartz H.F., Urrea C.A. (2011). Bacterial wilt of dry beans in western Nebraska. NebGuide G05-1562-A (revised).
- **Harveson R.M**., Schwartz H.F., Urrea C.A.; Yonts C.D. (2015). Bacterial Wilt of Dry-Edible Beans in the Central High Plains of the U.S.: Past, Present, and Future. Plant Disease, 99(12), 1665-1677.
- **Harveson R.M.,** Vidaver A.K. (2008). A new color variant of the dry bean bacterial wilt pathogen (*Curtobacterium flaccumfaciens* pv. *flaccumfaciens)* found in western Nebraska. Plant Health Progress.
- **He X.,** Szewczyk P., Karyakin A., Evin M., Hong W.X., Zhang Q., Chang G. (2010). Structure of a cation-bound multidrug and toxic compound extrusion transporter. Nature, 467(7318):991–994.
- **Hedges, F. (1926).** Bacterial wilt of beans (*Bacterium flaccumfaciens* Hedges) including comparison with *Bacterium phaseoli*. Phytopathology 16, 21.
- **Hsieh T.F.,** Huang H.C., Erickson R.S., Yanke L.J., Mündel H.H. (2002). First report of bacterial wilt of common bean caused by *Curtobacterium flaccumfaciens* in western Canada. Plant Disease, 86 (11), 1275.
- **Hu H.W.**, Wang J.T., Li J., Li J.J., Ma Y.B., Chen D., He J.Z. (2016) Field-based evidence for copper contamination induced changes of antibiotic resistance in agricultural soils. *Environmental microbiology* 18(11), 3896–3909.
- **Huang H.C**., Mundel H.H., Erickson R.S., Chelle C.D., Balasubramanian P.M., Kiehn F., Conner R.L. (2007). Resistance of common bean (*Phaseolus vulgaris* L.) cultivars and germplasm lines to the purple variant of bacterial wilt (*Curtobacterium flaccumfaciens* pv. *flaccumfaciens*). Plant Pathology Bullettine 16, 91-95.
- **Hulme** P.H. (2009). Trade, transport and trouble: managing invasive species pathways in an era of globalization Philip E. Journal of Applied Ecology, 46, 10–18.
- **IEEP.** (2009) TECHNICAL SUPPORT TO EU STRATEGY ON INVASIVE ALIEN SPECIES (IAS). Assessment of the impacts of IAS in Europe and the EU Service. Contract N° 070307/2007/483544/MAR/B2.
- **IUCN** (International Union for the Conservation of Nature) (2000). IUCN Guidelines for the Prevention of Biodiversity Loss caused by Alien Invasive Species (as approved by 51st Meeting of IUCN Council, February 2000). IUCN Information paper.
- **Jin Y.,** Nair A., van Veen H. W. (2014). Multidrug transport protein NorM from Vibrio cholerae simultaneously couples to sodium-and proton-motive force. The Journal of Biological Chemistry, 289, 14624–14632.
- **Knapp C.W**., Dolfing J., Ehlert P., and Graham D.W. (2010) Evidence of increasing antibiotic resistance gene abundances in archived soils since 1940. Environmental Science & Technology 44: 580–587.
- **Komárek M.**, E. Čadková, V. Chrastný, F. Bordas and J.C. Bollinger (2010). Contamination of vineyard soils with fungicides: a review of environmental and toxicological aspects. Environment International 36, 138–151.
- **Konstantinidis K.T**., Tiedje J.M. (2004). Trends between gene content and genome size in prokaryotic species with larger genomes. Proceedings of the National Academy of Sciences. USA101: 3160–3165.
- **Kunito T.,** K. Saeki, S. Goto, H. Hayashi, H. Oyaizu and S. Matsumoto (2001). Copper and zinc fractions affecting microorganisms in long term sludge-amended soils. Bioresource Technology 79, 135–146.
- **La Torre A.,** Iovino V. and Caradonia F. (2018). Copper in plant protection: current situation and prospects. Phytopathologia Mediterranea 57, 2, 201−236.

- **Lamichhane J. R.,** Osdaghi E., Behlau F., Jeffrey K., Jones J. B., Aubertot J.N. (20818). Thirteen decades of antimicrobial copper compounds applied in agriculture. Agronomy for Sustainable Development 38: 28.
- **Lu M.,** Radchenko M., Symersky J., Nie R., Guo Y. (2013b). Structural insights into H+-coupled multidrug extrusion by a MATE transporter. Nature Structural & Molecular Biology 20(11):1310-7.
- **Lu M.;** Symersky J., Radchenko M., Koide A., Guo Y., Nie R., Koide S. (2013). Structures of a Na+-coupled, substrate-bound MATE multidrug transporter. Proceedings of the National Academy of Sciences, 110, 2099–2104
- **M. Gonçalves**, M., Soman J.M., Krause-Sakate R., Passos J.R.S., Silva Júnior T.A.S., Maringoni A.C. (2018) Survival of *Curtobacterium flaccumfaciens* pv. *flaccumfaciens* in the soil under Brazilian conditions Ricardo European Journal of Plant Pathology (2018) 152:213–223.
- **M. Gonçalves**, M., Soman J.M., Krause-Sakate R., Passos J.R.S., Silva Júnior T.A.S., Maringoni A.C. (2018) Survival of *Curtobacterium flaccumfaciens* pv. *flaccumfaciens* in the soil under Brazilian conditions Ricardo European Journal of Plant Pathology (2018) 152:213–223.
- **Mackie K.A.,** T. Müller and E. Kandeler (2012). Remediation of copper in vineyards–a mini review. Environmental Pollution 167, 16–26.
- **MacLeod A.,** Pautasso M., Jeger M.J., Haines-Young R. (2010). Evolution of the international regulation of plant pests and challenges for future plant health. Food Security 2:49–70.
- **Maringoni A.C.,** Rosa E.F. (1997). Ocorrência de *Curtobacterium flaccumfacien*s pv. *flaccumfaciens* em feijoeiro no Estado de São Paulo. Summa Phytopatholica, 23 (1997), pp. 160-162.
- **Martinez L**., Sanchez M.B., Martınez-Solano L., Hernandez A., Garmendia L., Alicia Fajardo A., Alvarez-Ortega C. (2009). Functional role of bacterial multidrug efflux pumps in microbial natural ecosystems. FEMS Microbiology Reviews, 33(2009) 430–449
- **Mazzucchi U**. (1994). The fire blight monitoring network in Northern Italy: origin and development. OEPP/EPPO Bulletin, 24, 783-791.
- **McMurry L.,** Petrucci R.E. J., Levy S.B. (1980). Active efflux of tetracycline encoded by four genetically different tetracycline resistance determinants in *Escherichia coli*. Proceedings of the National Academy of Sciences. 77:3974–3977.
- **Ormsby M.,** Brenton-Rule E. (2017). A review of global instruments to combat invasive alien species in forestry Biological Invasions 19:3355–3364).
- **Osdaghi E.,** Taghavi S- M., Hamzehzarghani H., Fazliarab A, Harveson R.M., Lamichhane J.R. (2016). Occurrence and characterization of a new red-pigmented variant of *Curtobacterium flaccumfaciens*, the causal agent of bacterial wilt of edible dry beans in Iran. European Journal of Plant Pathology, 146:129–145.
- **Osdaghi E**., Taghavi S.M., Fazliarab A., Elahifard E., Lamichhane J.R. (2015). Characterization, geographic distribution and host range of *Curtobacterium flaccumfaciens*: An emerging bacterial pathogen in Iran. Crop Protection 78, 185:192.
- **Osdaghi E**., Taghavia S. M., Hamzehzarghania H., Fazliaraba A., Harvesonb R. M., Tegli S., Lamichhane J. R. (2018). Epiphytic *Curtobacterium flaccumfacien*s strains isolated from symptomless solanaceous vegetables are pathogenic on leguminous but not on solanaceous plants. Plant Pathology, 67,388–398
- **Painia** D.R., Shepparda A.W., David C. Cookc D.C., De Barroe P.J., Wornerf S.P., Thomasg M.B. (2016). Global threat to agriculture from invasive species. PNAS vol. 113 (27) 7575–7579.
- **Piddock L.** (2006). Multidrug-resistance efflux pumps— not just for resistance. NATURE REVIEWS|MICROBIOLOGY, volume 4.

- **Pimentel** D. (2001). Economic and environmental threats of alien plant, animal, and microbe invasions. Agriculture, Ecosystems and Environment' 84: 1–20.
- **Quacchia A**., Moriya S., Bosio G., Scapin I., Alma A. (2008). Rearing, release and settlement prospect in Italy of *Torymus sinensis*, the biological control agent of the chestnut gall wasp *Dryocosmus kuriphilus.* Bio Control (2008) 53:829–839.
- **Radchenko M.,** Symersky J., Nie R., Lu M. (2015). Structural basis for the blockade of MATE multidrug efflux pumps. Nature Communications, 6, 7995.
- **Sammer U.F.,** Reiher K. (2012). *Curtobacterium flaccumfaciens* pv. *flaccumfaciens* on Soybean in Germany - a threat for farming. Journal of Phytopathology 160 (6), 314e316.
- **Saponari M.,** Loconsole G., Cornara D., Yokomi R.K., De Stradis A., Boscia D., Bosco D., Martelli G. P., Krugner R., Porcelli F. (2014) Infectivity and Transmission of *Xylella fastidiosa by Philaenus spumarius* (Hemiptera: Aphrophoridae) in Apulia, Italy. Journal of Economic Entomology, 107(4):1316-1319.
- **Schuster M. L.,** Sayre R. M. (1967). A coryneform bacterium induces purple-colored seed and leaf hypertrophy of *Phaseolus vulgaris* and other Leguminosae. Phytopathology, 57, 1064–1066.
- **Schuster M.L**., Vidaver A.K., Mandel M. (1968). A purple pigment-producing bean wilt bacterium *Corynebacterium flaccumfaciens* var. *violaceum* n. var. The Journal of Microbiology. 14, 423e427.
- **Schuster, M. L.** (1959). Relation of root-knot nematodes and irrigation water to the incidence and dissemination of bacterial wilt of bean. Plant Disease Report, 43, 25–32.
- **Silva Júnior T.A.F.,** Negrão D.R., Itako A.T., Soman J.M. and Maringoni A.C. (2012). Survival of *Curtobacterium flaccumfaciens* pv. *flaccumfaciens* in soil and crop debris. Journal of Plant Pathology, 94 (2), 331-337.
- **Soares R.M**., Fantinato G.G.P., Darben L.M., Marcelino-Guimaraes F.C., Seixas C.D.S., Carneiro G.E.S. (2013). First report of *Curtobacterium flaccumfaciens* pv. f*laccumfaciens* on soybean in Brazil. Tropical Plant Pathology, 38 (5), 452e454.
- **Steed P. R.,** Stein R. A., Mishra S., Goodman M. C., Mchaourab H. S. (2013). Na+–substrate coupling in the multidrug antiporter NorM probed with a spin-labeled substrate. Biochemistry 52, 5790–5799.
- **Tanaka Y.,** Hipolito C.J., Maturana A.D., Ito K., Kuroda T., Higuchi T., Katoh T., Kato H.E., Hattori M., Kumazaki K., Tsukazaki T., Ishitani R., Suga H., Nureki O. (2013). Structural basis for the drug extrusion mechanism by a MATE multidrug transporter. Nature 496, 247.
- **Urrea C.A.,** Harveson R.M. (2014). Identification of sources of bacterial wilt resistance in common beans (*Phaseolus vulgaris* L.). Plant Disease, 98 (7), 973-976
- **Van Zwieten L.,** Rust J., Kingston T., Merrington G., Morris S. (2004). Influence of copper fungicide residues on occurrence of earthworms in avocado orchard soils. Science of the Total Environment, 329:29–41.
- **Vargas P.,** Felipe A., Michán C., Gallegos M.T. (2011). Induction of *Pseudomonas syringae* pv. *tomato* DC3000 MexAB-OprM Multidrug Efflux Pump by Flavonoids Is Mediated by the Repressor PmeR. Molecular Plant-Microbe Interactions Vol. 24, No. 10, 2011, pp. 1207–1219.
- **Wood B.A.,** Easdown W.J. (1990). A new bacterial disease of mung bean and cowpea for Australia. Australian Plant Pathology, 19 (1), 16-21.
- **Yerkes W.D**., Crispin A.M. (1956). Bean diseases of importance in Mexico in 1955. Plant Disease Rep. 40, 222:223.
- **Zaumeyer W.J.** and ThomasH.R. (1957). A monographic study of bean disease and methods for their control. USDA Technical Bulletins, 868 (revised).

Chapter 2

Aim of the thesis and study objectives

2.1 Aim and scope of this thesis

Within European Union (EU) the control of bacterial diseases of plants still mainly relies on the use of copper compounds as bactericides, whereas antibiotics are also allowed to be used just in the USA and other extra-EU Countries. However, the restriction of copper use in plant protection is a priority for EU. Therefore, the control and the management of phytopathogenic bacteria is going to get definitely more arduous in the next future. In addition, due to the increased globalization and connectedness via world trade, the threat from quarantine, alien and invasive plant pathogenic bacteria arrival and entry in Countries where they were previously absent is expected to increase.

This thesis aims to respond to this urgent need for innovation in plant protection against phytopathogenic bacteria, concerning the development of highly effective and eco-friendly alternatives to copper by applying. To this aim, a complementary research approach has been adopted, looking for several potential bacterial targets among new pathogenicity and virulence determinants of Gram-negative phytopathogenic bacteria, that have never been studied before and that here will be investigated. Moreover, the same approach will be also applied to Gram-positive plant pathogenic bacteria, which have been definitely less investigated until now, in spite of their relevant impact in recent times as emerging plant pathogens, with the support of genomic studies and cutting-edge approaches such as Phenotype MicroArray (PM). As a model, *Pseudomonas savastanoi* pv. *nerii* (*Psn23*) and *Curtobacterium flaccumfaciens* pv. *flaccumfaciens* (*Cff*) have been selected for Gram-negative and Gram-positive phytopathogenic bacteria, respectively.

- **Chapter 3**: The objectives of this study were to determinate the phenotypic characteristic (*i.e.* pathogenicity, arsenic resistance, and plasmid profile) of *C. flaccumfaciens* strains isolated from different annual crops in Iran and analyse the phylogenetic position of the *C. flaccumfaciens* strains having different geographical origins, in comparison to members of *Curtobacterium* spp., also with the aid of molecular fingerprint such as those obtained by rep-PCR.

- **Chapter 4:** The aim of this study has been to evaluate the role played in the plant pathogenic bacterium *Psn23* by the membrane protein *Psn*MATE on IAA efflux and homeostasis, as well as the consequences of these *Psn*MATE -mediated processes on the different stages of plant infection. To this purpose, in *silico* analysis of *Psn*MATE protein has been conducted,

to detect those amino acids supposed to be involved in substrate and ions bounding. Accordingly, several mutants have been produced and then phenotypical characterized (*i.e*. gene expression, pathogenicity tests, and evaluation of IAA production by Salkowski assay and HPLC-FLD). A model has been then drawn concerning the role of *Psn*MATE in the differential modulation of intracellular IAA levels.

- **Chapter 5**: In this study we have selected two strains isolated from Solanaceous plants, one demonstrated to be virulent on bean (*Cff s*train P990 / ICMP 22053) and the other avirulent on bean and not pathogenic (*C. flaccumfaciens* Tom827 / ICMP 22084), and the *Cff* type strain ICPM 2584^{T}. The genome of these three strains was sequenced, and a comprehensive comparison of genomes was conducted using DNA structural and annotation features, in order to identify genes putatively involved in *Cff* pathogenicity and/or virulence, in addition to the serine-protease coding gene that is the target of *Cff*-specific DNA based assay internationally adopted since the beginning of 2000's.

- **Chapter 6**: In this study, the chemical sensitivity to a wide number of metals and metalloids of three *Cff* strains, having distinct phenotypical characteristics and isolated from different hosts, was tested through Phenotype MicroArray analysis. In addition, the most significant metals/metalloids were further tested (*i.e.* caesium chloride, potassium tellurite and sodium metasilicate), including also the no pathogenic *C. flaccumfaciens* strain Tom 827 for comparison. At last, a genomic comparative analysis was conducted in order to detect the genetic determinants of tellurite and arsenic resistance, and that could be putatively related to the differential virulence on bean and other hosts of strains *Cff* P990, *Cff* type strain, and *C. flaccumfaciens* strain Tom827.

Chapter 3

Phenotypic and Molecular-Phylogenetic Analysis Provide Novel Insights into the Diversity of *Curtobacterium flaccumfaciens*

Phytopathology • 2018 • 108:1154-1164 • https://doi.org/10.1094/PHYTO-12-17-0420-R

Bacteriology

e-Xtra*

Phenotypic and Molecular-Phylogenetic Analysis Provide Novel Insights into the Diversity of *Curtobacterium flaccumfaciens*

Ebrahim Osdaghi,† S. Mohsen Taghavi, Silvia Calamai, Carola Biancalani, Matteo Cerboneschi, Stefania Tegli, and Robert M. Harveson

First and second authors: Department of Plant Protection, College of Agriculture, Shiraz University, Shiraz 71441-65186, Iran; third, fourth, fifth, and sixth authors: Dipartimento di Scienze delle Produzioni Agroalimentari e dell'Ambiente, Laboratorio di Patologia Vegetale Molecolare, Università degli Studi di Firenze, Via della Lastruccia 10, 50019 Sesto Fiorentino, Firenze, Italy; and seventh author: University of Nebraska, Panhandle Research & Extension Center, 4502 Ave. I., Scottsbluff 69361.
Accepted for publication 26 April 2018.

ABSTRACT

A multiphasic approach was used to decipher the phenotypic features, genetic diversity, and phylogenetic position of 46 *Curtobacterium* spp. strains isolated from dry beans and other annual crops in Iran and Spain. Pathogenicity tests, resistance to arsenic compounds, plasmid profiling and BOX-PCR were performed on the strains. Multilocus sequence analysis (MLSA) was also performed on five housekeeping genes (i.e., *atpD*, *gyrB*, *ppk*, *recA*, and *rpoB*) of all the strains, as well as five pathotype strains of the species. Pathogenicity test showed that six out of 42 strains isolated in Iran were nonpathogenic on common bean. Despite no differences found between pathogenic and nonpathogenic strains in their plasmid profiling, the former were resistant to different concentrations of arsenic, while the latter were sensitive to the same concentrations. Strains pathogenic on common bean were polyphyletic with at least two evolutionary lineages (i.e., yellow-pigmented strains versus red/orange-pigmented strains). Nonpathogenic strains isolated from solanaceous vegetables were clustered within either the strains of *C. flaccumfaciens* pv. *flaccumfaciens* or different pathovars of the species. The results of MLSA and BOX-PCR analysis were similar to each other and both methods were able to discriminate the yellow-pigmented strains from the red/orange-pigmented strains. A comprehensive study of a worldwide collection representing all five pathovars as well as nonpathogenic strains of *C. flaccumfaciens* is warranted for a better understanding of the diversity within this phytopathogenic bacterium.

Curtobacterium flaccumfaciens inhabits multiple ecological niches, and includes environmental (Chase et al. 2016), human-pathogenic (Francis et al. 2011) plant-pathogenic (Osdaghi et al. 2015a), and plant beneficial (Raupach and Kloepper 2000) strains. The plant-pathogenic strains consist of five pathovars, namely *C. flaccumfaciens* pv. *betae*, *C. flaccumfaciens* pv. *flaccumfaciens*, *C. flaccumfaciens* pv. *ilicis*, *C. flaccumfaciens* pv. *oortii*, and *C. flaccumfaciens* pv. *poinsettiae*, the causal agents of silvering disease of red beet, bacterial wilt of dry beans (*Fabaceae*), bacterial blight of American holly, bacterial wilt and spot of tulip, and bacterial canker of poinsettia, respectively (Collins and Jones 1983; Dye and Kemp 1977). Among them, *C. flaccumfaciens* pv. *flaccumfaciens* is an economically important quarantine pathogen which causes bacterial wilt of dry beans in several States in North and South America, Asia and Oceania (EPPO 2011). *C. flaccumfaciens* is one of the most ambiguous and poorly understood plant pathogenic bacteria in terms of its biology, epidemiology and population genetics (Harveson et al. 2015). The bacterium also can colonize a number of plant species without inducing any disease symptoms (Gonçalves et al. 2017; Harveson et al. 2015; Osdaghi et al. 2018a). While orange, pink, purple and yellow colony variants of *C. flaccumfaciens* pv. *flaccumfaciens* have been reported from the central high plains of the United States (Agarkova et al. 2012), multicolored populations of the pathogen have been found in Canada (Huang et al. 2009) and Brazil (Soares et al. 2013). In addition to the yellow and orange-pigmented variants, a new red-pigmented variant of *C. flaccumfaciens* pv. *flaccumfaciens* has been recently isolated from common bean seeds in Iran (Osdaghi and Lak 2015b; Osdaghi et al. 2015a, 2016a). Differences in aggressiveness of *C. flaccumfaciens* pv. *flaccumfaciens* variants were observed when they were tested on various dry bean cultivars (Osdaghi et al. 2016a).

Nucleic acid sequence-based methods, such as multilocus sequence analysis (MLSA), have been developed to phylogenetically analyze the multiple core genes and to obtain clustering patterns of microorganisms. In particular, MLSA is a powerful and well-accepted method to study the phylogeny of plant pathogenic bacteria (Jacques et al. 2012). While many MLSA studies have been conducted on several Gram-negative and Gram-positive plant pathogenic bacteria (Almeida et al. 2010; Jacques et al. 2012), no study has been conducted to determine the phylogenetic position of plant pathogenic C. *flaccumfaciens* strains. As a consequence, the relationships between the results of band-based fingerprinting (e.g., rep-PCR) and MLSA methods are yet to be determined for *C. flaccumfaciens*. In addition, unlike extensive molecular studies performed on several corynebacteria, (Gartemann et al. 2008), no information is available on mechanistic understanding of the virulence accessories and survival of *C. flaccumfaciens* on host plants, and other environmental habitats. This is a paradox based on the economic importance of this species, and the fact that high throughput techniques are available which could aid in making more accurate taxonomic classification.

The objectives of this study were to (i) determine the phenotypic characteristics (i.e., pathogenicity, arsenic resistance, and plasmid profile) of *C. flaccumfaciens* strains isolated from different annual

†Corresponding author: E. Osdaghi; E-mail: eosdaghi@shirazu.ac.ir

Funding: Financial support for this study was co-provided by Shiraz University (Iran) and University of Florence (Italy).

*The *e-X*tra logo stands for "electronic extra" and indicates that four supplementary figures are published online.

crops in Iran, (ii) analyze the phylogenetic position of the *C. flaccumfaciens* strains isolated in Iran and Spain, in relation to all members of *Curtobacterium* spp., and (iii) compare the results with those of BOX-PCR fingerprinting and phenotypic characteristics of the strains.

MATERIALS AND METHODS

Bacterial strains. *C. flaccumfaciens* and *Curtobacterium*-like strains isolated in Iran during 2013 to 2016, from either symptomatic dry bean plants or asymptomatic solanaceous vegetables and squash (*Cucurbita pepo*), were used in this study (Table 1). The strains isolated from solanaceous vegetables were associated with either symptomatic or symptomless tomato and pepper plants in Iran (Osdaghi et al. 2016b, 2017a, 2018a). Additionally, pure DNA of four *Curtobacterium* spp. strains isolated from common bean seeds of germplasm bank in Spain (provided by Ana J. González; Horticultural and Forest Crops Area, SERIDA, Asturias, Spain) were included in molecular and phylogenetic analysis (González et al. 2005). In total, 51 strains, which include 46 strains from Iran and Spain, as well as the type strains of *C. flaccumfaciens* pv. *flaccumfaciens* (ICMP 2584), *C. flaccumfaciens* pv. *betae* (ICMP 2594), *C. flaccumfaciens* pv. *ilicis* (ICMP 2608), *C. flaccumfaciens* pv. *oortii* (ICMP 2632), and *C. flaccumfaciens* pv. *poinsettiae*

TABLE 1. List of *Curtobacterium flaccumfaciens* and *Curtobacterium*-like strains used in this study, as well as the results of their morphological characterization, specific PCR, and pathogenicity tests[a]

Strain	Morphology	Host of isolation	Pathogenicity on common bean	CffFOR2/ CffREV4 PCR	Origin		Date of isolation	International collection number	Reference
					Province	County			
10eg	Y-F	Eggplant	+	+	East Azerbaijan	Marand	2014	ICMP 22079	Osdaghi et al. 2018a
50R	R-F	Common bean	+	+	Markazi	Arak	2014	ICMP 22071	Osdaghi et al. 2016a
80O	O-F	Common bean	+	+	Markazi	Arak	2014	ICMP 22069	Osdaghi et al. 2016a
Cb222	Y-F	Common bean	+	+	East Azerbaijan	Marand	2015	ICMP 21399	This study
Cb302	Y-F	Common bean	+	+	East Azerbaijan	Koshksaray	2015	–	This study
Cb926	Y-F	Common bean	+	+	Zanjan	Zanjan	2015	–	This study
Cb935	Y-F	Common bean	+	+	Zanjan	Zanjan	2015	–	This study
Cff110	Y-F	Common bean	+	+	Markazi	Khomein	2014	–	This study
Cff113	Y-F	Common bean	+	+	Markazi	Khomein	2014	–	This study
Cff114	Y-F	Common bean	+	+	East Azerbaijan	Marand	2014	–	This study
Cff120	Y-F	Common bean	+	+	Markazi	Khomein	2014	–	This study
Cff130	Y-F	Common bean	+	+	Markazi	Khomein	2014	–	This study
Cff132	O-F	Common bean	+	+	Markazi	Arak	2014	–	This study
Cff137	R-F	Common bean	+	+	Markazi	Arak	2014	ICMP 22066	Osdaghi et al. 2016a
Cff151	O-F	Common bean	+	+	Markazi	Arak	2014	–	This study
Cff153	O-F	Common bean	+	+	Markazi	Arak	2014	–	This study
Cff155	O-F	Common bean	+	+	Markazi	Arak	2014	–	This study
Cff156	O-F	Common bean	+	+	Markazi	Arak	2014	–	This study
Cff204	O-F	Common bean	+	+	Fars	Kazerun	2015	ICMP 22068	Osdaghi et al. 2016a
Cmmeg20	Y-F	Eggplant	–	–	Bushehr	Borazjan	2014	ICMP 22056	Osdaghi et al. 2018a
Cw101	Y-F	Cowpea	+	+	Markazi	Delijan	2015	–	This study
Cw104	Y-F	Cowpea	+	+	East Azerbaijan	Koshksaray	2015	–	This study
Cw110	Y-F	Cowpea	+	+	East Azerbaijan	Marand	2013	–	This study
Cw900	Y-D	Cowpea	+	+	Khuzestan	Dezful	2015	–	This study
Eg502	Y-F	Eggplant	+	+	East Azerbaijan	Koshksaray	2015	ICMP 22055	Osdaghi et al. 2018a
Eg505	Y-F	Eggplant	+	+	East Azerbaijan	Marand	2015	ICMP 22054	Osdaghi et al. 2018a
G105	R-F	Tomato	–	–	Bushehr	Borazjan	2015	ICMP 22064	Osdaghi et al. 2018a
G115	Y-F	Tomato	+	+	Fars	Khesht	2015	–	Osdaghi et al. 2018a
K31	Y-F	Tomato	+	+	Fars	Kazerun	2015	ICMP 22063	Osdaghi et al. 2018a
LPPA2199	O-ND	Common bean	ND	–	Northern Spain		2006	–	SERIDA*
LPPA2315	Y-ND	Common bean	ND	–	Northern Spain		2006	–	SERIDA
LPPA392	Y-ND	Common bean	ND	–	Southern Spain		2005	–	SERIDA
LPPA987	Y-ND	Common bean	ND	–	Northwestern Spain		2012	–	SERIDA
Mo01	Y-F	Squash	–	–	Golestan	Gorgan	–	–	This study
Mo04	O-F	Squash	–	–	Golestan	Gorgan	–	–	This study
P701	Y-F	Bell pepper	+	+	Zanjan	Zanjan	2015	ICMP 22078	Osdaghi et al. 2018a
P990	Y-F	Bell pepper	+	+	Zanjan	Zanjan	2015	ICMP 22053	Osdaghi et al. 2018a
Tom50	R-D	Tomato	+	+	Fars	Khesht	2015	ICMP 22062	Osdaghi et al. 2018a
Tom803	Y-F	Tomato	+	+	East Azerbaijan	Marand	2015	ICMP 22083	Osdaghi et al. 2018a
Tom805	Y-F	Tomato	+	+	West Azerbaijan	Urmia	2015	–	This study
Tom806	Y-F	Tomato	+	+	West Azerbaijan	Urmia	2015	ICMP 22059	Osdaghi et al. 2018a
Tom827	Y-F	Tomato	–	–	East Azerbaijan	Marand	2015	ICMP 22084	Osdaghi et al. 2018a
Tom929	Y-F	Tomato	+	+	Qazvin	Takestan	2015	–	This study
Tom930	Y-F	Tomato	+	+	Qazvin	Takestan	2015	ICMP 22057	Osdaghi et al. 2018a
Tom999	Y-F	Tomato	+	+	Fars	Abadeh	2015	ICMP 22082	Osdaghi et al. 2018a
Xeu15	Y-F	Chili pepper	–	–	East Azerbaijan	Marand	2013	ICMP 21400	Osdaghi et al. 2018a
ICMP 2594	Y-D	Red beet	ND	–	United Kingdom		1955	ICMP 2594^T	ICMP
ICMP 2584	Y-F	Bean	ND	+	Hungary		1957	ICMP 2584^T	ICMP
ICMP 2608	Y-D	American holly	ND	–	USA		1960	ICMP 2608^T	ICMP
ICMP 2632	Y-D	Tulip	ND	–	Netherlands		1967	ICMP 2632^T	ICMP
ICMP 2566	O-D	Poinsettia	ND	–	USA		1942	ICMP 2566^T	ICMP
Tom835	Y-M	Tomato	–	–	Iran		2015	ICMP 22052	Osdaghi et al. 2018b
ICMP 2550	Y-M	Tomato	ND	–	Hungary		1957	ICMP 2550	ICMP
Tom495	Peach color-M	Tomato	ND	–	Iran		2015	ICMP 22060	Osdaghi et al. 2018b

[a] ICMP: International Collection of Microorganisms from Plants (Auckland, New Zealand). T: type strain. * Indicates pure DNA of the strains were provided by Ana J. González (Horticultural and Forest Crops Area, SERIDA, Apdo 13. 33300, Asturias, Spain).

(ICMP 2566) were used in this study. Standard strains of *Clavibacter michiganensis* subsp. *michiganensis* (i.e., Tom835 = ICMP 22052, ICMP 2550, and NCPPB 382), as well as a nonpathogenic strain of *Clavibacter* spp. (Tom495 = ICMP 22060) were used as controls (Osdaghi et al. 2018b).

Morphological characteristics and pathogenicity tests of the strains. Morphological characteristics (e.g., colony color and fluidity) of the strains were determined on yeast extract-dextrose-calcium carbonate (YDC) agar medium, as well as nutrient agar (NA) medium supplemented with 5% sucrose, after 72 h incubation as described by Smith et al. (2001). Briefly, colony morphology was subdivided into three categories: fluidal (colonies flowed when plates were inclined at 45°), mucoid (colonies had a glutinous consistency due to the production of polysaccharide), and dry (little or no polysaccharide was produced) (Smith et al. 2001).

Pathogenicity tests were conducted on common bean (*Phaseolus vulgaris*) plants (cultivar Dorsa) grown in glasshouse conditions using the bacterial strains reported in Table 1. Plant growth conditions and inoculum preparation were described previously (Osdaghi et al. 2015b). Plants were inoculated at the 10 to 12 days postemergence. For each strain, six common bean plants (three/pot) were inoculated. Inoculation was made by inserting a sterile dissecting needle dipped into a fresh bacterial suspension (1×10^8 CFU/ml) throughout the internode between the first and the second node of each plant. All inoculated plants were maintained in the greenhouse at ambient temperature (25 to 28°C and 14 h natural light). A reference strain of *C. flaccumfaciens* pv. *flaccumfaciens* (ICMP 22071) and sterile distilled water were used as positive and negative controls, respectively. Plants were periodically monitored for the appearance of disease symptoms and the final evaluation of disease symptoms was performed at 20 days postinoculation (dpi). Disease severity on each plant was rated based on the number of primary or trifoliate leaves showing wilting symptoms as described previously (Osdaghi et al. 2016a). Koch's postulates were accomplished by re-isolating the inoculated strains on yeast-extract peptone glucose agar (YPGA) medium from all inoculated plants. The identity of re-isolated bacterial strains was confirmed using the primer pair CffFOR2/CffREV4 (Tegli et al. 2002) (Table 2). Since six strains (i.e., Cmmeg20, G105, Mo01 Mo04, Tom827, and Xeu15) did not induce any symptoms on the inoculated common bean cultivar Dorsa plants, the same procedure as described above was conducted on common bean cultivars Derakhshan and Sadri and cowpea (*Vigna unguiculata*) cultivar Mashhad. All the pathogenicity tests were repeated twice.

Screening for arsenic resistance. We evaluated a set of 31 representative strains (Table 3) for their resistant response to different concentrations of two arsenic compounds (i.e., sodium arsenite [$NaAsO_2$] and sodium arsenate [Na_3AsO_4]). Type strain of *C. flaccumfaciens* pv. *oortii* (ICMP 2632) was used as positive control as recommended by Hendrick et al. (1984). We also included the standard strains of either pathogenic (i.e., ICMP 2550, NCPPB 382, and ICMP 22052), or nonpathogenic *Clavibacter* spp. (ICMP 22060) strains as negative controls (Osdaghi et al. 2018b).

The bacterial strains were screened using the agar plating method as described previously (Hendrick et al. 1984). Briefly, nutrient broth-yeast extract (NBY) agar plates supplemented with three different concentrations of either sodium arsenite (2, 5, and 7 mM), or sodium arsenate (80, 100, and 130 mM) were used for bacterial inoculation. For each strain, serial tenfold dilutions were prepared from a starter suspension ($OD_{600} = 2.5$), obtained from a fresh culture grown at 27°C for 24 h on nutrient broth agar medium. For each dilution, 12 droplets (each droplet containing 5 µl of the suspension) were plated on each arsenic-containing plate. The plates were then incubated at 27°C for 48 h, after which the number of single colony forming units (CFU) were counted. The data (average values ± standard deviation [SD]) were subjected to one-way analysis of variance (ANOVA). Tukey's range test was also performed to identify statistically significant differences among the strains / salt concentrations, using PAST Version 3.17 (Hammer et al. 2001) (https://folk.uio.no/ohammer/past/).

Plasmid profiling. A set of 11 strains isolated in Iran was selected to carry out plasmid content analysis. This set was represented by candidate strains based on different isolation hosts and phenotypic features, including the type strain of *C. flaccumfaciens* pv. *flaccumfaciens* (ICMP 2584), pathogenic strains (50R, 80O, Cw110, P990, Tom50, and Tom930), as well as nonpathogenic strains (Cmmeg20, Mo04, Tom827, and Xeu15) of *C. flaccumfaciens*. The standard strains of *Clavibacter michiganensis* subsp. *michiganensis* (ICMP 2550 and NCPPB 382), harboring two plasmids (i.e., pCM1 and pCM2) (Meletzus et al. 1993) were also included in this study as positive controls.

Plasmids were isolated according to the procedure described by Klaenhammer (1984) with several modifications. The strains were grown overnight in 10 ml of Luria-Bertani (LB) medium, on a 110 rpm shaker at 27 °C. Bacterial cells were pelleted by centrifugation (6,000 × *g* for 5 min) and the pellets were resuspended in 1 ml of Tris-EDTA (TE) buffer (pH 7.5), with 25% sucrose and 75 µl of lysozyme (1 mg ml^{-1} in TE, pH 7.5), and incubated at 37°C for 1 h. Subsequently, 500 µl of lysis solution was added to the bacterial pellet and the samples were heated at 62 °C for 1 h. Finally, plasmid DNA was neutralized by the addition of 50 µl of 2 M Tris (pH 7) and 70 µl of 5 M NaCl. The presence of plasmids was analyzed on 0.9% agarose gel at 60 V for 4 to 5 h in TAE buffer. Agarose gel was stained with ethidium bromide at 0.5 µg/ml and visualized with UV light using Gel Doc XR+ (BioRad). The experiments were repeated three times.

TABLE 2. Primer pairs used in this study

Primer name	5′–3′ sequence	Target	Size of amplicon (bp)	Annealing temperature (°C)	Reference
atpD2F	GACATCGAGTTCCCGCAC	*atpD*	1,105	64	Jacques et al. 2012
atpD2R	CGATGATCTCCTGGAGCTCCTTGT				
2F	ACCGTCGAGTTCGACTACGA	*gyrB*	977	57	Richert et al. 2005
6R	AGSACGATCTTGTGGTA				
ppkCfF	GAGAACCTCATCCAGGCCCT	*ppk*	604	63	This study
ppkCfR	CGAGCTTCGAGTGCGTCTTCAG				
recACfF	GACCGCACTCGCCCAGATCGACCG	*recA*	723	66	This study
recACfR	GCCATCTTGTTCTTCACGACCTTG				
3Fs	GACAACTTCTACTTCAAC	*rpoB*	447	55	Richert et al. 2007
4Rs	GTTGTTCTGGTCCATGAAC				
CffFOR2	GTTATGACTGAACTTCACTCC	*C. flaccumfaciens* pv. *flaccumfaciens*	306	62	Tegli et al. 2002
CffREV4	GATGTTCCCGGTGTTCGA				
ERIC1R	ATGTAAGCTCCTGGGGATTCAC3	ERIC	–	42	Versalovic et al. 1994
ERIC2	AAGTAAGTGACTGGGGTGAGCG				
BOXA1R	CTACGCCAAGGCGACGCCTGACG	BOX	–	52	Versalovic et al. 1994
REPIR-I	IIICGICGICATCIGGC	REP	–	42	Versalovic et al. 1994
REP2I	ICGICTTATGIGGCCTAC				

DNA extraction, PCRs, and sequencing. DNA extraction was performed using Expin Combo-GP DNA extraction kit (GeneAll, Tic Tech Centre, Singapore) based on the manufacturer's recommendations. The quality and quantity of the DNAs were spectrophotometrically evaluated and adjusted to 50 ng μl^{-1} using Nanodrop ND-100 (Nanodrop Technologies, Waltham, MA). The DNA was kept at −20°C for further uses. Five housekeeping genes including *atpD*, *gyrB*, *ppk*, *recA*, and *rpoB* were employed for the sequencing and phylogenetic analyses on all the strains described in Table 1. Primer pairs were used for partial sequencing of *atpD*, *gyrB*, and *rpoB* as described previously (Table 2) (Jacques et al. 2012; Richert et al. 2005, 2007). While the primer pairs ppkCfF/ppkCfR and recACfF/recACfR were redesigned for *ppk* and *recA* genes, respectively, based on the sequence of *Curtobacterium* sp. (strain MR_MD2014, GenBank: CP009755.1) (Mariita et al. 2015) according to Jacques et al. (2012) (Table 2). For PCR reactions, Universal PCR Kit, Ampliqon Taq DNA Polymerase Master Mix Red (Ampliqon A/S, Odense, Denmark), was used according to the manufacturer's recommendations. For each strain, a 25 µl of PCR including 50 ng of total DNA and 1 µl of each primer (10 pmol μl^{-1}) were used. Purity and yield of PCR products were checked by running a 5-µl reaction mixture in 1.2% agarose gel stained with ethidium bromide. The PCR products were sent to Bioneer Corporation (www.Bioneer.com) (Daejeon, South Korea) to be sequenced using Sanger sequencing technology.

Resulting sequences were analyzed using the BLAST program (https://blast.ncbi.nlm.nih.gov/) and aligned with Clustal W program (Larkin et al. 2007) implemented in MEGA 6.06 software (Tamura et al. 2013). Partial sequences were deposited in the NCBI GenBank and assigned accession numbers as follows: *atp*D: KX591664 to KX591707 and MG737698 to MG737699; *gyr*B: KX591708 to KX591751, and MG737700 to MG737701; *ppk*: KX591752 to KX591795, and MG737702 to MG737703; *rec*A: KX591796 to KX591839, and MG737704 to MG737705; and *rpo*B: KX591840 to KX591883, and MG737706 to MG737707. For phylogenetic comparisons, the respective sequences of the five housekeeping genes were retrieved from 30 publicly available complete genome sequences of *Curtobacterium* spp. strains in the GenBank database.

Phylogenetic analysis. Sequences were concatenated following the alphabetic order of the genes, ending in a sequence of 2,977 bp: nucleotides 1 to 761 for *atpD*, 762 to 1507 for *gyrB* (746 bp), 1508 to 2021 for *ppk* (514 bp), 2022 to 2612 for *recA* (591 bp), and 2613 to 2977 for *rpoB* (365 bp). Phylogenetic analyses were performed on individual gene sequences as well as the data set of concatenated sequences. Phylogenetic trees were constructed using maximum likelihood method with MEGA 6.06 software (Tamura et al. 2013). The general time-reversible (GTR) model of evolution was selected for Maximum Likelihood analysis using the Modeltest tab in MEGA 6.06 (Hall, 2011). *Clavibacter michiganensis* subsp. *michiganensis* strain NCPPB 382 was used to root the trees. MEGA 6.06 was used to obtain the phylogenetic trees and bootstrap values (1000 replicates) for the nucleotide sequences of each individual gene and of concatenated sequences. Additionally,

TABLE 3. Growth rate of *Curtobacterium flaccumfaciens*, *Curtobacterium*-like, and *Clavibacter michiganensis* strains used in this study on different concentrations of sodium arsenite ($NaAsO_2$) and sodium arsenate (Na_3AsO_4)[a]

Strain		Resistance to						Pathogenicity on common bean
		Sodium arsenite			Sodium arsenate			
		2 mM^S	5 mM^S	7 mM^S	80 mM^S	100 mM^S	130 mM^S	
C. flaccumfaciens pv. *flaccumfaciens*	10eg	10^2–10^4	$\leq 10^2$	$\leq 10^2$	10^4–10^6	10^4–10^6	10^2–10^4	+
C. flaccumfaciens pv. *flaccumfaciens*	50R	10^4–10^6	$\leq 10^2$	$\leq 10^2$	10^4–10^6	10^4–10^6	10^2–10^4	+
C. flaccumfaciens pv. *flaccumfaciens*	80O	10^2–10^4	$\leq 10^2$	$\leq 10^2$	10^4–10^6	10^4–10^6	10^2–10^4	+
C. flaccumfaciens pv. *flaccumfaciens*	Cb222	10^2–10^4	$\leq 10^2$	$\leq 10^2$	10^4–10^6	10^4–10^6	10^2–10^4	+
C. flaccumfaciens pv. *flaccumfaciens*	Cb302	10^2–10^4	$\leq 10^2$	$\leq 10^2$	10^4–10^6	10^4–10^6	10^2–10^4	+
C. flaccumfaciens pv. *flaccumfaciens*	Cb926	10^2–10^4	$\leq 10^2$	$\leq 10^2$	10^4–10^6	10^4–10^6	10^2–10^4	+
C. flaccumfaciens pv. *flaccumfaciens*	Cff110	10^2–10^4	$\leq 10^2$	$\leq 10^2$	10^4–10^6	10^4–10^6	10^2–10^4	+
C. flaccumfaciens pv. *flaccumfaciens*	Cff137	10^2–10^4	$\leq 10^2$	$\leq 10^2$	10^4–10^6	10^4–10^6	10^2–10^4	+
C. flaccumfaciens pv. *flaccumfaciens*	Cff151	10^2–10^4	$\leq 10^2$	$\leq 10^2$	10^4–10^6	10^4–10^6	10^2–10^4	+
C. flaccumfaciens pv. *flaccumfaciens*	Cff153	10^2–10^4	$\leq 10^2$	$\leq 10^2$	10^4–10^6	10^4–10^6	10^2–10^4	+
C. flaccumfaciens pv. *flaccumfaciens*	Cff155	10^2–10^4	$\leq 10^2$	$\leq 10^2$	10^4–10^6	10^4–10^6	10^2–10^4	+
C. flaccumfaciens pv. *flaccumfaciens*	Cff156	10^2–10^4	$\leq 10^2$	$\leq 10^2$	10^4–10^6	10^4–10^6	10^2–10^4	+
C. flaccumfaciens pv. *flaccumfaciens*	ICMP 2584^T	$\leq 10^2$	–	–	$\leq 10^2$	$\leq 10^2$	$\leq 10^2$	+
C. flaccumfaciens pv. *flaccumfaciens*	Cw101	10^2–10^4	$\leq 10^2$	$\leq 10^2$	10^4–10^6	10^4–10^6	10^2–10^4	+
C. flaccumfaciens pv. *flaccumfaciens*	Cw110	10^4–10^6	$\leq 10^2$	$\leq 10^2$	10^4–10^6	10^4–10^6	10^2–10^4	+
C. flaccumfaciens pv. *flaccumfaciens*	Eg502	10^2–10^4	$\leq 10^2$	$\leq 10^2$	10^4–10^6	10^4–10^6	10^2–10^4	+
C. flaccumfaciens pv. *flaccumfaciens*	Eg505	10^2–10^4	$\leq 10^2$	$\leq 10^2$	10^4–10^6	10^4–10^6	10^2–10^4	+
C. flaccumfaciens pv. *flaccumfaciens*	Mo11	10^2–10^4	$\leq 10^2$	$\leq 10^2$	10^4–10^6	10^4–10^6	10^2–10^4	+
C. flaccumfaciens pv. *flaccumfaciens*	P701	10^2–10^4	$\leq 10^2$	$\leq 10^2$	10^4–10^6	10^4–10^6	10^2–10^4	+
C. flaccumfaciens pv. *flaccumfaciens*	P990	10^2–10^4	$\leq 10^2$	$\leq 10^2$	10^4–10^6	10^4–10^6	10^2–10^4	+
C. flaccumfaciens pv. *flaccumfaciens*	Tom50	10^2–10^4	$\leq 10^2$	$\leq 10^2$	10^4–10^6	10^4–10^6	10^2–10^4	+
C. flaccumfaciens pv. *flaccumfaciens*	Tom803	10^2–10^4	$\leq 10^2$	$\leq 10^2$	10^4–10^6	10^4–10^6	10^2–10^4	+
C. flaccumfaciens pv. *flaccumfaciens*	Tom806	10^2–10^4	$\leq 10^2$	$\leq 10^2$	10^4–10^6	10^4–10^6	10^2–10^4	+
C. flaccumfaciens pv. *flaccumfaciens*	Tom930	10^2–10^4	$\leq 10^2$	$\leq 10^2$	10^4–10^6	10^4–10^6	$\leq 10^2$	+
C. flaccumfaciens pv. *flaccumfaciens*	Tom999	10^2–10^4	$\leq 10^2$	$\leq 10^2$	10^4–10^6	10^4–10^6	10^2–10^4	+
C. flaccumfaciens pv. *oortii*	ICMP 2632^T	10^2–10^4	$\leq 10^2$	$\leq 10^2$	10^4–10^6	10^4–10^6	10^4–10^6	–
C. flaccumfaciens	Cmmeg20	–	–	–	–	–	–	–
C. flaccumfaciens	G105	–	–	–	–	–	–	–
C. flaccumfaciens	Tom827	–	–	–	–	–	–	–
C. flaccumfaciens	Xeu15	–	–	–	–	–	–	–
Curtobacterium spp.	Mo04	–	–	–	–	–	–	–
Clavibacter michiganensis subsp. *michiganensis*	ICMP 2550^T	–	–	–	–	–	–	–
Clavibacter michiganensis subsp. *michiganensis*	NCPPB 382	–	–	–	–	–	–	–
Clavibacter michiganensis subsp. *michiganensis*	Tom835	–	–	–	–	–	–	–
Clavibacter spp.	Tom495	–	–	–	–	–	–	–

[a] All strains, which were pathogenic on common bean, were able to grow on different concentrations of both compounds, while nonpathogenic strains were sensitive. *Clavibacter michiganensis* strains were sensitive to both the compounds regardless of their pathogenicity on tomato. S = data statistically significant (ANOVA and Tukey's test, $P < 0.05$).

the similarity matrix of the concatenated sequences of five housekeeping genes, in the type strains of five pathovars of *C. flaccumfaciens*, was prepared using the online service "Sequence Identity And Similarity" (SIAS) (http://imed.med.ucm.es/Tools/sias.html) with default settings.

Recombination analysis. Nucleotide diversity, the number of haplotypes, and haplotype diversity were determined using DnaSP 5.10 software (Librado and Rozas 2009). The class I neutrality tests (Tajima's D and Fu, and Li's D* and F*) were also calculated for detecting potential departure from the mutation/drift equilibrium (Librado and Rozas 2009). Detection of potential recombinant sequences and identification of likely parental sequences within *C. flaccumfaciens* strains were conducted using a set of seven nonparametric detection methods (i.e., RDP, Geneconv, MaxChi, Chimaera, BootScan, SiScan, and 3Seq) implemented in Recombination Detection Program (RDP) version 4.80 (Martin et al. 2015). The analysis was performed with default settings for the different detection methods, and the Bonferroni-corrected P value cutoff was set at 0.05. Two independent experiments, one including all the *Curtobacterium* sp. strains and the other including only *C. flaccumfaciens* strains, were performed in this analysis. Recombination events were accepted when they were identified by at least four out of seven detection methods (Martin et al. 2015). Splits-decomposition network was constructed and the pairwise homoplasy index (PHI) was calculated using SplitsTree version 4.14.4 (Huson and Bryant 2006). These calculations used the individual genes, as well as the entire data set of concatenated sequences (Huson and Bryant 2006).

Rep-PCR. Since the MLSA-based phylogeny was unable to differentiate pathogenic and nonpathogenic strains, BOX, enterobacterial repetitive intergenic consensus (ERIC), and repetitive element palindromic (REP) primers (Table 2) (Versalovic et al. 1994) were used to discriminate the putative diversity among *C. flaccumfaciens* strains from our collection. Fifty-one *C. flaccumfaciens* and one *Clavibacter michiganensis* (as out-group) strains were evaluated with rep-PCR analysis (Table 1). PCR reactions were similar to those described above, while the annealing temperatures are described in Table 2. Ten microliters of PCR products was run on 1.2% agarose gel, stained with ethidium bromide, and the digitized image was converted into a TIFF file for a subsequent analysis of the fingerprint patterns. Unweighted pair groups with arithmetic averages were calculated using NTSYS-pc software version 2.02e (Rohlf 2008). The procedure was repeated independently to test the reproducibility of the fingerprints.

RESULTS

Morphology and pathogenicity of the strains. Morphological characteristics of the strains are presented in Table 1. Among the bacterial strains isolated in Iran, all but two (i.e., Cw900 and Tom50) were shown to have fluidal colony on YDC medium. The strains Cw900 and Tom50 have had dried colonies on the same medium (Table 1). As for colony color, 30 strains had

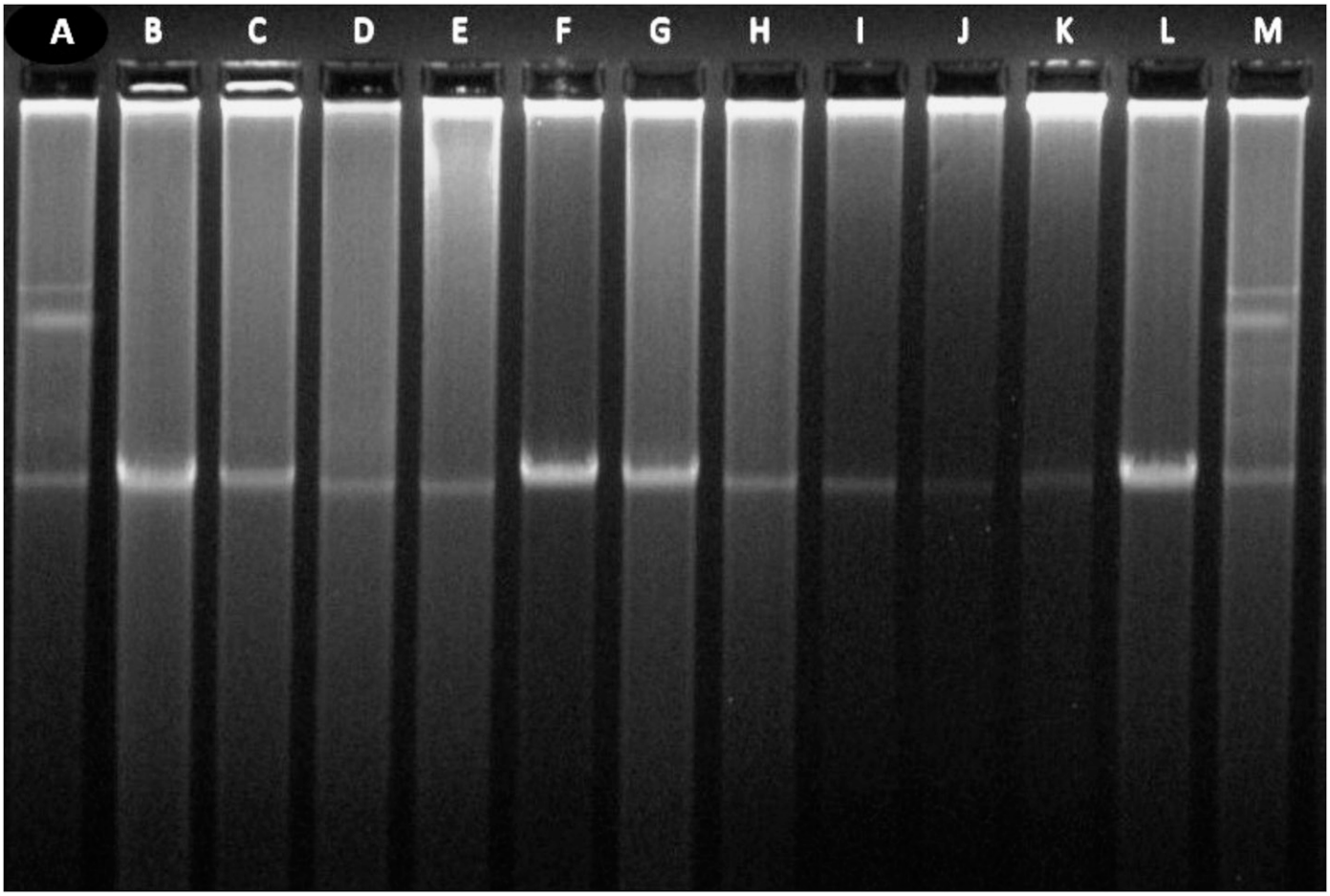

Fig. 1. Plasmid profile of *Curtobacterium flaccumfaciens* and *Curtobacterium*-like strains used in this study. Indigenous plasmids from *Clavibacter michiganensis* subsp. *michiganensis* (pCM1 and pCM2), whose sizes were 27.5 and 72 kb, respectively, were used as positive control. Chromosomal DNAs are seen as a common band in all strains. Lanes A and M, *Clavibacter michiganensis* subsp. *michiganensis* ICMP 2550 and NCPB 382, respectively; lane B, ICMP 2584; lane C, P990; lane D, Tom50; lane E, 50R; lane F, 80O; lane G, Tom827; lane H, Tom930; lane I, Xeu15; lane J, Cmmeg20; lane K, Cw110; and lane L, Mo04. No indigenous plasmids were found in *C. flaccumfaciens* and *Curtobacterium*-like strains used in this study.

yellow colonies, while eight were orange and four were red-pigmented (Table 1; Supplementary Fig. S1).

All the *C. flaccumfaciens* strains isolated from dry beans in Iran were pathogenic on common bean in greenhouse conditions (Table 1). Interveinal chlorosis, leading to necrotic areas on the leaves, and systemic wilting were observed at 8 to 14 days postinoculation (Supplementary Fig. S2). Among the strains isolated from solanaceous vegetables, all but four (i.e., Cmmeg20, G105, Tom827, and Xeu15) were pathogenic on common bean (Table 1). None of the strains isolated from squash (i.e., Mo01 and Mo04) were pathogenic on common bean. After inoculation, bacterial strains were re-isolated from the symptomatic plants, and

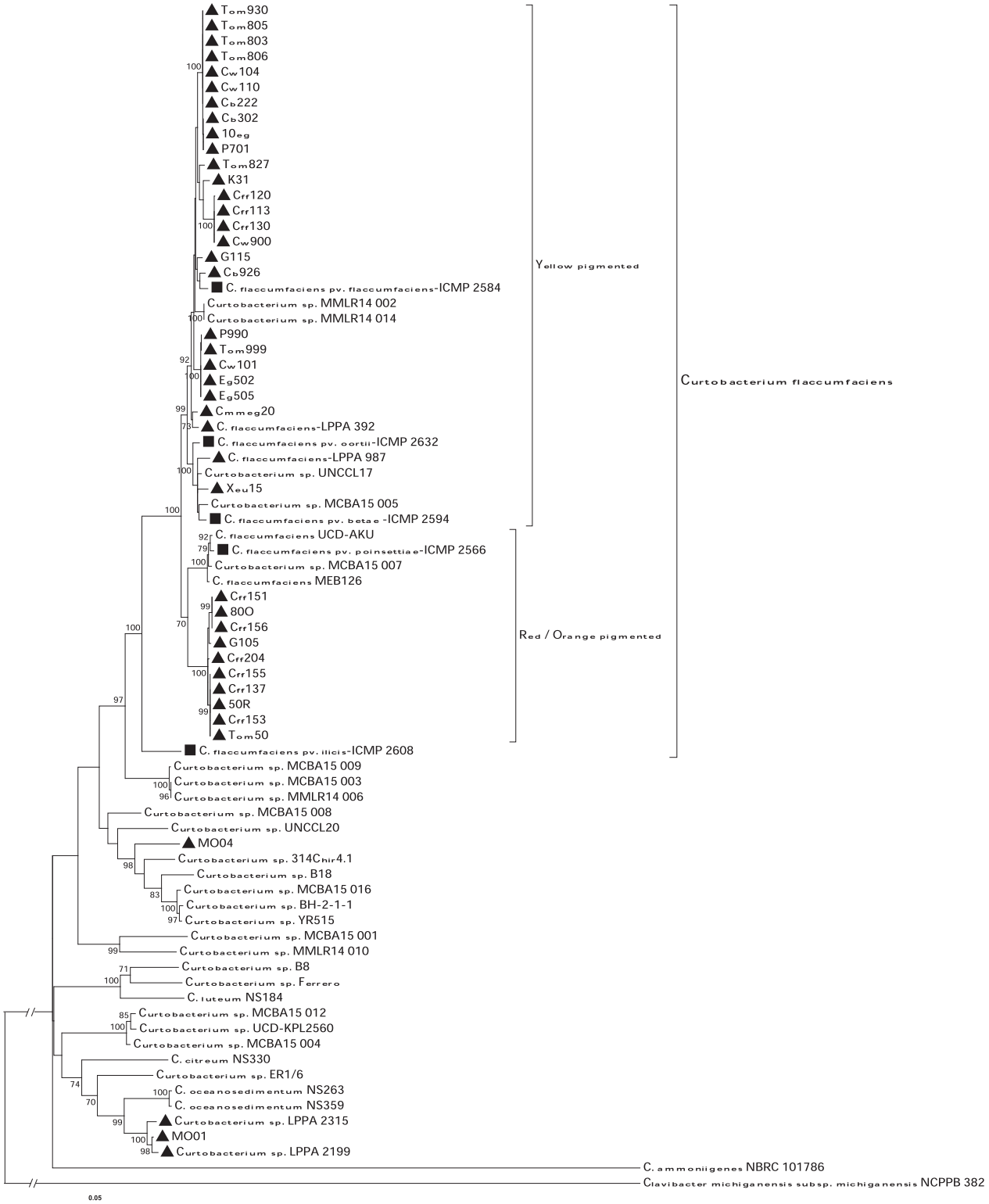

Fig. 2. Maximum likelihood tree based on the concatenated partial sequences of *atpD*, *gyrB*, *ppk*, *recA*, and *rpoB* genes in *Curtobacterium flaccumfaciens* and *Curtobacterium*-like strains used in this study. Bootstrap scores (1,000 replicates) are displayed at each node. *Clavibacter michiganensis* was used for rooting the tree. Yellow-pigmented strains of *C. flaccumfaciens* were phylogenetically different from those of red/orange-pigmented strains. Nonpathogenic strains of *C. flaccumfaciens* were scattered among the pathogenic strains. The strains isolated in Iran and Spain were labeled using black triangles, while the type strains of five pathovars of *C. flaccumfaciens* were labeled using black squares.

identified using specific PCR primers CffFOR2/CffREV4 (data not shown). Repetitive pathogenicity tests on common bean cultivars Derakhshan and Sadri, as well as on cowpea cultivar Mashhad with Cmmeg20, G105, Tom827, Xeu15, Mo01, and Mo04 strains produced similar results to those observed in the first set of pathogenicity tests. Control plants remained healthy.

Resistance to arsenic. All but five of the evaluated strains were resistant against arsenic compounds. The strains Cmmeg20, G105, Tom827, Xeu15, and Mo04 were unable to grow on any concentration of either sodium arsenite and sodium arsenate (Table 3). The level of resistance to arsenic compounds in the type strain of *C. flaccumfaciens* pv. *flaccumfaciens* (ICMP 2584) was statistically different from those of other strains. It was able to grow on sodium arsenite up to 2 mM (Table 3), with faint growth on all concentrations of sodium arsenate. None of the *Clavibacter* spp. strains evaluated was able to grow on arsenic compounds regardless of their pathogenicity status on tomato.

Plasmid profiling. As expected, *Clavibacter michiganensis* subsp. *michiganensis* strains ICMP 2550 and NCPPB 382 harbored two plasmids (pCM1 and pCM2); whose sizes were 27.5 and 72 kb, respectively (Fig. 1, lanes A and M). No plasmids were found in any of the *C. flaccumfaciens* strains tested here, regardless of their isolation host or pathogenicity on common bean (Fig. 1, lanes B to L).

Phylogenetic analysis. Phylogenetic analysis showed a clustering pattern based on colony color of *C. flaccumfaciens* strains used in this study (Fig. 2). Considering the data set of concatenated sequences of five housekeeping genes, the phylogenetic tree was strongly supported by a 100% bootstrap value, clear differentiation of yellow-pigmented *C. flaccumfaciens* strains from red/orange-pigmented strains (Fig. 2).

All the yellow-pigmented strains of *C. flaccumfaciens* clustered as a monophyletic group containing the nonpathogenic strains (i.e., Tom827, Cmmeg20, and Xeu15) isolated from solanaceous vegetables in Iran, as well as a number of cosmopolitan strains isolated from different environmental habitats (Fig. 2). The yellow-pigmented strains 10eg, Cb222, Cb302, Cw104, Cw110, P701, Tom803, Tom805, Tom806, and Tom930—all of which were isolated in northwestern Iran in 2015—were clustered as one haplotype (Table 1). This observation is consistent with the epidemic emergence of the bacterial wilt disease from all the northwestern provinces of the country in 2015. Nonpathogenic red-pigmented strain G105 was clustered among the other red/orange-pigmented pathogenic strains irrespective of their host of isolation. Furthermore, the strains LPPA2315, LPPA2199, and Mo01 were clustered as a monophyletic group apart from the core population of *C. flaccumfaciens*. Based on the results of MLSA data, none of the strains Mo01, Mo04, LPPA2315, and LPPA2199 are true members of *C. flaccumfaciens*. In all the five phylogenetic trees constructed using the individual housekeeping gene sequences, yellow-pigmented *C. flaccumfaciens* strains were separated from the red/orange-pigmented strains. Interestingly, there were no differences among all the yellow-pigmented *C. flaccumfaciens* strains in the *rpoB* gene sequence (data not shown).

Sequence statistics of the five housekeeping genes used for the phylogenetic analysis are summarized in Table 4. Among the 75 *C. flaccumfaciens* and *Curtobacterium* spp. strains used in this study, the highest number of haplotypes (53 haplotypes) were observed in *gyrB* gene sequences. Conversely, only 33 haplotypes were observed in *rpoB* gene sequences using the same number of strains (Table 4). Altogether, *gyrB* and *recA* genes were the most discriminative, and *rpoB* was the least discriminative gene for *C. flaccumfaciens* phylogeny evaluations (Table 4).

Sequence similarity matrix experiments using five housekeeping gene sequences showed that four pathotypes of *C. flaccumfaciens* (i.e., *C. flaccumfaciens* pv. *betae, C. flaccumfaciens* pv. *flaccumfaciens*, *C. flaccumfaciens* pv. *oortii*, and *C. flaccumfaciens* pv. *poinsettiae*) are closely related to each other with sequence similarity ranging between 97.31 to 99.09% (Table 5). However, *C. flaccumfaciens* pv. *ilicis* (previously known as *Arthrobacter ilicis*) (Young et al. 2004), which recently been included in *C. flaccumfaciens* species, is distinct from the core population of other *C. flaccumfaciens* isolates (Fig. 2). Indeed, the sequence similarity between C. *flaccumfaciens* pv. *ilicis* and the other four pathovars of the species is only 95.53 to 95.93% (Table 5).

Tajima's D, and Fu and Li's D* and F* statistics showed that there was no significant departure from the mutation drift equilibrium within *C. flaccumfaciens* strains used in this study (data not shown). Because the maximum likelihood phylogenies showed incompatible topologies (Fig. 2; Supplementary Fig. S3), phylogenetic networks were generated using the splits-decomposition method for the concatenated data set (Fig. 3), as well as all the individual gene sequences (data not shown). Considering the *C. flaccumfaciens* strains, pairwise homoplasy index (PHI) test did find statistically significant evidence suggesting the occurrence of recombination among the *gyrB* (PhiTest = 0.27568; $P < 0.02386$) and *recA* (PhiTest = 0.22906; $P < 0.3122$) genes but not in the *atpD*, *ppk*, and *rpoB* genes. Recombination Detection Program (RDP) discovered recombination in both the data set of *Curtobacterium* spp. strains, and *C. flaccumfaciens* strains (Table 6). Indeed, recombination was detected in the *C. flaccumfaciens* strains from all the seven tested methods. Additionally, when the individual gene sequences were considered using RDP, recombination was identified in *gyrB* (in six out of seven methods), *recA* (in four out of seven methods), and *rpoB* (in four out of seven methods) genes sequences.

Genetic diversity of the strains. ERIC-PCR produced 0 to 4 fragments in sizes ranging from 0.2 to 2 kb, while REP-PCR produced 0 to 3 fragments in sizes ranging from 0.1 to 3 kb (data not shown). Primer BOX A1R produced 4 to 12 fragments in sizes ranging from 0.2 to 2.6 kb (Supplementary Fig. S4). Hence, BOX A1R primer was selected to evaluate the genetic diversity of our collection of 51 *C. flaccumfaciens* strains. The dendrogram based on UPGMA cluster analysis showed all *C. flaccumfaciens* strains forming a group with similarity coefficient ranged from 31 to 93%

TABLE 4. Sequence statistics of the five housekeeping genes (i.e., *atpD*, *gyrB*, *ppk*, *recA*, and *rpoB*) of *Curtobacterium flaccumfaciens* strains used in this study

	Diversity parameters[a]					
Sequence	N	H	S	Pi	NM	HD
atpD	761	47	108	0.02091	124	0.964
gyrB	746	53	203	0.05783	267	0.983
ppk	514	46	130	0.06187	173	0.963
recA	591	48	138	0.05561	184	0.970
rpoB	365	33	66	0.04405	71	0.863
Concatenated	2,977	54	645	0.04696	819	0.983

[a] N: number of nucleotides; H: number of haplotypes; S: total number of segregating sites; Pi: nucleotide diversity; (π); NM: number of mutations (η); and HD: haplotype (gene) diversity.

TABLE 5. Similarity matrix of the concatenated sequences of five housekeeping genes (i.e., *atpD*, *gyrB*, *ppk*, *recA*, and *rpoB*) in five pathotype strains of *Curtobacterium flaccumfaciens*

Strain[a]	ICMP 2584	ICMP 2594	ICMP 2566	ICMP 2632	ICMP 2608
ICMP 2584	100.00				
ICMP 2594	98.25	100.00			
ICMP 2566	97.71	97.31	100.00		
ICMP 2632	98.52	99.09	97.61	100.00	
ICMP 2608	95.83	95.73	95.53	95.93	100.00

[a] ICMP 2584: *C. flaccumfaciens* pv. *flaccumfaciens*; ICMP 2594: *C. flaccumfaciens* pv. *betae*; ICMP 2566: *C. flaccumfaciens* pv. *poinsettiae*; ICMP 2632: *C. flaccumfaciens* pv. *oortii*; and ICMP 2608: *C. flaccumfaciens* pv. *ilicis*.

(Fig. 4). Cluster analysis using a cutoff level at 44% similarity produced six clusters (named G1 to G6)—two of them were major clusters (G1 = 25 and G2 = 16 strains) and four minor clusters (one to four strains). Cluster G1 included both yellow-pigmented and red/orange-pigmented strains, while clusters G2-G6 incorporated only yellow-pigmented strains. The strains in G1 were subclustered into three subgroups namely G1-1 to G1-3, with similarity values between 56 to 93%. All but one strain (Cff155) in G1-1 were yellow-pigmented, while the strains in G1-2 were red/orange-pigmented, except the strain LPPA392. The cluster G1-3 contained three strains, all of them isolated from tomato, and two of them (G105 and Tom827) were nonpathogenic on bean plants (Fig. 4; Table 1). Cluster G2 had similarity coefficients ranging from 55 to 91% and contained 15 yellow-pigmented strains in G2-1 and strain 10eg in G2-2 subclusters (Fig. 4). Cluster G3, contained four strains, which further divided into two subclusters in 49% cutoff value similarity. Cluster G4 contained four strains, three of which were isolated from in Spain (LPPA2199, LPPA2315, and LPPA987), and the type strain of C. *flaccumfaciens* pv. *poinsettiae*. Finally, cluster G5 contained only one strain (P701) as did cluster G6 (the type strain of *C. flaccumfaciens* pv. *oortii*) (Fig. 4).

The most prominent feature in the BOX-PCR fingerprint of *C. flaccumfaciens* is a band of approximately 500 bp, which is present in all the strains except for LPPA2199, LPPA2315, and the type strain of C. *flaccumfaciens* pv. *poinsettiae*. This is an interesting result because the strains LPPA2199 and LPPA2315 (G4-1) were isolated in Spain and were clustered apart from the core population of C. *flaccumfaciens* in MLSA-based phylogenetic trees (Fig. 2). A fragment of approximately 430 to 460 bp was produced in *Clavibacter michiganensis* but not in the *C. flaccumfaciens* strains. No discernible differences were found between C. *flaccumfaciens* strains isolated from dry beans and those isolated from asymptomatic solanaceous vegetables.

DISCUSSION

In this study, a multiphasic approach was used to decipher the phenotypic features, genetic diversity and phylogeny of *C. flaccumfaciens* strains isolated in Iran and Spain. Although no differences were found between the pathogenic and nonpathogenic strains in their plasmid profile, the former were resistant against all evaluated concentrations of arsenic compounds, while the latter were sensitive to the same concentrations. MLSA results revealed that the bacterial strains causing wilt disease on dry beans were distributed into two phylogenetic lineages (yellow-pigmented strains and red/orange-pigmented strains).

Most of the plant-pathogenic bacteria are reported to have nonpathogenic lineages (Jacques et al. 2012). For instance,

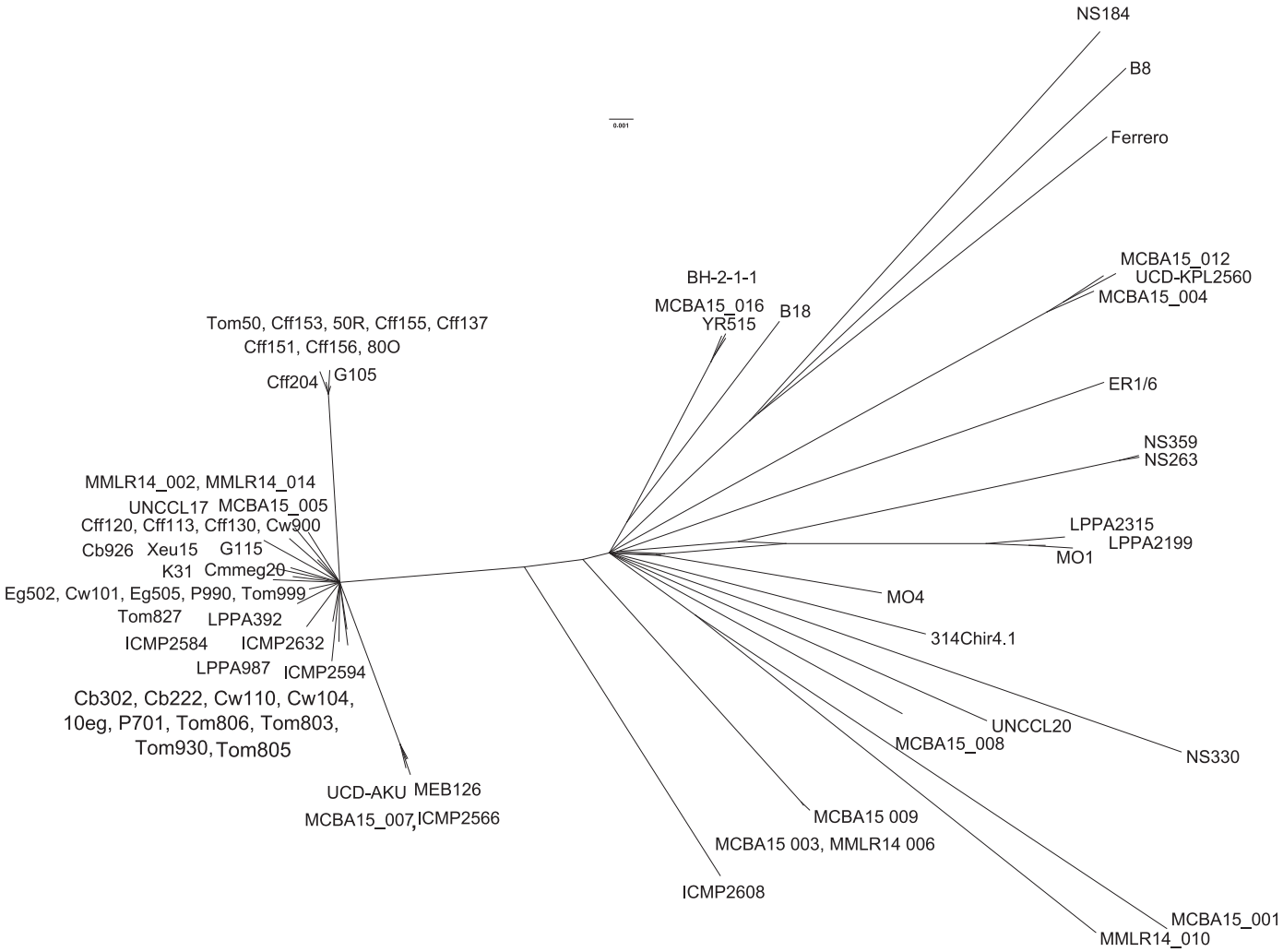

Fig. 3. Splits decomposition network generated from the concatenated sequences of *atpD*, *gyrB*, *ppk*, *recA*, and *rpoB* genes of *Curtobacterium flaccumfaciens* and *Curtobacterium*-like strains used in this study. All the red/orange-pigmented strains of *C. flaccumfaciens* pv. *flaccumfaciens* were clustered separately from the yellow-pigmented strains, while the type strain of *C. flaccumfaciens* pv. *poinsettiae* (ICMP 2566) was clustered within the cosmopolitan strains. Interestingly, the type strain of *C. flaccumfaciens* pv. *ilicis* (ICMP 2608) was clustered far from the core population of *C. flaccumfaciens* similar to that observed in multilocus sequence analysis scheme (Fig. 2).

nonpathogenic strains of *Clavibacter michiganensis* were reported to be isolated frequently from tomato seeds (Yasuhara-Bell and Alvarez 2015). Multiphasic studies, including pathogenicity tests, MLSA, and plasmid profiling, revealed that these strains form a separate phylogenetic group and thus could be considered as new subspecies namely *Clavibacter michiganensis* subsp. *californiensis* and *Clavibacter michiganensis* subsp. *chilensis* (Thapa et al. 2017; Yasuhara-Bell and Alvarez 2015). However, nonpathogenic strains of *C. flaccumfaciens* did not form a separate phylogenetic group and were scattered either within the core population of *C. flaccumfaciens* pv. *flaccumfaciens* or within the other pathovars of the species.

TABLE 6. Test of recombination among *Curtobacterium flaccumfaciens* and *Curtobacterium*-like strains using RDP4 with a Bonferroni test at a probability of 0.05

	Curtobacterium sp.		*C. flaccumfaciens*	
Test	Unique events	Recombination signals	Unique events	Recombination signals
RDP	4	4	1	1
GENECONV	4	4	1	1
BootScan	6	6	2	2
MaxChi	8	8	1	1
Chimaera	6	8	1	1
SiScan	9	11	2	2
3Seq	4	4	3	3
Total	14	44	4	11

We have demonstrated that unlike the nonpathogenic strains (i.e., Cmmeg20, G105, Tom827, Xeu15, and Mo04), the *C. flaccumfaciens* pv. *flaccumfaciens* strains which were pathogenic on common bean were resistant to arsenic compounds. The association between arsenic resistance and pathogenicity on common bean remains to be elucidated, although this could be due to the adaptation of *C. flaccumfaciens* pv. *flaccumfaciens* on bean plants. Indeed, common bean is an arsenic-accumulating plant (Carbonell-Barrachina et al. 1997; Stoeva et al. 2005). More specifically, *C. flaccumfaciens* pv. *flaccumfaciens* strains from Iran showed a higher resistance to arsenic compared to the type strain, which was originally isolated in Hungary. A high arsenic content was observed in surface and ground waters in several Iranian provinces, which might have favored the adaptation of the pathogen to this compound (Keshavarzi et al. 2011). However, no correlation was found between arsenic resistance and the MLSA data. Further analysis is needed to determine the effect of arsenic on the relationships of *C. flaccumfaciens* pv. *flaccumfaciens* and its hosts, as recently studied for the legume–rhizobia interaction (Lafuente et al. 2015).

In the original description of *C. flaccumfaciens* pathovars, it has been noticed that *C. flaccumfaciens* pv. *betae*, *C. flaccumfaciens* pv. *flaccumfaciens*, *C. flaccumfaciens* pv. *oortii*, and *C. flaccumfaciens*

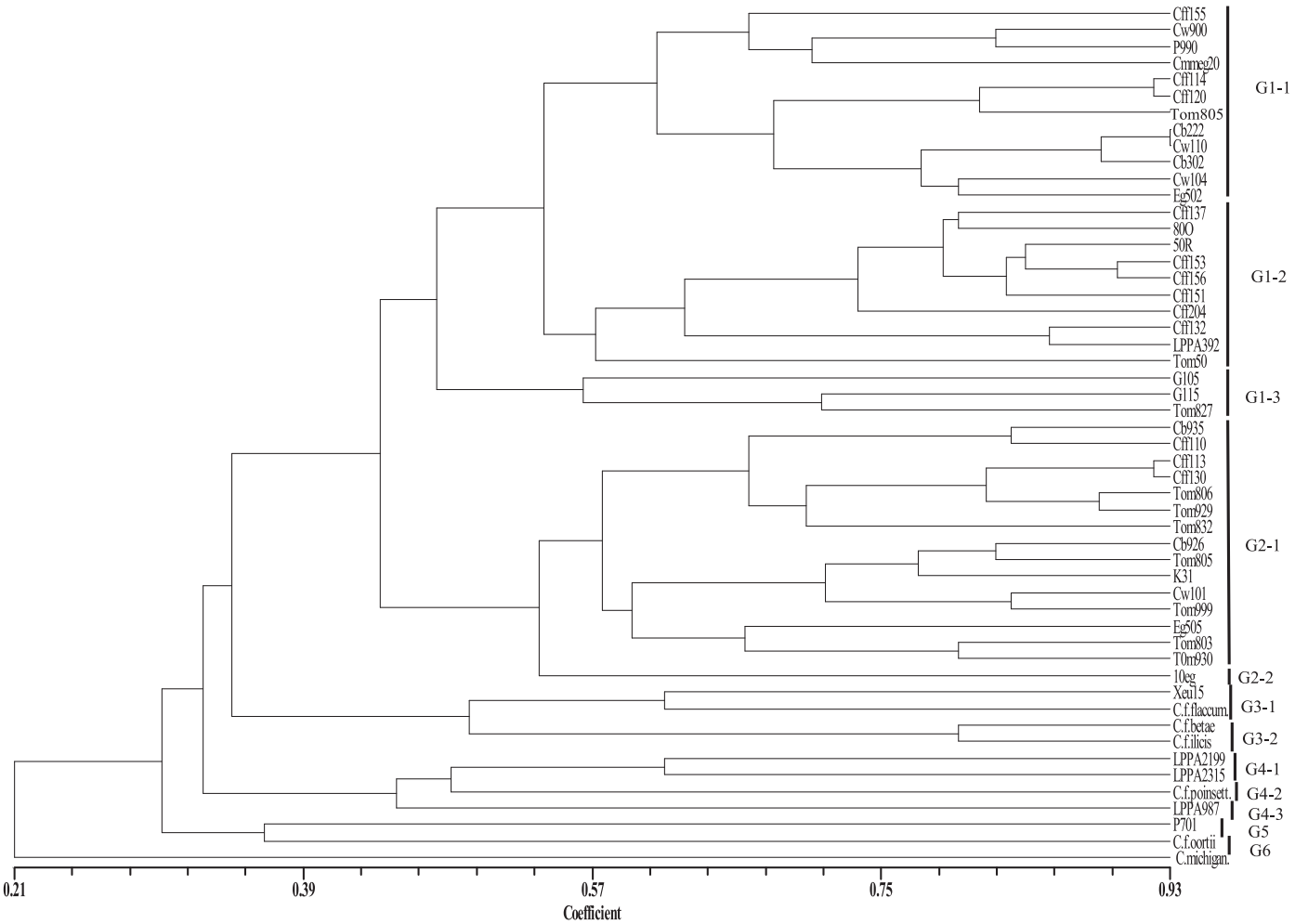

Fig. 4. Dendrogram generated from BOX-PCR fingerprints of *Curtobacterium flaccumfaciens* strains used in this study. Cluster analysis was performed using the simple matching similarity coefficient and unweighted pair group with arithmetic averages using NTSYS-pc software version 2.02e. The scale bar indicates levels of linkage between patterns. Cluster analysis using a cutoff level at 44% similarity produced six clusters (named G1 to G6)—two of them major (G1 = 25 and G2 = 16 strains) and four were minor (one to four strains) clusters. Red/orange-pigmented strains of *C. flaccumfaciens* were distinguished from the yellow-pigmented strains.

pv. *poinsettiae* are closely related to each other in terms of biochemical and physiological characteristics, and differences in host specificity and bacteriocin production are insufficient to justify differentiation at the subspecies level (Collins and Jones 1983; Dye and Kemp 1977). MLSA results from this study revealed that these four pathovars belong to the same species with 97.31 to 99.09% similarity in five housekeeping genes sequences (Table 5). However, *C. flaccumfaciens* pv. *ilicis* is distinct from the core population of *C. flaccumfaciens* pv. *flaccumfaciens* (Fig. 2). By contrast, it has been shown that phylogenetic distance between the yellow-pigmented strains of *C. flaccumfaciens* pv. *flaccumfaciens* and the red/orange-pigmented strains is higher than that of the distances among the type strains of *C. flaccumfaciens* pv. *betae*, *C. flaccumfaciens* pv. *flaccumfaciens*, and *C. flaccumfaciens* pv. *oortii* (Fig. 2; Table 5), all included in the cluster of yellow-pigmented *C. flaccumfaciens* pv. *flaccumfaciens* strains (Fig. 2; Table 5). Altogether, these results suggest that the taxonomy of *C. flaccumfaciens* should be reexamined using a large collection of strains from all the five pathovars of the species. Unlike to the other plant pathogenic corynebacteria, no molecular high throughput method to date has been used to confirm the classical taxonomy of *C. flaccumfaciens* proposed in late 1970s (Collins and Jones 1983; Dye and Kemp 1977). Recently, whole genome sequence analysis based on average nucleotide identity (ANI), digital DNA-DNA hybridization, and MLSA of seven housekeeping genes supported the concept of raising many *Clavibacter michiganensis* subspecies to five new species/combination level (Li et al. 2017). A similar approach has been started for the members of *C. flaccumfaciens* using the complete genome sequencing of type /pathotype strains of the species (Osdaghi et al. 2017b, 2018a).

In conclusion, the results obtained in this study provide several new findings, including the phylogenetic relationships between the two different lineages (i.e., yellow-pigmented strains versus red/orange-pigmented strains) of the bean pathogen *C. flaccumfaciens* pv. *flaccumfaciens*, as well as the remaining four pathovars of *C. flaccumfaciens*. Results of MLSA and phenotypic features (i.e., colony color) are in congruence among *C. flaccumfaciens* strains, although further detailed and multiphasic evaluations are needed to determine if the different colony variants of *C. flaccumfaciens* pv. *flaccumfaciens* could be reclassified as different subspecies/pathovars of the species. We also found a distinctive phenotypic feature (arsenic resistance) which is capable to discriminating pathogenic strains of *C. flaccumfaciens* from nonpathogenic strains. However, a comprehensive multiphased study using a collection of worldwide isolates should illustrate the phylogenetic history and intraspecies relationships of *C. flaccumfaciens* strains.

ACKNOWLEDGMENTS

Pure DNA of the strains isolated in Spain were provided by A. J. González (Cultivos Hortofrutícolas y Forestales, SERIDA, Villaviciosa, Asturias, Spain). We thank J. Ram Lamichhane (UMR AGIR, INRA, Castanet-Tolosan, France) for critical reading of the first draft of the manuscript. E. Osdaghi thanks DISPAA, University of Florence, for financial support during his sabbatical stay in Italy.

LITERATURE CITED

Agarkova, I. V., Lambrecht, P. A., Vidaver, A. K., and Harveson, R. M. 2012. Genetic diversity among *Curtobacterium flaccumfaciens* pv. *flaccumfaciens* populations in the American High Plains. Can. J. Microbiol. 58:788-801.

Almeida, N. F., Yan, S., Cai, R., Clarke, C. R., Morris, C. E., Schaad, N. W., Schuenzel, E. L., Lacy, G. H., Sun, X., and Jones, J. B. 2010. PAMDB, a multilocus sequence typing and analysis database and website for plant-associated microbes. Phytopathology 100:208-215.

Carbonell-Barrachina, A. A., Burlò, J. F., Mataix, J., Burgos-Hernkdez, A., Lopez, E., and Mataix, J. 1997. The influence of arsenite concentration on arsenic accumulation in tomato and bean plants. Sci. Hortic. (Amsterdam) 71:167-176.

Chase, A. B., Arevalo, P., Polz, M. F., Berlemont, R., and Martiny, J. B. H. 2016. Evidence for ecological flexibility in the cosmopolitan genus *Curtobacterium*. Front. Microbiol. 7:1874.

Collins, M. D., and Jones, D. 1983. Reclassification of *Corynebacterium flaccumfaciens, Corynebacterium betae*, *Corynebacterium oortii* and *Corynebacterium poinsettiae* in the genus *Curtobacterium*, as *Curtobacterium flaccumfaciens* comb. nov. J. Gen. Microbiol. 129:3545-3548.

Dye, D. W., and Kemp, W. J. 1977. A taxonomic study of plant pathogenic *Corynebacterium* species. N.Z. J. Agric. Res. 20:563-582.

EPPO. 2011. *Curtobacterium flaccumfaciens pv. flaccumfaciens*. Bull. OEPP/EPPO Bull. 41:320-328.

Francis, M. J., Doherty, R. R., Patel, M., Hamblin, J. F., Ojaimi, S., and Korman, T. M. 2011. *Curtobacterium flaccumfaciens* septic arthritis following puncture with a Coxspur Hawthorn thorn. J. Clin. Microbiol. 49:2759-2760.

Gartemann, K. H., Abt, B., Beke, T., Burger, A., Engemann, J., Flugel, M., Gaigalat, L., Goesmann, A., Grafen, I., Kalinowski, J., Kaup, O., Kirchner, O., Krause, L., Linke, B., McHardy, A., Meyer, F., Pohle, S., Ruckert, C., Schneiker, S., Zellermann, E., Puhler, A., Eichenlaub, R., Kaiser, O., and Bartels, D. 2008. The genome sequence of the tomato-pathogenic actinomycete *Clavibacter michiganensis* subsp. *michiganensis* NCPPB382 reveals a large island involved in pathogenicity. J. Bacteriol. 190:2138-2149.

Gonçalves, R. M., Schipanski, C. A., Koguishi, L., Soman, J. M., Sakate, R. K., Silva Júnior, T. A. F., and Maringoni, A. C. 2017. Alternative hosts of *Curtobacterium flaccumfaciens* pv. *flaccumfaciens*, causal agent of bean bacterial wilt. Eur. J. Plant Pathol. 148:357-365.

González, A. J., Tello J. C., Rodicio, M. R., 2005. Bacterial wilt of beans (*Phaseolus vulgaris*) caused by *Curtobacterium flaccumfaciens* in South-eastern Spain. Plant Dis. 89:1361.

Hall, B. G. 2011. Phylogenetic Trees Made Easy, a How To Manual. 4th ed., Sinauer Associate Inc., Sunderland, MA.

Hammer, Ø., Harper, D. A. T., and Ryan, P. D. 2001. PAST: Paleontological statistics software package for education and data analysis. Palaeontol. Electronica 4:1-9.

Harveson, R. M., Schwartz, H. F., Urrea, C. A., and Yonts, C. D. 2015. Bacterial wilt of dry-edible beans in the Central High Plains of the U.S.: Past, present, and future. Plant Dis. 99:1665-1677.

Hendrick, C. A., Haskins, W. P., and Vidaver, A. K. 1984. Conjugative plasmid in *Corynebacterium flaccumfaciens* subsp. *oortii* that confers resistance to arsenite, arsenate, and antimony(III). Appl. Environ. Microbiol. 48:56-60.

Huang, H. C., Erickson, R. S., Balasubramanian, P. M., Hsieh, T. F., and Conner, R. L. 2009. Resurgence of bacterial wilt of common bean in North America. Can. J. Plant Pathol. 31:290-300.

Huson, D. H., and Bryant, D. 2006. Application of phylogenetic networks in evolutionary studies. Mol. Biol. Evol. 23:254-267.

Jacques, M. A., Durand, K., Orgeur, G., Balidas, S., Fricot, C., Bonneau, S., Quillévéré, A., Audusseau, C., Olivier, V., Grimault, V., and Mathis, R. 2012. Phylogenetic analysis and polyphasic characterization of *Clavibacter michiganensis* strains isolated from tomato seeds reveal that non-pathogenic strains are distinct from *C. michiganensis* subsp. *michiganensis*. Appl. Environ. Microbiol. 78:8388-8402.

Keshavarzi, B., Moore, F., Mosaferi, M., and Rahmani, F. 2011. The source of natural arsenic contamination in groundwater, west of Iran. Water Qual. Expo. Health 3:135-147.

Klaenhammer, T. R. 1984. A general method for plasmid isolation in lactobacilli. Curr. Microbiol. 10:23-28.

Lafuente, A., Pérez-Palacios, P., Doukkali, B., Molina-Sánchez, M. D., Jiménez-Zurdo, J. I., Caviedes, M. A., Rodríguez-Llorente, I. D., and Pajuelo, E. 2015. Unraveling the effect of arsenic on the model Medicago–Ensifer interaction: A transcriptomic meta-analysis. New Phytol. 205:255-272.

Larkin, M. A., Blackshields, G., Brown, N. P., Chenna, R., McGettigan, P. A., McWilliam, H., Valentin, F., Wallace, I. M., Wilm, A., Lopez, R., Thompson, J. D., Gibson, T. J., and Higgins, D. G. 2007. ClustalW and ClustalX version 2. Bioinformatics 23:2947-2948.

Li, X., Tambong, J., Yuan, K., Chen, W., Xu, H., Lévesque, C. A., and De Boer, S. H. 2017. Re-classification of *Clavibacter michiganensis* subspecies on the basis of whole-genome and multi-locus sequence analyses. Int. J. Syst. Evol. Microbiol. 68:234-240.

Librado, P., and Rozas, J. 2009. DnaSP v5: a software for comprehensive analysis of DNA polymorphism data. Bioinformatics 25:1451-1452.

Mariita, R. M., Bhatnagar, S., Hanselmann, K., Hossain, M. J., Korlach, J., Boitano, M., Roberts, R. J., Liles, M. R., Moss, A. G., Leadbetter, J. R., Newman, D. K., and Dawson, S. C. 2015. Complete genome sequence of *Curtobacterium* sp. strain MR_MD2014, isolated from topsoil in Woods Hole, Massachusetts. Genome Announc. 3:e01504-e01515.

Martin, D. P., Murrell, B., Golden, M., Khoosal, A., and Muhire, B. 2015. RDP4: Detection and analysis of recombination patterns in virus genomes. Virus Evol. 1:vev003.

Meletzus, D., Bermphol, A., Dreier, J., and Eichenlaub, R. 1993. Evidence for plasmid-encoded virulence factors in the phytopathogenic bacterium *Clavibacter michiganensis* subsp. *michiganensis* NCPPB382. J. Bacteriol. 175:2131-2136.

Osdaghi, E., Ansari, M., Taghavi, S. M., Zarei, S., Koebnik, R., and Lamichhane, J. R. 2018b. Pathogenicity and phylogenetic analysis of *Clavibacter michiganensis* strains associated with tomato plants in Iran. Plant Pathol. 67:957-970.

Osdaghi, E., Forero Serna, N., Bolot, S., Fischer-Le Saux, M., Jacques, M.-A., Portier, P., Carrère, S., and Koebnik, R. 2017b. High-quality draft genome sequence of *Curtobacterium* sp. strain Ferrero. Genome Announc. 5: e01378-e17.

Osdaghi, E., and Lak, M. R. 2015. Occurrence of a new orange variant of *Curtobacterium flaccumfaciens* pv. *flaccumfaciens*, causing common bean wilt in Iran. J. Phytopathol. 163:867-871.

Osdaghi, E., Pakdaman Sardrood, B., Bavi, M., Akbari Oghaz, N., Kimiaei, S., and Hadian, S. 2015a. First report of *Curtobacterium flaccumfaciens* pv. *flaccumfaciens* causing cowpea bacterial wilt in Iran. J. Phytopathol. 163: 653-656.

Osdaghi, E., Taghavi, S. M., Fazliarab, A., Elahifard, E., and Lamichhane, J. R. 2015b. Characterization, geographic distribution and host range of *Curtobacterium flaccumfaciens*: An emerging bacterial pathogen in Iran. Crop Prot. 78:185-192.

Osdaghi, E., Taghavi, S. M., Hamzehzarghani, H., Fazliarab, A., Harveson, R. M., and Lamichhane, J. R. 2016a. Occurrence and characterization of a new red-pigmented variant of *Curtobacterium flaccumfaciens*, the causal agent of bacterial wilt of edible dry beans in Iran. Eur. J. Plant Pathol. 146: 129-145.

Osdaghi, E., Taghavi, S. M., Hamzehzarghani, H., Fazliarab, A., Harveson, R. M., Tegli, S., and Lamichhane, J. R. 2018a. Epiphytic *Curtobacterium flaccumfaciens* strains isolated from symptomless solanaceous vegetables are pathogenic on leguminous but not on solanaceous plants. Plant Pathol. 67: 388-398.

Osdaghi, E., Taghavi, S. M., Hamzehzarghani, H., Fazliarab, A., and Lamichhane, J. R. 2017a. Monitoring the occurrence of tomato bacterial spot and range of the causal agent *Xanthomonas perforans* in Iran. Plant Pathol. 66:990-1002.

Osdaghi, E., Taghavi, S. M., Hamzehzarghani, H., and Lamichhane, J. R. 2016b. Occurrence and characterization of the bacterial spot pathogen *Xanthomonas euvesicatoria* on pepper in Iran. J. Phytopathol. 164:722-734.

Raupach, G. S., and Kloepper, J. W. 2000. Biocontrol of cucumber diseases in the field by plant-growth promoting rhizobacteria with and without methyl bromide fumigation. Plant Dis. 84:1073-1075.

Richert, K., Brambilla, E., and Stackebrandt, E. 2005. Development of PCR primers specific for the amplification and direct sequencing of *gyrB* genes from microbacteria, order Actinomycetales. J. Microbiol. Methods 60: 115-123.

Richert, K., Brambilla, E., and Stackebrandt, E. 2007. The phylogenetic significance of peptidoglycan types: Molecular analysis of the genera *Microbacterium* and *Aureobacterium* based upon sequence comparison of *gyrB, rpoB, recA* and *ppk* and 16SrRNA genes. Syst. Appl. Microbiol. 30: 102-108.

Rohlf, F. J. 2008. NTSYSpc: Numerical Taxonomy System, ver. 2.20. Exeter Publishing, Ltd., Setauket, NY.

Smith, N. C., Hennessy, J., and Stead, D. E. 2001. Repetitive sequence-derived PCR profiling using the BOX-A1R primer for rapid identification of the plant pathogen *Clavibacter michiganensis* subspecies *sepedonicus*. Eur. J. Plant Pathol. 107:739-748.

Soares, R. M., Fantinato, G. G. P., Darben, L. M., Marcelino-Guimarães, F. C., Seixas, C. D. S., and Carneiro, G. E. S. 2013. First report of *Curtobacterium flaccumfaciens* pv. *flaccumfaciens* on soybean in Brazil. Trop. Plant Pathol. 38:452-454.

Stoeva, N., Berova, M., and Zlatev, Z. 2005. Effect of arsenic on some physiological parameters in bean plants. Biol. Plant. 49:293-296.

Tamura, K., Stecher, G., Peterson, D., Filipski, A., and Kumar, S. 2013. MEGA6: Molecular evolutionary genetics analysis version 6.0. Mol. Biol. Evol. 30:2725-2729.

Tegli, S., Sereni, A., and Surico, G. 2002. PCR-based assay for the detection of *Curtobacterium flaccumfaciens* pv. *flaccumfaciens* in bean seeds. Lett. Appl. Microbiol. 35:331-337.

Thapa, S. P., Pattathil, S., Hahn, M. G., Jacques, M.-A., Gilbertson, R. L., and Coaker, G. 2017. Genomic analysis of *Clavibacter michiganensis* reveals insight into virulence strategies and genetic diversity of a gram-positive bacterial pathogen. Mol. Plant-Microbe Interact. 30:786-802.

Versalovic, J., Schneider, M., de Bruijn, F. J., and Lupski, J. R. 1994. Genomic fingerprinting of bacteria using repetitive sequence-based polymerase chain reaction. Methods Mol. Cell. Biol. 5:25-40.

Yasuhara-Bell, J., and Alvarez, A. M. 2015. Seed-associated subspecies of the genus *Clavibacter* are clearly distinguishable from *Clavibacter michiganensis* subsp. *michiganensis*. Int. J. Syst. Evol. Microbiol. 65: 811-826.

Young, J. M., Watson, D. R. W., and Dye, D. W. 2004. Reconsideration of *Arthrobacter ilicis* (Mandel et al. 1961) Collins et al. 1982 as a plant-pathogenic species. Proposal to emend the authority and description of the species. Request for an opinion. Int. J. Syst. Evol. Microbiol. 54: 303-305.

Chapter 4

A MATE transporter involved in pathogenicity and IAA homeostasis in the hyperplastic plant pathogen *Pseudomonas savastanoi* pv. *nerii*

microorganisms

MDPI

Article

A MATE transporter is involved in pathogenicity and IAA homeostasis in the hyperplastic plant pathogen *Pseudomonas savastanoi* pv. *nerii*

Stefania Tegli[1,*], Lorenzo Bini[1], Silvia Calamai[1], Matteo Cerboneschi[2] and Carola Biancalani[1]

[1] Dipartimento di Scienze e Tecnologie Agrarie, Alimentari Ambientali e Forestali, Laboratorio di Patologia Vegetale Molecolare, Università degli Studi di Firenze, Via della Lastruccia 10, 50019 Sesto Fiorentino (Firenze), Italy

[2] Next Genomics srl, Via Madonna del Piano, 6, 50019 Sesto Fiorentino (Firenze), Italy

*Correspondence: stefania.tegli@unifi.it; Tel.: +39 0554573427

Received: date; Accepted: date; Published: date

Abstract:

During the last years, many evidences has been accumulating about the phytohormone indole-3-acetic acid (IAA) as a multifaceted compund also in the microbial world, with IAA playing a role as a bacterial intra- and inter-cellular signaling molecule, or as an effector during pathogenic or beneficial plant-bacteria interactions. However, pretty much nothing is known on the mechanisms that bacteria use to modulate IAA homeostasis, in particular on IAA active transport systems. Here, by an approach combining *in silico* 3D structural modeling and docking, mutagenesis, quantitative gene expression analysis and HPLC FLD auxin quantitative detection, for the first time a bacterial Multidrug And Toxic compound Extrusion (MATE) transporter was demonstrated to be involved in the efflux of IAA, as well as of its conjugate IAA-Lysine, in the plant pathogenic hyperplastic bacterium *Pseudomonas savastanoi* pv. *nerii* strain *Psn23*. Furthermore, accordingly to the role proved to be played by *Psn23* MATE in the development of plant disease, and to the presence of *Psn23* MATE homologs in all the genomospecies of the *P. syringae* complex, this membrane transporter could likely represent a promising target for the design of novel and selective anti-infective molecules for plant disease control.

Keywords: *Pseudomonas savastanoi*; IAA; IAA-Lysine; Multidrug And Toxic compound Extrusion transporter; MATE; TTSS

1. Introduction

Auxin are plant hormones whose correct homeostasis is pivotal for proper plant growth and development, as well as for plant defense [1]. Indole-3-acetic acid (IAA) is the main and most abundant naturally occurring auxin in plants, as well as the best studied, whose *de novo* biosynthesis is mainly through four interlinked pathways having L-tryptophan (Trp) as a precursor. Generally, the Trp-dependent pathways are two-step reactions, named accordingly to their specific key intermediate molecule, specifically indole-3-pyruvic acid (IPyA), indole-3-acetamide (IAM), tryptamine (TAM), or indole-3-acetaldoxime (IAOX). Less information is definitely available for Trp-independent IAA biosynthesis, where indole-3-glycerol phosphate or indole are considered the main precursors. The IPyA and IAM pathways are considered the most conserved and used routes for IAA biosynthesis in plants. However, many other important aspects still remain to be fully elucidated,

such as which pathways are used in the different plant species and if they are likely to play alternative roles [2, 3].

Firstly discovered in human urine and structurally similar to melatonin in animals [4], in addition to plants IAA is also produced by microalgae, archaea, bacteria, fungi, and yeasts [5]. Although the ability to synthesise IAA in bacteria and fungi is not restricted to those associated to plants, the role of microbial IAA in the interactions between plants and phytopathogenic or beneficial bacteria and fungi is the most studied [6].

Microbial IAA biosynthesis is strictly Trp-dependent, according to at least five different routes, including the IPyA and TAM pathways, as well as the tryptophan side-chain oxidase (TSO) pathway [7, 8]. In gall- and tumor-forming bacteria and fungi, IAA has been shown pivotal for the development of hyperplastic symptoms, and its biosynthesis is generally through the IAM pathway. Conversely, the IPyA pathway is mainly represented in beneficial bacteria and fungi. Interestingly, the hyperplastic plant pathogenic bacterium *Pantoea agglomerans* has both the IPyA and IAM pathways, that are mainly expressed during plant colonization and the pathogenetic process, respectively [9, 10].

Phylogenetic analysis carried out on key genes for IAA biosynthesis in organisms and microorganisms indicate that an independent but convergent evolution was occurred [5]. This finding strongly suggests a universal role of IAA as a signal molecule, both for the producers and during their biotic interactions at different taxonomic levels (*e.g.* intra- and interspecies and even inter-kingdom) [11]. Plant pathogens have been demonstrated to produce IAA to hijack plant immunity, by subverting plant auxin signaling to increase host susceptibility to infection [6, 12-14]. In addition, microbial IAA is also essential as signal molecules within the producer populations, and in plant pathogenic bacteria IAA was demonstrated to affect the expression of genes of their virulence network [7, 15-17].

However, the multiple effects triggered or dynamically modulated by IAA do not exclusively depend on its *de novo* biosynthesis. In plants, significant and coordinated changes occur during the time for local IAA content, as well as for its bioactive forms, also as a consequence of the IAA active polar transport throughout the whole plant and of other processes, such as its catabolism, conjugation, oxidation, storage, and even its signal transduction [18]. A similar fine and dynamic control of IAA homeostasis seems to occur also in bacteria, such as clearly demonstrated for the hyperplastic plant pathogen *Pseudomonas savastanoi* pv. *nerii*. Its ability to cause 'knots' on its hosts relies on a functional Type Three Secretion System (TTSS) as well as on the bacterial IAA biosynthesis by the IAM pathway [19-21]. In addition, during the pathogenetic process, *P. savastanoi* pv. *nerii* regulates free IAA levels in the infected tissues by its conversion to IAA-Lys through the enzyme IAA-Lys synthase, encoded by the *iaaL* gene [17]. Interestingly, most of the *P. syringae* pathovars and strains possess the *iaaL* gene in their genomes, even when not hyperplastic, and this gene appears to be very well conserved and present independently from the genes for IAA biosynthesis [22, 23]. It is worth to point out that the conversion of IAA to IAA-Lys is an exclusive trait of bacteria belonging to the *P. syringae* complex, and plants neither produce IAA-Lys nor are able to degrade it. Overall these findings suggest for the bacterial conversion of IAA to IAA-Lys a widely conserved role in the dynamic regulation of the IAA content at and near the infection site. In this frame, it is thus not surprising that in *P. savastanoi* pv. *nerii* both the expression of the operon for IAA biosynthesis and that of *iaaL* gene are also under the control of TTSS, in addition to be auxin-regulated, to further stress the involvement of bacterial IAA and IAA-Lys in the plant-pathogen dialogue since the very first steps of their interaction [17].

Obviously, if a similar dialogue has to take place, it is reasonable to assume that bacterial IAA, and perhaps also its IAA-Lys conjugate, needs to be transported some way out of the bacterial cell into the apoplast. In the *P. savastanoi* pv. *nerii* strain *Psn23* genome, a gene coding a putative Multidrug and Toxic compound Extrusion (MATE) efflux transporter (hereafter named *matE*) was found upstream to the *iaaL* gene, and whose expression was demonstrated to be TTSS-regulated [17]. MATE transporters are widely distributed in Gram-positive and Gram-negative bacteria, where they are usually associated with the efflux of organic cations for multidrug resistance. Conversely, MATE

pumps found so far in plants have been demonstrated to be involved in the transport of a broader range of substrates than in bacteria, and having many other roles beyond detoxification, including the efflux of plant hormones and the regulation of plant disease resistance to pathogens, respectively [24, 25].

The aim of this study was to analyse the structure of putative MATE transporter in *Psn23* through the application of bioinformatics tools and, to evaluate the role played by *Psn23* MATE in the development of plant disease and its relationship with the IAA efflux and homeostasis.

2. Materials and Methods

2.1. Bacterial strains and growth conditions

The bacterial strains used in this study are listed in Table S1. *Pseudomonas savastanoi* pv. *nerii* strain *Psn23* and its mutants were routinely grown at 26°C on King's B (KB) [26] or *hrp*-inducing Minimal Medium (MM) [27], while *Escherichia coli* strains TOP10 and ER2925 were grown on Luria-Bertani (LB) [28], as liquid or agarized cultures. Bacterial growth in liquid media was monitored by measuring optical density (OD) at 600 nm (OD_{600}) with a spectrophotometer (Infinite® M200 PRO Multimode Reader, Tecan Group Ltd., Männedorf, Switzerland), while the concentration of viable bacteria was evaluated by plate counts and expressed as Colony Forming Units per milliliter (CFU/ml). For long term storage, bacteria were maintained at -80°C on 40% (v/v) glycerol, and *P. savastanoi* cultures were periodically monitored by using specific PCR-based assays to exclude any bacterial contamination [29, 30]. Antibiotics were added to growth medium if needed, and used at the following final concentrations: 20 μg/ml streptomycin, 50 μg/ml nitrofurantoin, 10 μg/ml gentamicin, and 50 μg/ml kanamycin.

2.2. Molecular techniques

Unless otherwise stated, routine DNA manipulations and PCR were carried out using standard procedures [31] or according to manufacturers' instructions. The plasmids used in this study are reported in Table S1. Genomic DNA from *P. savastanoi* strains was extracted from single bacterial colonies using thermal lysis [29], or from bacterial cultures (OD_{600}=0.8), using Puregene® Genomic DNA Purification Kit (QIAGEN, Hilden, Germany). DNA concentration was evaluated both spectrophotometrically with NanoDrop™ ND-1000 (NanoDrop Technologies Inc., DE, USA), and visually by standard agarose gel electrophoresis on 1% agarose (w/v) in TBE 1X [31]. For plasmid DNA extraction, NucleoSpin® Plasmid (Macherey-Nagel GmbH & Co. KG, Düren, Germany) was used according to the manufacturer's protocol. Amplicons were purified from agarose gel using NucleoSpin® Gel and PCR clean-up (Macherey-Nagel GmbH & Co. KG), and then double-strand sequenced at Eurofins Genomics (Ebersberg, Germany). Primers were designed using Beacon Designer 7.7 software (Premier Biosoft International, Palo Alto, CA, USA), and their sequences and features are reported in Table S2.

2.3. Construction of Psn23 *mutants for* matE *gene*

Five mutants were here produced from the wild type strain *Psn23* for the *matE* gene. The primers were designed according to the *matE* nucleotidic sequence of *Psn23* strain (GenBank Accession Number KU351686), and here used to generate and analyze the mutants listed in Table S2. The suicide vector for *P. syringae sensu lato* pK18-*ΔhrpA* [17, 32] was used to clone the mutated *matE* constructs into *E. coli* cells, and then for their transfer into electrocompetent *Psn23* cells by using Gene Pulser XCell™ (Bio-Rad Laboratories Inc., Hercules, CA, USA) to replace the native *matE* gene by marker exchange [17]. A preliminary PCR screening of the putative *matE* mutants was carried out on transformed *Psn23* Suc^R/Kan^S colonies, and then the marked mutations were confirmed by DNA sequencing. A stable knockout Δ*matE* mutant was constructed by an in-frame deletion of *matE* gene from the *Psn23* genome. Three alanine-substituted mutants for the putative *Psn23* MATE were also generated. The *matE* gene from *Psn23* was cloned into the *PstI* and *EcoRI* sites of pK18-*ΔhrpA* to

produce the pK18-*matE* recombinant vector (Table S1). On this plasmid, the alanine substitutions D182A, Y200A and T17035A were introduced into *matE* by using mutagenic PCR primers and QuikChange II Site-Directed Mutagenesis Kit (Agilent Technologies, La Jolla, CA, USA). The over-expressing mutant *Psn23*_pT3-*matE* was also constructed. The recombinant plasmid pT3-*matE* (Table S1) was produced starting from the vector pLPVM-T3A, which contains the native promoter of *hrpA* gene for *Psn23* [33]. The *matE* gene, amplified from pK18-*matE* using the primers pT3_matE_BamHI_For/pT3_matE_KpnI_Rev, was cloned into the *KpnI* and *BamHI* restriction sites of pLPVM-T3A and then electroporated into *Psn23* cells.

2.4. In planta *phenotypic characterization of* Psn23 matE *mutants*

Hypersensitive Response (HR) assay was carried out on 2 months old *Nicotiana tabacum* plants (var. Burley White), grown at 24°C and at 75% relative humidity with a photoperiod of 16/8 h of light/dark. Bacterial cultures grown overnight in KB medium at 26°C were wash twice in sterile physiological solution (SPS, 0.85% NaCl in distilled water), and then resuspended to reach an OD_{600}=0.5. Bacteria were then injected into the mesophyll of fully expanded leaves of Tobacco plants, using a 2 ml blunt-end syringe pressed against the abaxial surface (approximately 100 µl/spot) [34]. The appearance of macroscopic symptoms associated to the development of HR was monitored in the next 48 hours post-infiltration, taking photographic records of the results obtained. Pathogenicity trials with *Psn23* and its mutants were carried out on *in vitro* micropropagated oleander plants (var. Hardy Red), grown on Murashige-Skoog medium (MS) [35] without addition of any phytohormone for 3 weeks, at 26°C and with a photoperiod of 16 h/light and 8 h/dark, as described previously [30, 36]. Plants were periodically monitored for symptoms appearance, and the bacterial growth was estimated at 7, 14 and 21 days post inoculation (dpi). Three independent experiments were performed, and three plants for each *P. savastanoi* strain were used in each run.

2.5. Reverse transcription-quantitative PCR (qRT-PCR) and gene expression analysis

Liquid cultures of the wild-type strain *Psn23* and its mutants were grown overnight at 26°C in KB, on an orbital shaker (100 rpm), then washed twice with SPS and transferred into MM medium supplemented with L-Trp (0.25mM) to reach an OD_{600}=0.5. After 24 hours at 26°C and under shaking condition, bacterial cultures were collected and used for RNA extraction, performed with NucleoSpin® RNA Plus (Macherey-Nagel GmbH & Co. KG) and after a treatment with NucleoSpin® gDNA Removal Column (Macherey-Nagel GmbH & Co. KG) to eliminate any genomic DNA. Then, RNA Reverse transcription was carried out on about 5 µg of total RNA per sample, by using iScript™ Advanced cDNA Synthesis kit (Bio-Rad Laboratories Inc.). Diluted cDNA was analyzed with SsoFast™ EvaGreen® Supermix (Bio-Rad Laboratories Inc.), according to manufacturer's protocols, using the CFX96 Real Time PCR Detection System and CFX Manager software v1.6 (Bio-Rad Laboratories Inc.). The specific primers pairs here designed and used are listed in Table S2. The expression of each monitored gene was quantified using the $2^{-\Delta\Delta Ct}$ method and the 16S rRNA gene for normalization. For each sample, three biological replicates were processed in each of the three independent qRT-PCR experiments here carried out.

2.6. Quantification of bacterial IAA synthesis

The amount of IAA produced *in vitro* by the wild type strain *Psn23* and its mutants was assessed both by the colorimetric Salkowski's method [37] and by high-performance liquid chromatography coupled with fluorescence detection (HPLC FD). Bacterial cultures were grown overnight at 26°C in KB on an orbital shaker (100 rpm), then washed twice with SPS and transferred into MM supplemented with L-Trp (0.25mM). At 24 and 48 h post-inoculation, bacterial growth was recorded as OD_{600}. The bacterial cultures were centrifuged in a microcentrifuge at 5,000 rpm for 10 minutes. The supernatants were collected, filter sterilized on 0.2µm pore size membranes (Sarstedt, Nümbrecht, German), and then used as such for IAA determination both by Salkowski's assay and HPLC FD. The residual pellets were then resuspended into the same volume of MM of the original

cultures. The bacterial suspensions thus obtained were boiled at 100°C for ten minutes, then centrifuged and the supernatants filter sterilized as above. The supernatants obtained after bacterial cell lysis were used for IAA quantification by HPLC FD, further diluted 1:100 in 35% MeOH. Standards for IAA, L-Trp and IAM at high purity grade (98%) for analytical applications were purchased from Sigma-Aldrich Co. (St. Louis, MO, USA), while IAA-Lysine was kindly synthesized by Department of Chemistry of the University of Padova, Italy. Standard curves were prepared by five ten-fold dilutions of each molecule, starting from 100 ppm in 35% MeOH. The HPLC analyses were performed on a HP 1100 Series chromatograph (Agilent Technologies, Waldbronn, Germany), equipped with diode array (DAD) and fluorescence (FLD) detectors. Chromatographic separations were carried out using a reverse-phase HPLC column ZORBAX ODS (4.6 mm x 250 mm; 5µm) (Agilent Technologies), whose temperature was set up at 40°C. A 50 µl injection volume and flow rate at 0.9 ml/min were selected. Analytes were separated with an isocratic elution in 35% MeOH. The detection was performed in absorbance at 273 nm and in fluorescence using λ_{ex} 280 nm and λ_{em} 340 nm. The HPLC-DAD/FLD system control, as well as data acquisition and analysis were performed using the ChemStation A.10.01 software (Agilent Technologies).

2.7. Bioinformatic analysis

Multiple sequence alignments and comparisons were performed by using the computer package Clustal Omega (https://www.ebi.ac.uk/Tools/msa/clustalo/) [38], and Basic Local Alignment Search Tool (BLAST) (http://www.ncbi.nlm.nih.gov/blast) [39]. Phylogenetic analyses were carried out using Neighbor-joining statistical method [40] and phylogenetic trees were generated in MEGA, version 7.0.18 [41]. Bootstrap analysis used 500 replications, Poisson model for substitutions and pairwise deletion method for data treatments (gaps). The cut-off value for condensed tree was 90%. According to the putative MATE protein from *Psn23*, 3D structural models were produced by Phyre2 (http://www.sbg.bio.ic.ac.uk/phyre2/html/page.cgi?id=index) [42] and RaptorX (http://raptorx.uchicago.edu/) under default settings [43]. Molecular models visualization was performed using the software USCF Chimera (https://www.cgl.ucsf.edu/chimera/) [44]. The *in silico* prediction of ligand-binding-sites for the interaction with target molecules was made by molecular docking, using the GEMDOCK software (BioXGEM) [45] and AutoDock Vina [46], and the molecular structure of L-Trp, IAM, IAA and IAA-lysine were assembled in digital format using MarvinSketch 17.6 software (ChemAxon) (http://www.chemaxon.com).

2.8. Data collection and statistical analysis

The experiments reported in this study were always carried out in triplicate, and at least three independent experiments were performed. The results are reported as means values ± standard deviation (SD). PAST software version 3.11 was used [47] to perform one-way ANOVA followed by Tukey-Kramer's post-test analysis, and p values ≤ 0.05 were considered to be statistically significant.

3. Results

3.1. In vitro *IAA production by* Psn23 *depends from a functional* matE *gene*

Upstream to the gene *iaaL*, an ORF encoding a putative MATE efflux transporter (GenBank AOR51355) was found near the *iaaM*/*iaaH* operon in *P. savastanoi* pv. *nerii Psn23*, having a TTSS-dependent expression and hypothesised to mediated IAA efflux, in addition to confer resistance to drugs such as 8 hydroxyquinoline [17]. To test this hypothesis, the in-frame deleted mutant *ΔmatE* was produced. As a control, the overexpressing mutant pT3-*matE* also was generated. Here the *matE* gene was under the control of an inducible promoter, that is the promoter driving the expression of *hrpA* in the TTSS of *Psn23*, hereafter named pT3. This promoter is switched on *in vitro* on Minimal Medium (MM), mimicking the apoplast conditions [27]. No significant differences were observed between the *in vitro* growth of *Psn23* and its mutants *ΔmatE* and pT3-*matE*, when incubated at 26°C on MM or on KB, during the first 72 h in shaking condition (100 rpm) (data not shown). Similarly, no

differences were found in the ability the wild type strains *Psn23* and the mutants *ΔmatE* and pT3-*matE* to cause HR after their infiltration into the mesophyll of Tobacco leaves (Figure 1).

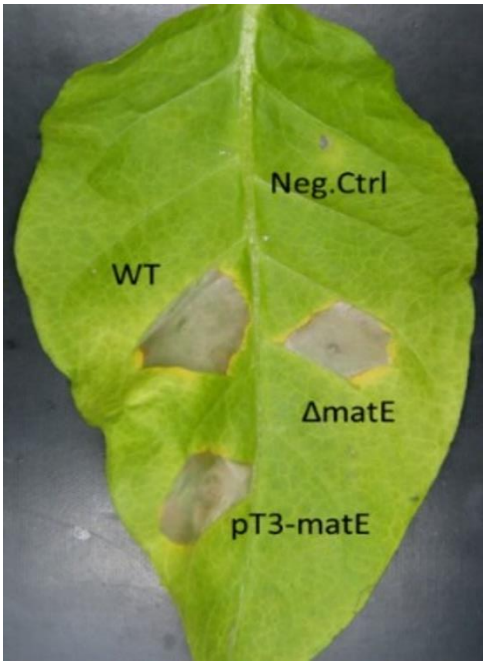

Figure 1. Hypersensitive Response assay on *N. tabacum*. Tobacco leaves were infiltrated with bacterial suspensions of *ΔmatE* and pT3-*matE* mutants. For comparison the wild-type *Psn23* (WT) was also tested. As negative control, sterile physiological solution was used (Neg.Ctrl). Picture was taken 48 h post-infiltration.

Conversely, strongly statistically significant differences were found between *Psn23* and its mutants as far as the *in vitro* production of IAA is concerned. After 24 and 48 h of incubation at 26°C on MM supplemented with Trp, the concentration of IAA in the bacterial free culture supernatants was evaluated by the colorimetric assay based on Salkowski's reagent [17, 48]. As shown in Figure 2, after 24 h the amounts of IAA released into the culture medium by the mutants *ΔmatE* and pT3-*matE* were significantly lower and higher, respectively, than that of the wild type *Psn23*. The exceptionally increased value in IAA production obtained for the mutant pT3-*matE* was then confirmed as statistically significant also after 48 hours.

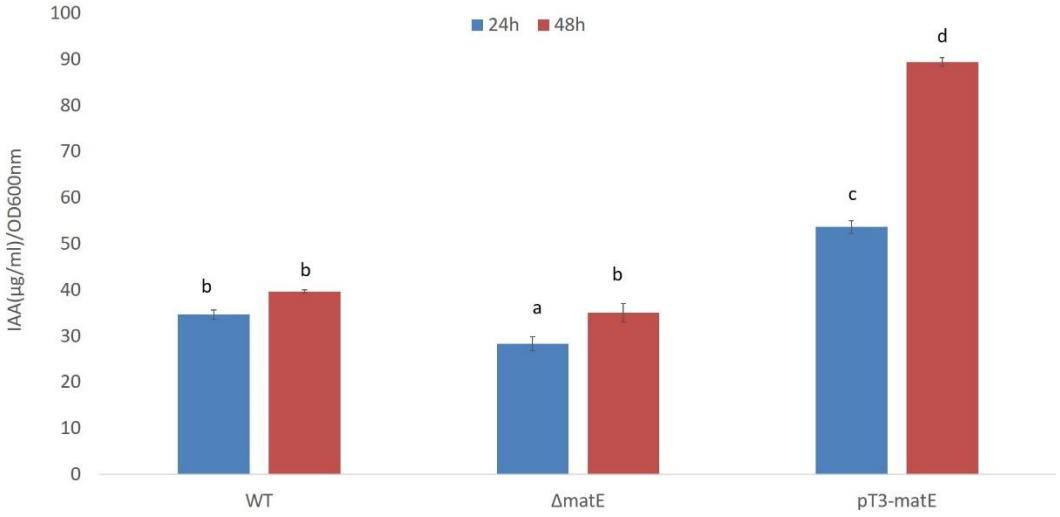

Figure 2. IAA *in vitro* production by *Psn23*, and its *ΔmatE* and pT3-*matE* mutants. Bacteria were grown on MM supplemented with Trp (0.25mM), at 26°C in shaking condition. Salkowski assay was carried out on bacterial supernatants collected after 24 h (blue) and 48 h (red) of growth. The data represent the average of three independent experiments, each with replicates ± standard deviation (SD). Different letters indicate significant differences among means of mutants at $P < 0.05$, according to Tukey's test.

3.2. *Expression of* matE *gene influences expression of genes for IAA production and pathogenicity*

The expression of genes related to IAA biosynthesis (*iaaM* and *iaaH*) and metabolism (*iaaL*), to the activation of the master pathogenicity system TTSS (*hrpRS* and *hrpA*) as well as to the putative MATE transporter here studied (*matE*), was then evaluated by RealTime PCR on *Psn23* and its *matE* mutants, grown on MM supplemented with Trp. The mutants *ΔiaaM* and *ΔiaaL* were also included for comparison. Coherently with the data on *in vitro* IAA production, the expression of *iaaM* and *iaaH* was statistically significantly reduced in the mutant *ΔmatE* in comparison to the wild type *Psn23*, while it was upregulated in the overexpressing mutants pT3-*matE* (Figure 3).

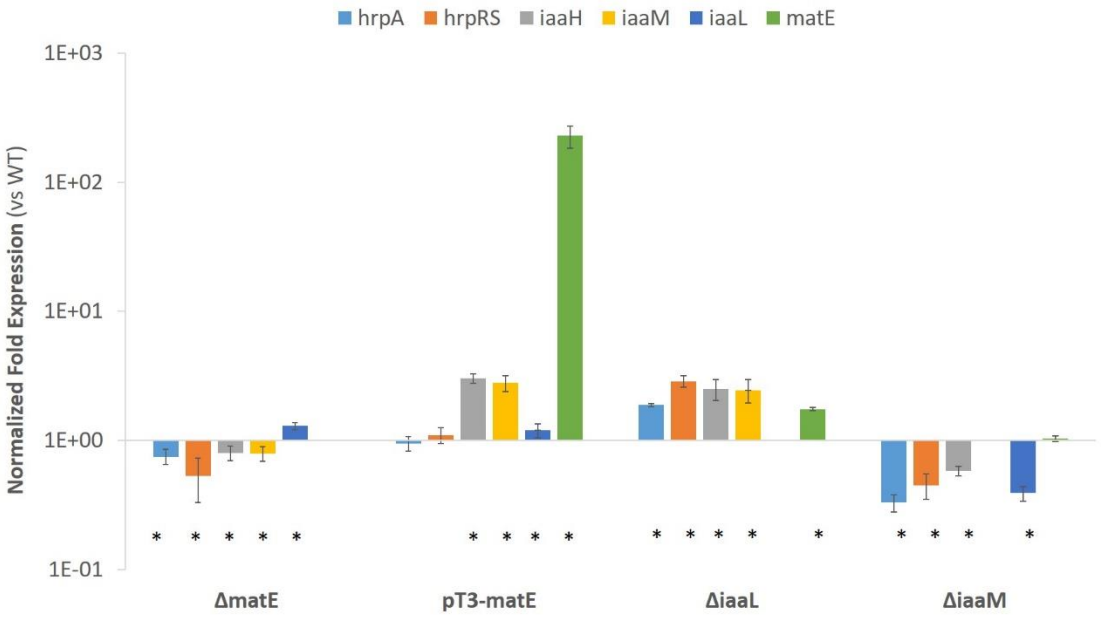

Figure 3. *In vitro* gene expression analysis of the *Psn23* mutants *ΔmatE*, pT3-*matE*, *ΔiaaL* and *ΔiaaM*. Bacteria were grown *in vitro* on MM for 24 h, and their gene expression was compared with that of the wild-type *Psn23*, for the genes *hrpA* (light blue), *hrpRS* (orange), *iaaH* (grey), *iaaM* (yellow), *iaaL* (blue) and *matE* (green). Data are averages of triplicates ± standard deviation (SD). Asterisks indicate significant differences compared with the untreated sample at $p<0.05$.

Interestingly, in the mutant *ΔmatE* also the gene related to the TTSS were downregulated, and just the gene *iaaL* appeared to be overexpressed in comparison to the wild type *Psn23*. The gene expression profile of the *ΔmatE* mutant resulted here quite close to that of *ΔiaaM* mutant, with the exception of the gene *iaaL*.

Similarly to the pT3-*matE* mutant, the genes for IAA biosynthesis and *matE* were statistically significantly overexpressed in the *ΔiaaL* mutant. Overall these findings strongly suggest the involvement of the putative *Psn23* membrane protein encoded by *matE* also in bacterial IAA homeostasis, in particular to mediate IAA efflux.

3.3. *Virtual 3D modelling of* Psn23 *MATE and prediction of IAA and IAA-Lys as putative substrates*

Concerning microbial IAA, up to know just the fungal MATE transporter Mte1 of *Tricholoma vaccinum* has been demonstrated to have a role in IAA efflux, by an indirect approach based on the

use of the IAA transport inhibitor 2,3,5-triiodobenzoic acid (TIBA) [49]. Unfortunately, the crystal structure of Mte1 is not available yet, to perform the most appropriate structure-activity studies to unequivocally demonstrate its involvement in IAA active transport. Conversely, the crystal structures of some bacterial MATE transporters are already available, and all of them are membrane proteins characterized by the presence of twelve transmembrane helices (TM 1-12), forming an internal cavity. In this pocket, several quite specific and conserved residues provide the binding sites for the substrates and for those ions (H^+ or Na^+), whose gradient across the membrane serves as energy source [50]. As shown in Figure 4, also the putative *Psn23* MATE transporter consists of twelve TMs arranged as two bundles (TM 1-6 and TM 7-12), one at the N- and the other at the C-terminal domain, forming the above mentioned pocket with a typical V-shaped conformation.

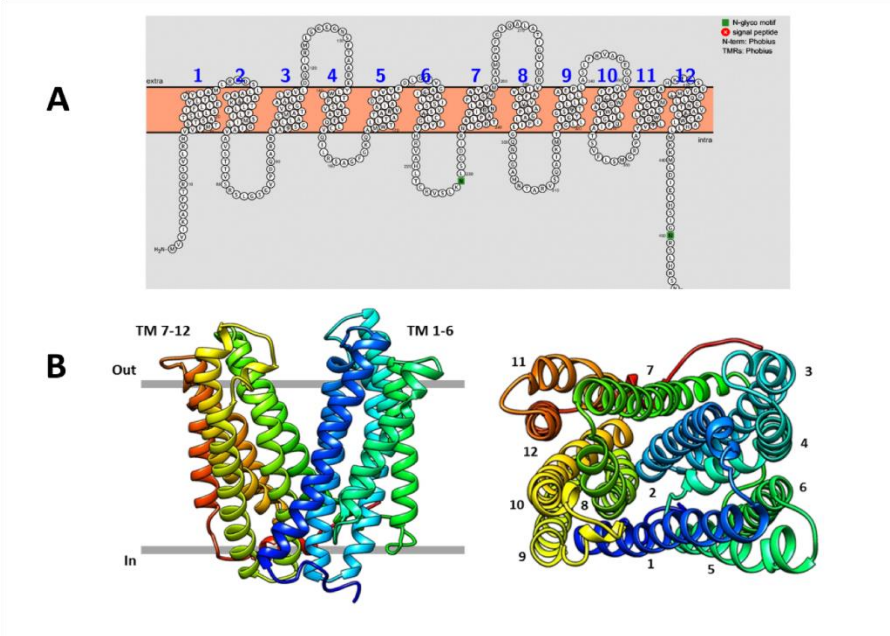

Figure 4. Predicted membrane topology and structure of the *Psn23* MATE transporter. A) Twelve putative TM domains were predicted for *Psn23* MATE, on the basis of amino acid hydrophobicity; B) Ribbon 3D model of *Psn23* MATE, viewed parallel to the membrane (left) and along the membrane normal from the periplasmic side (right), with the twelve TM helices numbered starting from the first N amino acid (methionine).

According to this 3D model, in the TM1 and TM5 of the N lobe of *Psn23* MATE two negative amino acids (E35 and D182) were found to be located, as occurring in the same TMs (D41 and D184) of the H^+ driven MATE transporter from *Pyrococcus furiosus* (hereafter *Pf*MATE) to give the cation-binding site [51, 52]. In contrast, no negative charged amino acids were found in the TM7 and TM10 of *Psn23* MATE as well as of *Pf* MATE, as occurring in the NorM-type MATE transporters which usually use the Na^+ - motive force to drive the substrate transport across the membrane [52, 53].

Overall these findings support the hypothesis of *Psn23* MATE transporter belonging to the DinF subfamily of the prokaryotic MATE transporters. On these bases, a virtual structure-based ligand analysis was then performed to assess if IAA and its conjugate IAA-Lys could be substrate for *Psn23* MATE, by using the GEMDOCK software (BioXGEM) and *Pf* MATE as comparative protein structure model [45]. The binding free energy calculations showed that free IAA and IAA-lysine could be realistically considered among the potential substrates transported by *Psn23*MATE across the bacterial membrane, and that the Y200, T170, T173 and T175 residues are important in substrate binding (Table 1).

Table 1. Energy values of interaction between selected *Psn23* MATE aminoacids and several putative ligands. The value for each aminoacid residue represents the energy of the single bond (expressed as kcal/mol). H= hydrogen bonding; V= van der Waals forces.

Ligand	Energy	H T175	H Y200	V T170	V T173	V T175	V Y200
L-Trp	-72.1	0	0	0	0	0	-11.1
IAM	-71.2	-2.9	-1.4	0	0	-0.9	-10.6
IAA-free	-102.5	0	0	0	0	-1.5	-28.5
IAA-lysine	-95.1	-5.9	0	-2.1	-3.5	-3.9	-16.8

While Y200 has to be considered potentially involved in the binding of both free IAA and of its conjugate with Lysine, the residues T170, T173 and T175 showed to have a stronger interaction with IAA-Lys than IAA, probably because of a specific affinity of polar uncharged amino acids for lysine, such as occurring for threonine.

3.4. Site-directed mutagenesis of Psn23 *MATE to confirm its involvement in pathogenicity and IAA secretion*

According to the data from virtual 3D modelling and docking analysis performed on *Psn23* MATE, site-directed mutagenesis was then carried out on those residues of its N-lobe supposed to be involved in cation-binding (*i.e.* D182), or in substrate recognition and interaction (*i.e.* T170, T173, T175 and Y200). Therefore, the alanine-substituted mutants D182A and Y200A were obtained by single substitution events, while by a triple substitution the mutant T17035A was generated. As previously reported for the *Psn23* mutants *ΔmatE* and pT3-*matE*, the *in vitro* growth of the alanine-substituted mutants D182A, Y200A and T17035A was not impaired in comparison to the wild type *Psn23*, when incubated at 26°C on MM or on KB in shaking condition (data not shown).

Pathogenicity tests were then carried out on these mutants, as well as on the *ΔmatE* and pT3-*matE* mutants, by using *in vitro* micropropagated oleander plants (var. Hardy Red) [17]. For comparison, the wild type *Psn23* was also used. Plants were periodically monitored for symptoms appearance, and the development of the typical hyperplastic knot was firstly visible at naked eyes at about 7 dpi. The *in planta* bacterial growth was also periodically evaluated at 7, 14 and 21 dpi.

The results obtained at 21 dpi are shown in Figure 5, where it is obvious the significant reduction in the size of the knots occurring in the *ΔmatE* inoculated plants, as well as on those infected by the alanine-substituted mutants D182A and Y200A.

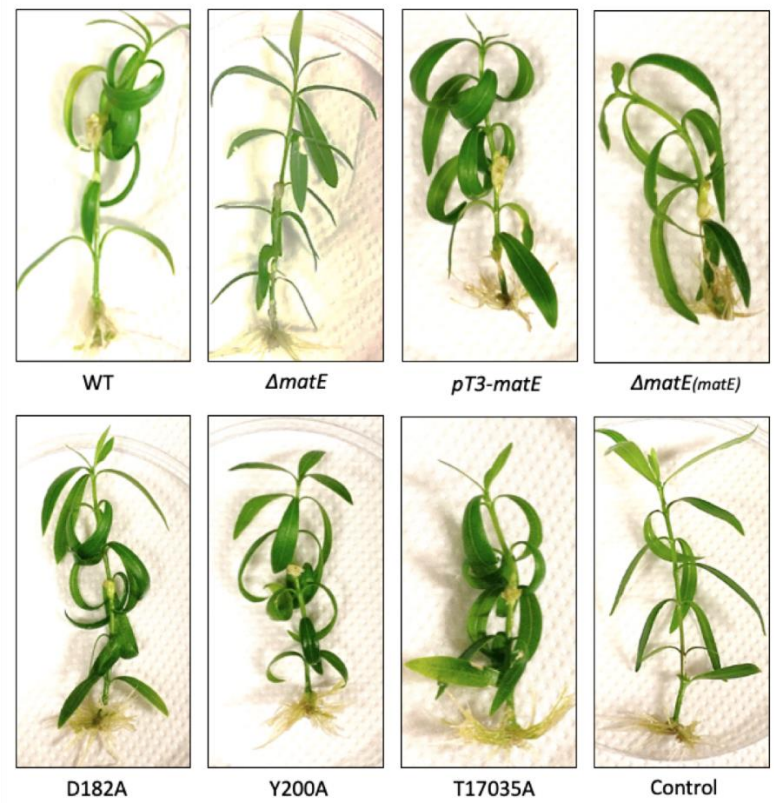

Figure 5. Hyperplastic symptoms obtained at 21 dpi in pathogenicity tests carried out on micropropagated oleander plants with *Psn23* wild type and its mutants *ΔmatE*, pT3-*matE*, D182A, Y200A and T17035A. Control: sterile physiological solution (SPS, NaCl 0,85%) inoculated plants. Complemented mutant for *ΔmatE*: *ΔmatE*(*matE*).

Their hypovirulent phenotype is further confirmed by the data on their growth *in planta*, which was statistically significantly reduced in comparison to the wild type *Psn23* (Figure 6). A reduction in their *in planta* growth ability was also observed at 21 dpi for the mutants T17035A and pT3-*matE*, although the hyperplastic galls they generated on infected plants were slightly bigger or comparable in size to those for the wild-type *Psn23*, for pT3-*matE* and T17035A, respectively (Figure 6).

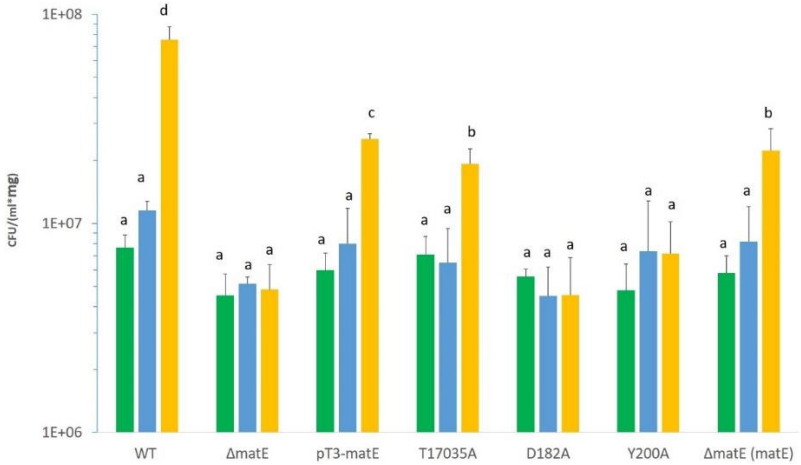

Figure 6. *In planta* bacterial growth of *Psn23* wild type and its mutants *ΔmatE*, pT3-*matE*, D182A, Y200A and T17035A, at 7 (green), 14 (blue) and 21 (yellow) dpi. Values are the mean of 3 independent experiments, with 9 replicates for run and for each strain ± standard deviation (SD). Different letters indicate statistically significant differences among means at $P < 0.05$, according to Tukey's test. Complemented mutant for *ΔmatE*: *ΔmatE*(*matE*).

These findings undoubtedly demonstrated that the putative transporter MATE coded in *Psn23* by *matE* gene is definitely involved in the virulence of this plant pathogen, expressed as ability to cause symptoms and to grow inside the infected plant host. Most importantly, this role appears to depend on *Psn23* MATE ability to transport bacterial biosynthesised IAA using the H^+ motive force, similarly to *Pf*MATE [52]. It was therefore essential to increase the resolution of the analysis for the quantification of IAA and its conjugate IAA-Lys, as well as its intermediate IAM, synthesised *in vitro* by *Psn23* and its MATE-mutants by using high-performance liquid chromatography coupled with a fluorescent detector (HPLC-FLD). In Figure 7, the data related to the *in vitro* production of IAA and IAA-Lys are evaluated by HPLC-FLD on the cell-free filtrates of *Psn23* and the mutants *ΔmatE* and pT3-*matE*, after 24 and 48 h of growth on MM supplemented with Trp. For comparison, the hypovirulent *ΔiaaM* and the hypervirulent *ΔiaaL* mutants were also tested, thus to confirm what already known and expected, that is the *ΔiaaM* inability to synthesise IAA as well as the hyperproduction of free IAA obtained by *ΔiaaL*. The mutants *ΔmatE* and pT3-*matE* have been here shown to have a behaviour similar to *ΔiaaM* and *ΔiaaL*, respectively, for both IAA production and virulence.

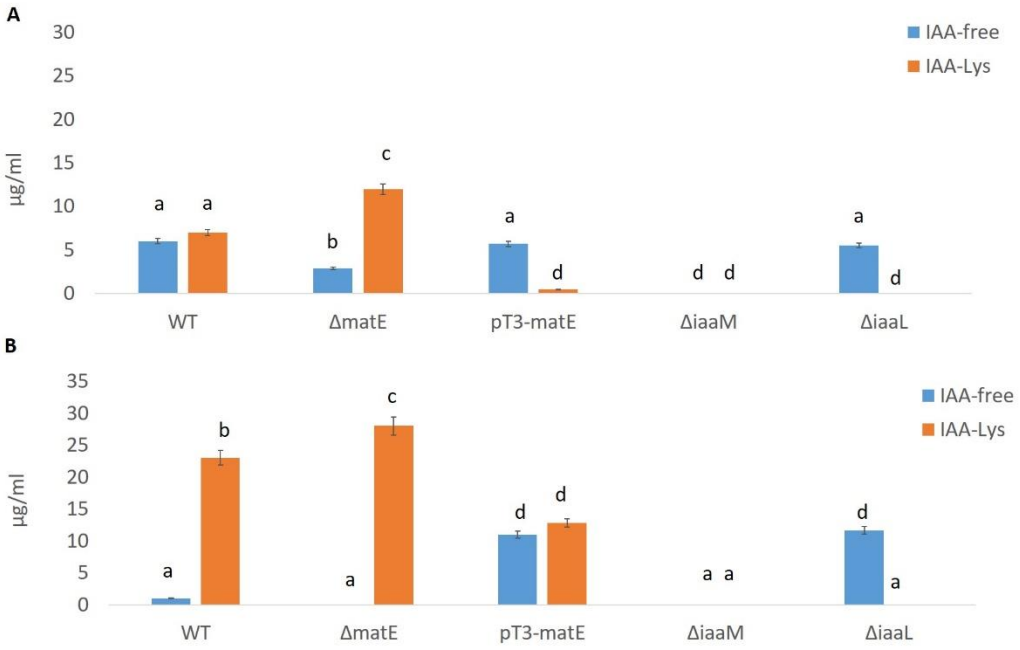

Figure 7. IAA *in vitro* production by the wild type *Psn23* (WT) and its mutants *ΔmatE*, pT3-*matE*, *ΔiaaM* and *ΔiaaL*. After 24h (A) and 48h (B) of *in vitro* growth on MM supplemented with Trp, free IAA and IAA-Lys were quantified in the bacterial supernatants by HPLC-FLD. Data are averages of triplicates ± standard deviation (SD). Different letters indicate significant differences among means of mutants at $P < 0.05$, according to Tukey's test.

As far as the MATE alanine-substituted mutants are concerned, in Figure 8 the results obtained are reported. As expected, the hypovirulent mutants D182A and Y200A showed a reduce production of IAA and increased levels of IAA-Lys, with a behaviour coherent to that of the other hypovirulent mutant *ΔmatE*. Accordingly, no particular differences were found in the biosynthesis of IAA and its metabolite for the T17035 mutant in comparison to the *Psn23* wild type, as occurring also for its ability to cause symptoms on the host plant.

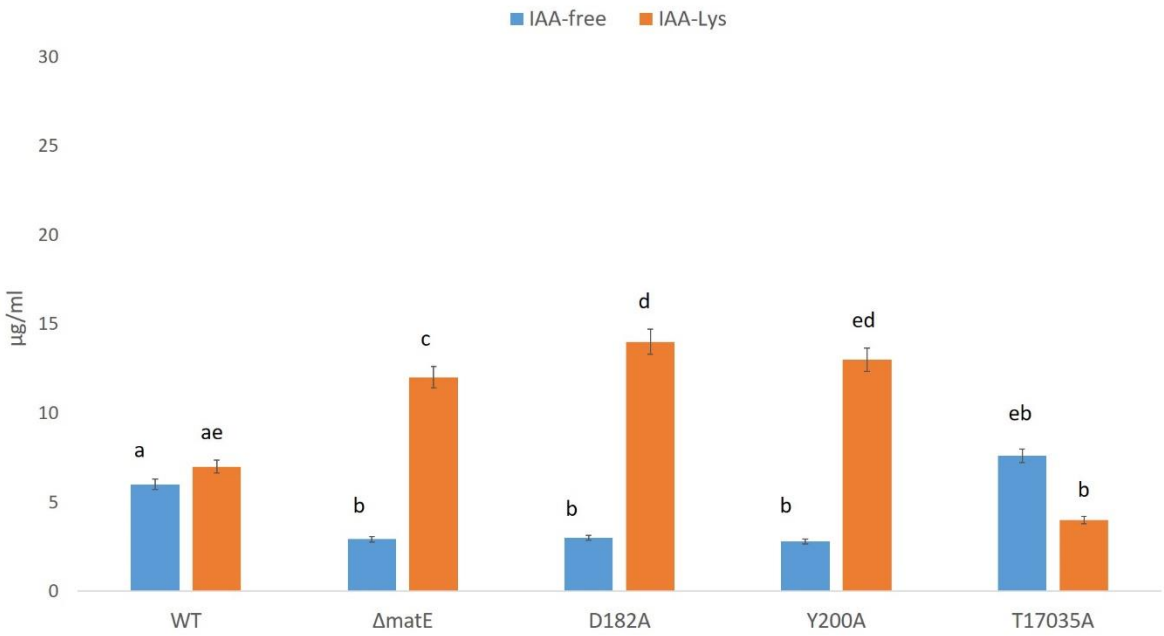

Figure 8. IAA *in vitro* production by the wild type *Psn23* (WT) and its MATE alanine-substituted mutants D182A, Y200A and T17035A. For comparison, the mutant *ΔmatE* was also used. After 24h of *in vitro* growth on MM supplemented with Trp, free IAA and IAA-Lys were quantified in the bacterial supernatants by HPLC-FLD. Data are averages of triplicates ± standard deviation (SD). Different letters indicate significant differences among means of mutants at $P < 0.05$, according to Tukey's test.

4. Discussion

In plants, phytohormones are known to finely regulate plant morphogenesis and development, and their involvement in plant-microbe interactions has been demonstrated as well [1]. In this frame, a pivotal role is played by the auxin IAA, whose levels in plant can be modulated by phytopathogens to promote susceptibility in their potential hosts. Gram negative phytopathogenic bacteria belonging to the so called *P. syringae* complex have been shown to hijack IAA accumulation or auxin signaling by specific virulence factors, such as several TTSS effectors. In addition, most *P. syringae* bacteria produce IAA, even if they do not cause any hyperplastic symptom, and its role as a signaling molecule able to regulate bacterial gene expression as well as virulence has been ascertained [9, 10]. The hyperplastic activity of *P. savastanoi* pv. *nerii* strain *Psn23* on Oleander was shown to depend from the balance between free IAA and its conjugate IAA-Lys in the infected tissues, and this process was demonstrated to be under the control of TTSS [17]. In this auxin-based dialogue with plants, up to now the aspect definitely less investigated has been how IAA-producing phytopathogenic bacteria secrete this phytohormone into the apoplast.

Here, for the first time a bacterial MATE transporter was demonstrated to mediate IAA efflux in the plant pathogen *P. savastanoi* pv. *nerii* strain *Psn23*, as already known for some plant MATE membrane proteins which mediate transport of several phytohormones, including auxins [24]. The same role has been demonstrated just for a microbial MATE, that is Mte1 from *T. vaccinum* [49]. By targeted mutagenesis, several aminoacid residues involved in *Psn23* MATE functionality have been identified. According to these data and to its putative structure, obtained by *in silico* 3D modeling, *Psn23* MATE appears to belong to the DinF subfamily of the prokaryotic MATE transporters, such as the H^+ driven MATE transporter from *P. furiosus* [51].

Just another bacterial MATE transporter has been identified so far in plant pathogenic bacteria, particularly in *Erwinia amylovora*. The *norM* gene from *E. amylovora* codes for a protein higly homologous to the NorM MATE transporter of *E. coli* and *Vibrio parahaemolyticus*, and it was demonstrated to confer resistance to toxins produced by several epiphytic bacteria colonizing the same habitat in addition to the canonical resistance to some hydrophobic cationic antibiotics [54].

Here for the first time a bacterial MATE transporter was demonstrated to be involved in the molecular dialogue between a phytopathogenic bacterium and its potential host plant, by modulating IAA homeostasis in *Psn23* through the MATE-mediated auxin transport. It is well established that in *P. savastanoi* the expression of several TTSS genes is down-regulated by IAA. Therefore, in the first step of the infection process induced by *P. savastanoi* it is reasonable to hypothesize that the intracellular IAA levels have to be carefully modulated by some homeostatic mechanisms, for the most part unknown but which certainly include IAA conjugation, to give less active auxin metabolites such as IAA-Lys. In the *ΔiaaL* mutant, unable to conjugate IAA with Lysine, IAA secretion is strongly increased in association with a hypervirulent phenotype [17]. The same phenotype was here found for the overexpressing mutant pT3-*matE*. Conversely, a hypovirulent phenotype was scored for the *Psn23* mutants having their MATE transporter somehow impaired, as occurring for the deleted mutant *ΔmatE* and for the alanine-substituted mutants D182A and Y200A. In addition, these mutants also showed a reduced *in vitro* IAA production in comparison to the wild type *Psn23*. Overall these data demonstrated that *Psn23* MATE mediates IAA efflux, thus to contribute to maintain the most appropriate IAA intracellular concentrations in each step of the whole infective process, as also suggested by its TTSS-dependent expression, in order to maximise the chances of success. This regulation of IAA homeostasis is played together with IAA-Lysine synthase. The *iaaL* expression is also TTSS-dependent, as well as coordinated with that of *matE* and IAA-inducible [17]. According to the experimental data obtained by HPLC-MS on the IAA *in vitro* production by *Psn23* and its MATE-mutants, *Psn23* MATE can be fairly hypothesised to transport IAA but not its conjugate IAA-Lys, for which additional secretion mechanisms have to be taken into consideration.

However, in addition to the virtual structure-based ligand analysis here carried out, the crystal structure determination and analysis of *Psn23* MATE is the next key step to definitely elucidate those substrates specifically recognised and trasported by this membrane protein, as well as the actual antiporter cation (H^+ or Na^+). A deeper understanding of mechanisms underlying the physiology and the activity of these evolutionarily conserved transport proteins also in bacterial plant pathogens is advisable. For its role in the efflux of a virulence factor such as IAA and also in the resistance to several antimicrobials [17], *Psn23* MATE has indeed to be considered an important promising target for the development of innovative and ecofriendly strategies for the control of *Psn23* as well as of other pathogenic bacteria, possibly by the use of natural indole-mimicking competitors.

Supplementary Materials: Table S1: Bacterial strains, mutants and plasmids used in this study; Table S2: Primers used in this study.

Author Contributions: conceptualization and experiment design, S.T. and L.B.; investigation and data analysis, L.B.; C.B.; S.C.; M.C.; S.T.; draft preparation, S.T.; L.B.; M.C.; writing, review and editing, S.T.; S.C.; L.B.; C.B. supervision, project administration and funding acquisition, S.T.

All authors read and approved the final manuscript.

Funding: This research was funded by EU commission, project "Environmentally friendly biomolecules from agricultural wastes as substitutes of pesticides for plant diseases control", EVERGREEN, LIFE13 ENV/IT/000461, and Fondazione Cassa di Risparmio di Firenze (ref. 2014/0724).

Acknowledgments: Thanks are due to Alessio Sacconi for his support in HPLC analysis, and to Dr Marta De Zotti and Prof. Fernando Formaggio, Università di Padova, for the synthesis of IAA-Lysine.

Conflicts of Interest: The authors declare no conflict of interest. The funders had no role in the design of the study; in the collection, analyses, or interpretation of data; in the writing of the manuscript, or in the decision to publish the results.

References

1. Naseem, M.; Kaltdorf, M.; Dandekar, T. The nexus between growth and defence signalling: auxin and cytokinin modulate plant immune response pathways. *J Exp Bot* **2015**, *66*, 4885-4896, doi: 10.1093/jxb/erv297.
2. Enders, T.A.; Strader, L.C. Auxin activity: Past, present, and future. *Am J Bot* **2015**, *102*, 180-196, doi: 10.3732/ajb.1400285.
3. Di, DW.; Zhang, C.; Luo, P.; An, C.W.; Guo, G.Q. The biosynthesis of auxin: how many paths truly lead to IAA? *Plant Growth Regul* **2016**, *78*, 275-285, doi: 10.1007/s10725-015-0103-5.
4. Kögl, F.; Haagen-Smit A.J.; Erxleben, H. Über ein neues Auxin (Heteroauxin) aus Harn. Hoppe-Seyler's Zeitschrift fur Physiologische Chemie. **1934**, *228*, 90-103, doi: 10.1515/bchm2.1934.228.1-2.90.
5. Fu, S.F.; Wei J.Y.; Chen, H.W.; Liu Y.Y.; Lu, H.Y.; Chou, J.Y. Indole-3-acetic acid: A widespread physiological code in interactions of fungi with other organisms. *Plant Signal Behav* **2015**, *10(8)*: e1048052, doi: 10.1080/15592324.2015.1048052.
6. Kunkel, B.N; Harper, C.P. The roles of auxin during interactions between bacterial plant pathogens and their hosts, J Exp Bot **2018**, *69*, 245-254, doi: 10.1093/jxb/erx447.
7. McClerklin, S.A; Lee S.G.; Harper, C.P.; Nwumeh, R.; Jez, J.M.; Kunkel, B.N. Indole-3-acetaldehyde dehydrogenase-dependent auxin synthesis contributes to virulence of *Pseudomonas syringae* strain DC3000. *PLoS Pathog* **2018,** *14(1)* :e1006811, doi: 10.1371/journal.ppat.1006811.
8. Zhang, P.; Jin, T.; Kumar Sahu, S.; Xu, J.; Shi, Q.; Liu, H.; Wang, Y. The distribution of Tryptophan-dependent Indole-3-Acetic Acid synthesis pathways in bacteria unraveled by large-scale genomic analysis. *Molecules* **2019**, *24(7)*, E1411, doi: 10.3390/molecules24071411.
9. Duca, D.; Lorv, J.; Patten, C.L.; Rose, D.; Glick, B.R. Indole-3-acetic acid in plant-microbe interactions. *A Van Leeuw J Microb* **2014**, *1*, 85-125, doi: 10.1007/s10482-013-0095-y.
10. Ludwig-Müller J. Bacteria and fungi controlling plant growth by manipulating auxin: balance between development and defense. *J Plant Physiol* **2015**, *172*, 4-12, doi: 10.1016/j.jplph.2014.01.002.
11. Spaepen, S.; Vanderleyden, J.; Remans, R. Indole-3-acetic acid in microbial and microorganism-plant signaling, *FEMS Microbiol Rev* **2007**, *31*, 425-448, doi: 10.1111/j.1574-6976.2007.00072.x.
12. Ma, K.W.; Ma, W. Phytohormone pathways as targets of pathogens to facilitate infection. *Plant mol biol* **2016**, 91: 713-725, doi: 10.1007/s11103-016-0452-0.
13. Dermastia, M. Plant hormones in phytoplasma infected plants. *Front. Plant Sci*. **2019**, *10*, 477, doi: 10.3389/fpls.2019.00477.
14. Han, X.; Kahmann, R. Manipulation of phytohormone pathways by effectors of filamentous plant pathogens. *Front Plant Sci* **2019**, *10*, 822, doi: 10.3389/fpls.2019.00822.
15. Yang, S.; Zhang, Q.; Guo, J.; Charkowski, A.O.; Glick, B.R., Ibekwe, A.M.; Cooksey, D.A.; Yang, C.H. (2007) Global effect of indole-3-acetic acid biosynthesis on multiple virulence factors of *Erwinia chrysanthemi* 3937. *Appl Enviromental Microbiol* **2007**, *73*, 1079-1088, doi: 10.1128/AEM.01770-06.
16. Castillo-Lizardo, M.G.; Aragón, I.M.; Carvajal, V., Matas, I.M.; Pérez-Bueno, M.L.; Gallegos, M.T.; Barón, M.; Ramos, C. Contribution of the non-effector members of the HrpL regulon, *iaaL* and *matE*, to the virulence of *Pseudomonas syringae* pv. *tomato* DC3000 in tomato plants. *BMC Microbiol* **2015**, *15*, 165, doi:10.1186/s12866-015-0503-8.
17. Cerboneschi, M.; Decorosi, F.; Biancalani, C.; Ortenzi, M. V.; Macconi, S.; Giovannetti, L.; Viti, C.; Campanella, B.; Onor, M., Bramanti, E.; Tegli, S. Indole-3-acetic acid in plant-pathogenic interactions: a key

molecule for in planta bacterial virulence and fitness. *Res Microbiol* ***2016***, *167*, 774-787, doi:10.1016/j.resmic.2016.09.002.

18. Leyser, O. Auxin Signaling. *Plant physiol* **2018**, *176*, 465-479, doi: 10.1104/pp.17.00765.
19. Sisto, A.; Cipriani, M. G.; Morea, M. Knot formation caused by *Pseudomonas syringae* subsp. *savastanoi* on olive plants is *hrp*-dependent. *Phytopathology* **2004**, *94*, 484-489, doi: 10.1094/PHYTO.2004.94.5.484.
20. Pérez-Martínez, I.; Rodríguez-Moreno, L.; Lambertsen, L.; Matas, I.M.; Murillo, J.; Tegli, S.; Jiménez, A.J.; Ramos, C. Fate of a *Pseudomonas savastanoi* pv. *savastanoi* Type III Secretion System mutant in olive plants (*Olea europaea* L.). *Appl Environ Microbiol* **2010**, *76*, 3611-3619, doi: 10.1128/AEM.00133-10.
21. Caballo-Ponce, E.; Murillo, J.; Martínez-Gil, M.; Moreno-Pérez, A.; Pintado, A.; Ramos, C. Knots Untie: molecular determinants involved in knot formation induced by *Pseudomonas savastanoi* in woody hosts. *Front Plant Sci* **2017**, *8*, 1089, doi:10.3389/fpls.2017.01089.
22. Glickmann, E.; Gardan, L.; Jacquet, S.; Hussain, S.; Elasri, M.; Petit, A.; Dessaux, Y. Auxin production is a common feature of most pathovars of *Pseudomonas syringae*. *Mol Plant Microbe Interact* **1998,** *11*, 156-162, doi: 10.1094/MPMI.1998.11.2.156.
23. Xin, X.F.; Kvitko, B.; He, S.Y. *Pseudomonas syringae*: what it takes to be a pathogen. *Nat Rev Microbiol* **2018**, *16*, 316-328, doi: 10.1038/nrmicro.2018.17.
24. Sun, X,; Gilroy, E.M.; Chini, A.; Nurmberg, P.L..; Hein, I.; Lacomme, C.; Birch, P.R.; Hussain, A.; Yun, B.; Loake, G.J. *ADS1* encodes a MATE-transporter that negatively regulates plant disease resistance. *New Phytol* **2001**, *192*, 471-482, doi: 10.1111/j.1469-8137.2011.03820.x.
25. Remy, E.; Duque, P. Beyond cellular detoxification: a plethora of physiological roles for MDR transporter homologs in plants. *Front physiol* **2014**, *5*, 201, doi: 10.3389/fphys.2014.00201.
26. King, E.O., Ward, M.K., Raney, D.E. Two simple media for the determination of pyocianine and fluorescein. *J Lab Clin Med 1954, 44, 301-307,* doi*:10.5555/uri:pii:002221435490222X.*
27. Huynh, T.V.; Dahlbeck, D.; Staskawicz, B.J. Bacterial blight of soybean: Regulation of a pathogen gene determining host cultivar specificity. *Science* **1989**, *245*, 1374-1377, doi: 10.1126/science.2781284.
28. Miller, J. H. Experiments in molecular genetics. J.H. Miller Ed. *Cold Spring Harbor Laboratory. Cold Spring Harbor, New York, NY, USA*, **1972**, pp. 1-466.
29. Sisto, A.; Cipriani, M.; Tegli, S.; Cerboneschi, M.; Stea, G.; Santilli, E. Genetic characterization by fluorescent AFLP of *Pseudomonas savastanoi* pv. *savastanoi* strains isolated from different host species. *Plant Pathol* **2007**, *56*, 366-372, doi: 10.1111/j.1365-3059.2007.01567.
30. Tegli, S.; Cerboneschi, M.; Marsili Libelli, I.; Santilli, E. Development of a versatile tool for the simultaneous differential detection of *Pseudomonas savastanoi* pathovars by End Point and Real-Time PCR. *BMC Microbiol* **2010**, *10,* 156, doi:10.1186/1471-2180-10-156.
31. Sambrook, J.; Fritsch, E.F.; Maniatis, T.A. Molecular Cloning: A Laboratory Manual, *2nd ed. Cold Spring Harbor Laboratory Press. New York, NY, USA*, **1989**, pp. 1-1469.
32. Schäfer, A.; Tauch, A.; Jäger, W.; Kalinowski, J.; Thierbach, G.; Pühler, A. Small mobilizable multi-purpose cloning vectors derived from the *Escherichia coli* plasmids pk18 and pk19: selection of defined deletions in the chromosome of *Corynebacterium glutamicum. Gene* **1994**, *145*, 69-73, doi: 10.1016/0378-1119(94)90324-7.
33. Biancalani, C.; Cerboneschi, M.; Tadini-Buoninsegni, F.; Campo, M.; Scardigli, A.; Romani, A.; Tegli, S. Global analysis of Type Three Secretion system and Quorum Sensing inhibition of *Pseudomonas savastanoi* by polyphenols extracts from vegetable residues. *PLoS ONE* **2016**, *11*, doi: 10.1371/journal.pone.0163357.
34. Baker, C.J.; Atkinson, M.M.; Collmer, A. Concurrent loss in Tn5 mutants of *Pseudomonas syringae* pv. *syringae* of the ability to induce the Hypersensitive Response and host plasma membrane K+/H^+ exchange in Tobacco. *Phytopathotogy* **1987**, *77*, 1268-1272, doi: 10.1094/Phyto-77-1268.

35. Murashige, T.; Skoog, F. A revised medium for rapid growth and bioassays with tobacco tissue cultures. *Physiol Plant* **1962**, *5*, 473–497, doi:10.1111/j.1399-3054.1962.tb08052.
36. Gori, A.; Cerboneschi, M.; Tegli, S. High-Resolution Melting Analysis as a powerful tool to discriminate and genotype *Pseudomonas savastanoi* pathovars and strains. *PLoS ONE* **2012**, *7(1): e30199*, doi: 10.1371/journal.pone.0030199.
37. Ehmann, A. The Van Urk-Salkowski reagent - a sensitive and specific chromogenic reagent for silica gel thin-layer chromatographic detection and identification of indole derivatives. *J Chromatogr* **1977**, *132*, 267-276.
38. Thompson, J.D.; Higgins, D.G.; Gibson, T.J. ClustalW: improving the sensitivity of progressive multiple sequence alignment through sequence weighting, position-specific gap penalties and weight matrix choice. *Nucleic Acids Res* **1994**, 22, 4673-4680, doi: 10.1093/nar/22.22.4673.
39. Altschul, S.F.; Gish, W.; Miller, W.; Myers, E.W.; Lipman, D.J. Basic local alignment search tool. *J Mol Biol* **1990**, *215*, 403-410, doi: 10.1016/S0022-2836(05)80360-2.
40. Tajima, F.; Nei, M. Estimation of evolutionary distance between nucleotide sequences. *Mol Biol Evol* **1984**, *1*, 269-285, doi: 10.1093/oxfordjournals.molbev.a040317.
41. Kumar, S.; Stecher, G.; Tamura K. MEGA7: Molecular Evolutionary Genetics Analysis Version 7.0 for Bigger Datasets. *Mol Biol Evol* **2016**, *33*, 1870-1874, doi: 10.1093/molbev/msw054.
42. Kelley, L.A.; Mezulis, S.; Yates, C.M.; Wass, M.N.; Sternberg, M.J.E. The Phyre2 web portal for protein modeling, prediction and analysis. *Nat Protoc* **2015**, *10*, 845-858, doi: 10.1038/nprot.2015.053.
43. Källberg, M.; Wang, H.; Peng, J.; Wang, Z.; Lu, H.; Xu, J. Template-based protein structure modeling using the RaptorX web server. *Nat Protoc* **2012**, *7*, 1511-1522, doi: 10.1038/nprot.2012.085.
44. Pettersen, E.F.; Goddar, T.D.; Huang, C.C.; Couch, G.S.; Greenblatt, D.M.; Meng, E.C.; Ferrin, T.E. UCSF Chimera: A visualization system for exploratory research and analysis. *J Comput Chem* **2004**, *25*, 1605-1612, doi: 10.1002/jcc.20084.
45. Jacobson, M.; Sali, A. Comparative protein structure modeling and its applications to drug discovery. *Annu Rep Med Chem* **2004**, *39*, 259-276, doi: 10.1016/S0065-7743(04)39020-2.
46. Trott, O.; Olson, A.J. AutoDock Vina: improving the speed and accuracy of docking with a new scoring function, efficient optimization and multithreading. *J Comput Chem* **2010**, *31*, 455-461, doi: 10.1002/jcc.21334.
47. Hammer, Ø.; Harper, D.A.T.; Paul D. Ryan, P.D. PAST: Paleontological Statistics Software Package for Education and Data Analysis. *Palaeontol Electron* **2001,** *4*, 1-9.
48. Gordon, S.A.; Weber, R.P. Colorimetric estimation of indoleacetic acid. *Plant Physiol* **1951,** *26*, 192-196, doi: 10.1104/pp.26.1.192.
49. Krause, K.; Henke, C.; Asiimwe, T.; Ulbricht, A.; Klemmer, S.; Schachtschabel, D.; Boland, W.; Kothe, E. Indole-3-acetic acid biosynthesis, secretion, and its morphological effects on *Tricholoma vaccinum*-Spruce ectomycorrhiza. *Appl Environ Microb* **2015**, *81*, 7003-7011, doi: 10.1128/AEM.01991-15.
50. Du, D.; Wang-Kan, X.; Neuberger, A.; Van Veen, H.W.; Pos, K.M.; Piddock, L.J.V.; Luisi, B.F. Multidrug efflux pumps: structure, function and regulation. *Nat Rev Microbiol* **2018**, *16*, 523-539, doi: 10.1038/s41579-018-0048-6.
51. Jin, X.; Shao, Y.; Bai, Q.; Xue, W.; Liu, H.; Yao, X. Insights into conformational regulation of *Pf*MATE transporter from *Pyrococcus furiosus* induced by alternating protonation state of Asp41 residue: A molecular dynamics simulation study. *Biochim Biophys Acta* **2016**, *1860*,1173-1180, doi: 10.1016/j.bbagen.2016.02.007.

611 52. Tanaka, Y.; Hipolito, C.J.; Maturana, A.D.; Ito, K.; Kuroda, T.; Higuchi, T.; Katoh, T.; Kato, H.E.; Hattori,
612 M.; Kumazaki, K.; Tsukazaki, T.; Ishitani, R.; Suga, H.; Nureki, O. Structural basis for the drug extrusion
613 mechanism by a MATE multidrug transporter. *Nature* **2013**, *496*, 247-251, doi: :10.1038/nature12014.
614 53. Miyauchi, H.; Moriyama, S.; Kusakizako, T.; Kumazaki, K.; Nakane, T.; Yamashita, K., Hirata, K.; Dohmae,
615 N.; Nishizawa, T.; Ito, K.; Miyaji, T.; Moriyama, Y.; Ishitani, R.; Nureki, O. Structural basis for xenobiotic
616 extrusion by eukaryotic MATE transporter. *Nat Commun* **2017**, *8*, 1633, doi: 10.1038/s41467-017-01541-0.
617 54. Burse, A.; Weingart, H.; Ullrich, M.S. NorM, an *Erwinia amylovora* multidrug efflux pump involved in *in*
618 *vitro* competition with other epiphytic bacteria. *Appl Environ Microbiol* **2004**, *70*, 693-703, doi:
619 10.1128/aem.70.2.693-703.2004.
620

621

Chapter 5

Comparative genome analysis of *Curtobacterium flaccumfaciens* strains

5.1 Introduction

Members of the *Curtobacterium* genus are Gram-positive, obligately aerobic chemoorganotrophs in the family Microbacteriaceae, phylum Actinobacteria (Evtushenko and Takeuchi, 2006). *Curtobacterium flaccumfaciens* is the only pathogenic species of this genus (Young et al., 1996). Furthermore, different pathovars of *C. flaccumfaciens* were described as economically important plant pathogens on annual crops, such as dry bean (Harveson *et al*., 2015) and sugar beet (Chen *et al.*, 2007).

Under field conditions, *C. flaccumfaciens* can survive on a wide number of nonhost plant species, including alfalfa, maize, eggplant, pepper, sunflower, tomato and wheat (Harveson *et al.*, 2015). Recently, pathogenicity test on common bean plants (*Phaseolus vulgaris*) were conducted with epiphytic *C. flaccumfaciens* strains isolated from symptomless Solanaceous vegetables (Osdaghi *et al*., 2018). Only a small number of tested strains were no pathogenic on these plants, instead the most of them showed wilt symptoms, exactly such as those caused by *C. flaccumfaciens* pv. *flaccumfaciens (Cff)* (Osdaghi *et al*., 2018). *Cff* is the causal agent of bacterial wilt of dry beans worldwide, and it is responsible for severe yield losses and seed quality reduction (Osdaghi *et al*, 2015; Chase *et al.*, 2016).

Studies on the genome of *C. flaccumfaciens*, as well as *Cff*, are in their infancy as well as poorly understood. It is known that a pair of PCR primers (CffFOR2-CffREV4) amplify a 306-bp DNA specific fragment using DNA *Cff* as template (Tegli *et al.*, 2002). The specific primers were designed targeting a sequence of cloned DNA fragment of 550 bp which had high identity with a putative serine protease. The serine proteases are known to be involved in the in plant–microbe interaction in different phytopathogenic bacteria, such as *Clavibacter* spp. and *Xanthomonas* spp. (Eichenlaub *et al.*, 2011, Hotson et al., 2003). Information about genes involved in virulence of *Cff* are not available, also as a results of the lack of genome studies on these bacteria.

In this study, we have selected two *C. flaccumfaciens* strains isolated from Solanaceous plants, one virulent and the other not virulent on bean (P990 /ICMP 22053 and Tom827 / ICMP 22084, respectively). The *Cff* type strain ICPM 2584 was used for comparison. At first, it was verified through gene expression studies that the specific *Cff*-fragment was not expressed by the strain which was not virulent on bean. Then, the genome of these three strains was sequenced and a comprehensive comparison of their genomes was conducted, using DNA structural and annotation features in order to identify genes involved in

pathogenicity and/or virulence of the two strains virulent on bean plants, and thus belonging to *Cff*.

5.2 Materials and methods

Bacterial strains, media and growth condition

The *Curtobacterium* sp. using in this study are listed in Table 1. The bacteria strains were routinely grown at 26°C as liquid or solid cultures in Luria-Bertani LB (Miller, 1972) or YDC (tryptone at 10 g/liter, yeast extract at 5g/liter, NaCl at 5 g/liter, pH 7.5) medium.

Table 1: list of strains used in this study.

Strain	Host of isolation	Date of isolation	International collection n°	Reference
P990	Bell pepper	2015	ICMP 22053	Osdaghi et *al.* 2018
Tom827	Tomato	2015	ICMP 22084	Osdaghi *et al.* 2018
Type	Bean	1957	ICMP 2584^{T}	ICMP

T: Type strain

Quantitative gene expression analysis

Bacterial gene expression was evaluated by real-time PCR. Bacterial cells of strain Tom827 and type strain ICPM2584 were grown overnight in LB (starting concentration OD_{600}=0.1), washed twice with SPS and transferred into LB. Cells were collected after 24 h of incubation at 26°C on an orbital shaker (100 rpm). Total RNA was purified from bacteria using NucleoSpin® RNA Plus (Macherey-Nagel GmbH and Co. KG, Düren, Germany). The RNA quality was evaluated both spectrophotometrically, with NanoDrop™ ND-1000 (NanoDrop Technologies Inc., DE, USA), and visually by standard agarose gel electrophoresis [1% agarose (w/v) in TBE 1×] (Sambrook *et al.,* 1989). About 1 µg of RNA for each treatment was reverse transcribed, using iScript™ Advanced cDNA Synthesis kit (Bio-Rad Laboratories Inc., Hercules, CA, USA), according to the manufacturer's instructions. Diluted cDNA was analysed by real-time PCR, with SsoFast™ EvaGreen®Supermix (Bio-Rad Laboratories Inc.) and using the CFX96 cycler–real-time PCR Detection System and CFX-manager software v1.6 (Bio-Rad Laboratories Inc.). To normalise the expression of monitored gene, the 16S rDNA expression level was used as a housekeeping gene. For each

sample, three replicates were analised, and three independent experiments were conducted. The primers used are listed in Table 2.

Table 2: Primers designed and used in this study for real time-PCR experiments

Primer name	Primer sequence (5' → 3')
Cff B3	CGTTAGTGAAGGCTGACGAA
Cff F3	TTCCCGGTGTTCAGTTGAC
16sF_CffRT _FOR	TGGCCGCATGGTCTGG
16s_CffRT_REV	GCCGTGTCTCAGTCCCA

Genome sequencing and annotation

Genomic DNA was extracted from bacteria liquid culture using Gentra PureGene™ Yeast/Bacterial Kit (QIAGEN) according to the supplier's instructions. Genome sequencing was conducted using Illumina HiSeq 3000 platform (Italy). Sequence assembly was performed with SPAdes algorithm (Bankevich *et al.,* 2012). Moreover, whole contigs (≥ 0 bp) of the three strains where aligned with reference genome using MeDuSa (Bosi et al., 2015) in order to reduce contigs number. Then, contig thus reduced were used to functional annotation which were performed with Prokka1.13.3 (Seemann, 2014), setting up a database of genomes of *Curtobacterium* sp. In addition, tRNA, rRNA, gene and signal peptide calling were performed respectively with ARAGORN, (Laslett *et al.,* 2004) Barrnap (Lagesen *et al.,* 2007), Prodigal (Chen *et al.,* 2010) and SignalP (Nielsen, 2017) program. Assigned function were checked with BLAST (Altschul *et al.,* 1990).

Comparative analysis

Comparative genomics of the three strains were carried out using Roary (Page *et al.,* 2015). Finally, IslandViewer (Langille *et al.,* 2009) was used to assess the presence of putative genomic islands (GIs) on the draft genomes. IslandViewer integrates two sequence composition GIs prediction methods, namely IslandPathDIMOB (Hsiao *et al.,* 2005) and SIGI-HMM (Waack et al., 2006), and one single comparative GI prediction method, namely IslandPick (Langille *et al.,* 2009) for genomic island prediction. The presence of possible virulence-related gene and genes theoretically expressed during bean infection in the draft

genome of *Cff* strains was analysed by comparing them with the *C. flaccumfaciens* strain Tom827 which is avirulent on bean.

Data analysis

Statistically significant differences among treatments were calculated by one-way ANOVA with Tukey-Kramer post-test ($p<0.05$) with PAST software (Version 3.11, Øyvind Hammer, Natural History Museum, University of Oslo).

5.3 Results

Quantitative gene expression analysis

Previous studies have shown that a primer pairs (CffFOR2-CffREV4), which targeted a sequence of cloned DNA fragment of 550 bp encoding for a putative serine protease, amplify a specific fragment using *Cff*-DNA as template (Tegli *et al.*, 2001). Moreover, it is known that the *C. flaccumfaciens* strain Tom827 neither gives any amplicon by using these *Cff* specific primers nor is positive on pathogenicity tests on bean plants (Osdaghi *et al*., 2018). Bacterial gene expression of this putative serine protease was evaluated by real-time PCR, by designing and using the primer pair B3-F3 (Table 2). As shown in Figure 1 and as expected, no expression was observed for this gene for the *C. flaccumfaciens* strain Tom827 when grown *in vitro* on LB, while a positive signal was found for the *Cff* type strain ICPM 2584. These data confirm that the sequence targeted by the CffFOR2-CffREV4 primer pair, encoding a putative serine protease, is present and expressed only by *Cff* strains and likely linked to their virulence on bean plants.

General features of the chromosomes

The shotgun sequence of *Cff* type strain ICP2584 yielded 2,038,269 read pairs (313,770 250pb paired-end reads and 1,724,499 180pb mate pair reads). Furthermore, the shotgun sequence of *Cff* P990 strain yielded 4,078,563 read pairs (2,474,933 250pb paired-end reads and 1,603,630 180pb mate pair reads). Finally, the shotgun sequence *C. flaccumfaciens* Tom827 strain yielded 4,103,038 read pairs (2,484,762 250pb pair-end reads and 1,618,275 mate pair reads).

Genome assembly using paired-end and mate-paired reads resulted in a 3.83 Mb for *Cff* type strain ICPM 2584), 3.94 Mb for *Cff* P990 and 3.81Mb for *C. flaccumfaciens* Tom827 strain. Moreover, the assembly resulting in 131 contigs 500 bp (N50 190,112) for the *Cff* type stain

(ICP2584), in 179 contigs 500bp (N50 816,167) for the *C. flaccumfaciens* Tom827 strain and 171 contigs 500bp (N50 755,151) for the *Cff* P990 strain. The GC % content of the chromosome is 70.81% for *Cff* type strain (PM 2584), 70.78% for *Cff* P990 strain, and 70.93 for *C. flaccumfaciens* strain Tom827. Moreover, the number of CDSs, signal peptides and RNAs which have been identified are listed in Table 3.

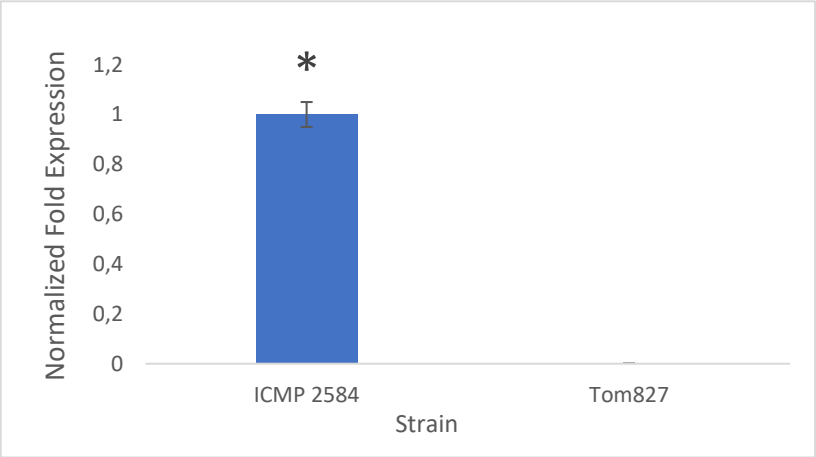

Figure 1: Differential gene expression of pathogenic strain (ICPM 2584) and the non-pathogenic strain (*Tom827*) with B3/F3 primer pairs. Bacteria grown in vitro on LB alone for 24h. Data are the averages of triplicates ± standard deviation (SD). Asterisks indicate significant differences compared with

Table 3: comparison of genome characteristics (based on Prokka server)

Genome name	Type strain	*P990*	*Tom827*
Host	Bean	Bean	/
Disease	Bacterial wilt	Bacterial wilt	/
Size (pb)	3838786	3944189	3812828
n° contigs (>500pb)	131	179	171
Largest contig size (pb)	902486	9375563	1360892
GC (%)	70.81	70.78	70.93
CDS	3723	3767	3630
rRNA	4	5	5
tRNA	51	52	54
Signalp	287	368	274

Comparative analysis

The analysis of the three genomes with IslandPath-DIMOB method showed that at least 8 regions with lower GC content, distributed among different contigs, could be distinguished (Table 4). The putative genomic islands 1, 2, 3, 4 and 5 count have been excluded from further analysis because of their very low number of bases. The genomic island 6 of *Cff* type strain (ICPM 2584) counts 22.76kb and does not overlap with any genomic region of P990. On reverse, the genomic island 7 of *Cff* P990 strain does not overlap with any genomic region of *Cff* type strain ICPM 2584. Conversely, the genomic island 8 of *Cff* type strain ICPM 2584 and the genomic island 9 of the *Cff* P990 strain have several genes in common although different lengths. Moreover, a comparative analysis conducted with Roary showed a region of 115 genes which are common to these *Cff* strains, but absent in the avirulent *C.flaccumfaciens* strain Tom827. This region partially overlaps the genomic island 8 and 9 and includes several genes involve on virulence (Additional data Table S1), a high number of integrases (Additional data Table S2) and a considerable number of genes related to conjugative systems (Additional data Table S3).

Table 4: Low GC regions detected by IslandViewer.

N°	Size (bp)	GI prediction program	Strain
1	8.229	IslandPath-DIMOB	Type
2	11.585	IslandPath-DIMOB	Type
3	5.114	IslandPath-DIMOB	*P990*
4	8.195	IslandPath-DIMOB	*Tom827*
5	9.469	IslandPath-DIMOB	*Tom827*
6	22.758	IslandPath-DIMOB	Type
7	24.908	IslandPath-DIMOB	*P990*
8	27.653	IslandPath-DIMOB	Type
9	76.382	IslandPath-DIMOB	*P990*

5.4 Discussion

The starting point of the genomic studies here carried out on *Cff* was the 550 bp DNA fragment targeted by the PCR primer pair CffFOR2-CffREV4, routinely used for a specific *Cff* diagnostic test (Tegli *et al.,* 2002). This fragment encodes for a putative serine-protease

(Osdaghi et al, 2018) whose gene expression was exclusive of the *Cff* strains as here assessed by real-time PCR (Figure 1) Therefore, these results raised the question of the potential role of this protein in the interaction between *Cff* and its hosts, In particular, this putative serine protease could be hypothesised to be involved in *Cff* virulence on bean, as occurring for these proteins in other plant pathogen bacteria (Gartemann *et al.,* 2008). Genome sequencing and comparative genome analysis have been demonstrated pivotal to detect genomic differences among virulent and no virulent strains of the same bacterial species, according to an untargeted approach (Tambong *et al.,* 2017; Zaluga *et al.,* 2014**)**. Therefore, we sequenced the genome of the three strains (*Cff* type strain, *Cff* P990 strain and *C. flaccumfaciens* Tom827 strain), and then the data obtained were used for a genomic comparative analysis to try to discover genes potentially related to *Cff* pathogenicity and virulence on bean plants.
The analyses carried out with Roary and IslandViewer clearly showed a 115 genes region which was exclusive of *Cff* type strain and *Cff* P990strain. This region includes the *Cff*-specific DNA fragment targeted by CffFOR2-CffREV4 primers, in addition to several other genes putatively involve in virulence, a high number of integrases and a considerable number of genes related to bacterial conjugative systems (Additional data Table S1, Table S2, Table S3).

Several serine proteases are among those proteins hypothetically involved in *Cff* virulence (Table S1), as occurring in other plant pathogens (Stork *et al*., 2008). The proteases XopD of *Xanthomonas campestris* pv. *vesicatoria* affects several plant signalling pathways leading to stress responses or defence reactions against pathogens (Hotson *et al*., 2003). It is well known that serine proteases have a role in plant pathogen interaction for *Clavibacter michiganensis* subsp. *michiganensis* (*Cmm)* NCPPB382, as well as *Clavibacter michiganensis* subps. *sepedonicus* (*Cms*) (Nissinen *et al.,* 2009, Stork *et al*., 2008).
Still in the same region supposed to be involved in *Cff* pathogenicity and virulence, a gene encoding for a putative pectate lyase (p990_03615; type.fna_03755) is included (Table S1). Pectin or pectic substances have been demonstrated to play an important role in the defence mechanisms against plant pathogens, and their degradative action contributes to disease development in pepper and tomato respectively in *Clavibacter michiganensis* subsp. *capsici* and *Clavibacter michiganensis* subsp. *michiganensis* (Hwang *et al,* 2018; Thapa *et al*., 2017; Voragen *et al.,* 2009).

The *C. flaccumfaciens* Tom827 strain, avirulent on bean, completely lacks all these genes. In light of these results, we can strongly hypothesise these genes could have a role in plant-pathogen interaction for *Cff*, as it is already known for *Clavibact*er spp. and

Xanthomonas spp. (Hotson et al., 2003, Nissinen *et al.*, 2009, Stork *et al*., 2008, Hwang *et al*, 2018; Thapa *et al*., 2017). According to homology studies it is reasonable to presume *Cff* acquiring these determinants from other plant pathogenic bacteria by horizontal gene transfer (HGT) events. Conjugation, which is one of the major mechanisms of gene transfer, requires cell-to-cell contact and is able to deliver the whole genome of one cell into another (Guglielmini *et al.*, 2014). Probably the mating pair formation (MPF) was occurred on those most common host plants for *Clavibacter* spp. and *Xanthomonas* spp., which are Solanaceous and on which *Cff* has been demonstrated able to survive and multiply (Harveson *et al.*, 2015).

Moreover, integrase genes and presence of known conjugative genes are hall-marks for presence of Integrative Conjugative Elements (ICE), supporting the assumed horizontal gene transfer (Ambroset *et al*., 2015). The 115 genes region, occurring exclusively on *Cff* strains, counts two integrases which are essential to catalyse the integration reaction (Delavat *et al*., 2017) (Table S2). In addition, the same region includes two of the major components of a conjugative system: a relaxosome and a type IV secretion system (T4SS) (Table S3) (Guglielmini *et al*., 2014). Conjugation relies another component, the coupling protein (T4CP). Annotation results did not show a specific T4CP, but only one AAA+ ATPase (Table S3) which could be responsible for coupling the relaxosome with the DNA transport apparatus during cell mating (Alvarez Martinez *et al*, 2009). Furthermore, lacking considerable genomic information about *Curtobacterium* spp., it is also possible that other not identified proteins among those placed adjacent to the relaxosome could be T4CP coupling proteins.

In conclusion, genomes comparative analysis and gene expression studies had allowed to detect at least a genomic island in *Cff*, containing genes putatively involved in the pathogenicity and virulence of these strains. In addition, the presence of integrases and conjugative genes suggest its acquisition by horizontal gene transfer event, likely occurred with other phytopathogenic bacteria such as *Clavibacter*, which allowed to transfer genes involved in disease development and plant-pathogen interaction.

5.5 Additional materials

Table S1: Putative virulence genes found in the *Cff* type strain and *Cff* P900 strain genomes (Based on the annotation results from Prokka1.13.3)

CDS identifiers P990 strain	CDS identifiers Type strain	Annotation
p990_03611	type.fna_03759	trypsin-like serine protease
p990_03612	type.fna_03758	trypsin-like serine protease
p990_03613	type.fna_03757	serine protease
p990_03614	type.fna_03756	putative Serine/cysteine peptidase protein
p990_03615	type.fna_03755	pectate lyase
p990_03652	type.fna_03718	trypsin-like serine protease

Table S2: Mobile genetic elements found in the *Cff* type strain and *Cff* P900 strain genomes (Based on the annotation results from Prokka1.13.3)

CDS identifiers P990 strain	CDS identifiers Type strain	Annotation
p990_03610	type.fna_03760	transposase
p990_03627	type.fna_03743	transposase
p990_03648	type.fna_03722	transposase
p990_03649	type.fna_03721	integrase
p990_03650	type.fna_03720	integrase

Table S3: Putative genes involved on conjugative system found in the *Cff* type strain and *Cff* P900 strain genomes (Based on the annotation results from Prokka1.13.3)

CDS identifiers P990 strain	CDS identifiers Type strain	Annotation
p990_03651	type.fna_03719	conjugative relaxase
p990_03672	type.fna_03698	AAA family ATPase
p990_03691	type.fna_03679	putative Flp pilus-assembly protein
p990_03692	type.fna_03678	pilus assembly protein
p990_03693	type.fna_03677	pilus assembly protein
p990_03695	type.fna_03675	TadC protein
p990_03697	type.fna_03673	type II/IV secretion system ATPase subunit
p990_03703	type.fna_03667	type IV secretion system protein VirB4

5.6 References

- **Altschul S.F.,** Gish W., Miller W., Myers E.W., Lipman D.J. (1990) Basic local alignment search tool. Journal of Molecular Biology, 215(3):403–410.
- **Alvarez-Martinez C.E**, Christie P.J. (2009) Biological Diversity of Prokaryotic Type IV Secretion Systems. Microbiology and Molecular Reviews p. 775–808.
- **Ambroset C**, Coluzzi C, Guedon G et al. New insights into the classification and integration specificity of Streptococcus Integrative Conjugative Elements through extensive genome exploration. Frontieres Microbiology 6:1483.
- **Bankevich A**., Nurk S., Antipov D., Gurevich A., Dvorkin M., Kulikov A. S.,Lesin V.M., Nikolenko S.I., Pham S., Prjibelski A.D., Pyshkin A.V., Sirotkin A. V., Vyahhi N., Tesler G., Alekseyev M.A., Pevzner P.A. (2012). SPAdes: A New Genome Assembly Algorithm and Its Applications to Single-Cell Sequencing. Journal of computational biology, 19(5).
- **Bosi E**., Donati B., Galardini M., Brunetti S., Sagot M.F., Lio´ P., Crescenzi P., Fani R., Fondi M. (2015). MeDuSa: a multi-draft based scaffolder. Bioinformatics, 31(15) 2443–2451.
- **Chase A.B**., Arevalo P., Polz M.F., Berlemont R. and Martiny J.B.H. (2016). Evidence for Ecological Flexibility in the Cosmopolitan Genus *Curtobacterium*. Frontiers in Microbiology, 7:1874.
- **Chen G.L.,** LoCascio P.F. Land M.L., Larimer F. W., Hauser L.J. (2010). Prodigal: prokaryotic gene recognition and translation initiation site identification. Hyatt D., Gwo-Liang. C Bioinformatics, 11:119
- **Chen Y.F**., Yan-Ni Yin Y.N., Zhang X.M., Guo J.H. (2007). *Curtobacterium flaccumfaciens* pv. *beticola*, A New Pathovar of Pathogens in Sugar Beet. Plant Disease / Vol. 91 No. 6.
- **Delavat F**., Miyazaki R., Carraro N., Pradervand N., Van Der Meer J.R. (2017) The hidden life of integrative and conjugative elements. FEMS Microbiology Reviews, 41(4): 512–537.
- **Eichenlaub R**., Gartemann K.H. (2011). The *Clavibacter michiganensis* subspecies: molecular investigation of Gram-positive bacterial plant pathogens. The Annual review of phytopatology, 49:445-464.
- **Evtushenko L. I.,** Takeuchi, M. (2006). "The family Microbacteriaceae," in *The Prokaryotes*, eds M. Dworkin, S. Falkow, E. Rosenberg, K.-H. Schleifer, and E. Stackebrandt (New York, NY: Springer), 1020–1098.
- **Gartemann K.H**., Abt B., Bekel T., Burger A., Engemann J., Flügel M., Gaigalat L., Goesmann A., Gräfen I., Kalinowski J., Kaup O., Kirchner O., Krause L., Linke B., McHardy A., Meyer F., Pohle S., Rückert C., Schneiker S., Zellermann E.M., Pühler A., Eichenlaub R., Kaiser O., Bartels D. (2008). The genome sequence of the tomato-pathogenic actinomycete *Clavibacter michiganensis* subsp. *michiganensis* NCPPB382 reveals a large island involved in pathogenicity. Journal of Bacteriol. 190(6):2138-49.
- **Guglielmini J.**, Néron B., Abby S.S., Garcillán-Barcia M.P., De La Cruz F., Rocha E.P. (2014). Key components of the eight classes of type IV secretion systems involved in bacterial conjugation or protein secretion. Nucleic Acids Research, 42(9):5715-27.
- **Harveson R.M.,** Schwartz H.F., Urrea C.A., Yonts C.D. (2015). Bacterial wilt of dry-edible beans in the central high plains of the U.S.: past, present, and future. Plant Dis 99:1665–1677.
- **Harveson R.M.**, Schwartz H.F., Urrea C.A., Yonts C.D. (2015). Bacterial wilt of dry-edible beans in the central High Plains of the U.S.: past, present, and future. Plant Disease, 2015.
- **Hotson A.,** Chosed R., Shu H., Orth K., Mudgett M.B. (2003) *Xanthomonas* type III effector XopD targets SUMO-conjugated proteins in planta. Molecular Microbiology, 50, 377–389.

- **Hsiao W.W.,** Ung K., Aeschliman D., Bryan J., Finlay B.B., Brinkman F.S. (2005). Evidence of a large novel gene pool associated with prokaryotic genomic islands. PLoS Genet, 1(5):62.
- **Hwang I.S**., Hom-Ji Oh E.J., Kim D., Oh C.S. (2018). Multiple plasmid-borne virulence genes of *Clavibacter michiganensis* ssp. *capsici* critical for disease development in pepper. New Phytologist, 217: 1177–1189.
- **Lagesen K.,** Hallin P., Rodland E.A., Staerfeldt H.H., Rognes T., Ussery D.W. (2007). RNAmmer: consistent and rapid annotation of ribosomal RNA genes. Nucleic Acids Res 35:3100 –3108.
- **Langille M.G.,** Brinkman F.S. (2009). IslandViewer: an integrated interface for computational identification and visualization of genomic islands. Bioinformatics, 25(5):664–665.
- **Laslett D.,** Canback B. (2004). ARAGORN, a program to detect tRNA genes and tmRNA genes in nucleotide sequences. Nucleic Acids Research 32(1): 11–16.
- **Miller H.** Experiments in molecular genetics. Cold Spring Harbor Laboratory Press: New York, 1972.
- **Nielsen H**. (2017) Predicting Secretory Proteins with SignalP. Protein Function Prediction pp 59-73
- **Nissinen R.,** Xia Y., Mattinen L., Ishimaru C.A., Knudson D.L., Knudson S.E., Metzler M., Pirhonen M. (2009). The putative secreted serine protease Chp-7 is required for full virulence and induction of a nonhost hypersensitive response by *Clavibacter michiganensis* subsp. *sepedonicus*. Molecular Plant Microbe Interaction. 22(7):809-19.
- **Osdaghi E.,** Taghavi S.M., Calamai S., Biancalani C., Cerboneschi M., Tegli S., Harveson R.M. (2018). Phenotypic and Molecular-Phylogenetic Analysis Provide Novel Insights into the Diversity of *Curtobacterium flaccumfaciens*. Phytopathology, 108:1154-1164
- **Osdaghi E**., Taghavi S.M., Fazliarab A., Elahifard E., Lamichhane J.R. (2015). Characterization, geographic distribution and host range of *Curtobacterium flaccumfaciens*: An emerging bacterial pathogen in Iran. Crop Protection 78, 185:192.
- **Osdaghi E**., Taghavi S.M., Hamzehzarghani H., Fazliarab A., Harveson R.M., Tegli S., Lamichhane J.R. (2017). Epiphytic *Curtobacterium flaccumfaciens* strains isolated from symptomless solanaceous vegetables are pathogenic on leguminous but not on solanaceous plants. Plant Pathol.
- **Page, A. J.,** Cummins C. A., Hunt M., Wong V. K., Reuter S., Holden M. T. G., et al. (2015). Roary: rapid large-scale prokaryote pan genome analysis. *Bioinformatics* 31, 3691–3693.
- **Sambrook J**, Fritsch EF, Maniatis TA. Molecular Cloning. In *A Laboratory Manual*, Cold Spring Harbor Laboratory Press: New York, 1989.
- **Seemann T.** (2014). Prokka: rapid prokaryotic genome annotation. Bioinformatic application note 30 (14), 2068–2069.
- **Stork I.,** Gatermann K.H., Burger A., Eichenlaub R. (2008). A family of serine proteases of *Clavibacter michiganensis* subsp. *michiganensis*: chpC plays a role in colonization of the host plant tomato. Molecular Plant Pathology, 9(5), 599–608
- **Tambong J.T**. (2017) Comparative genomics of Clavibacter michiganensis subspecies, pathogens of important agricultural crops. https://doi.org/10.1371/journal.pone.0172295
- **Tegli S.,** Sereni A., Surico G. (2002). PCR-based assay for the detection of *Curtobacterium flaccumfaciens* pv. *flaccumfaciens* in bean seeds. Letters in Applied Microbiology,35, 331–337.
- **Thapa S.P.,** Pattathil S., Hahn M.G., Jacques M.A., Gilbertson R.L., Coaker. (2017). Genomic Analysis of *Clavibacter michiganensis* Reveals Insight Into Virulence Strategies and Genetic Diversity of a Gram-Positive Bacterial Pathogen. Molecular plant-microb interaction 30 (10).

- **Voragen A.G.J.,** Coenen G.J., Verhoef R.P., Henk A. Schols H.A. (2009). Pectin, a versatile polysaccharide presents in plant cell walls. Structural Chemistry, 20:263–275
- **Waack S.,** Keller O., Asper R., Brodag T., Damm C., Fricke W.F., Surovcik K., Meinicke P., Merkl R. (2006). Score-based prediction of genomic islands in prokaryotic genomes using hidden Markov models. BMC Bioinformatics, 7(1):142.
- **Young, J.,** Saddler, G., Takikawa, Y., De Boer, S., Vauterin, L., Gardan, L., et al. (1996). Names of plant pathogenic bacteria 1864-1995. *Rev. Plant Pathol.* 75, 721–763
- **Zaluga J**., StragierP., Baeyen S., Haegeman A., Van Vaerenbergh J., Maes M., De Vos P. (2014). Comparative genome analysis of pathogenic and non-pathogenic *Clavibacte*r strains reveals adaptations to their lifestyle. BMC Genomics, 15:392.

Chapter 6

Genomic and phenotypic metal resistance profile of *Curtobacterium flaccumfaciens* strains

6.1 Introduction

Curtobacterium flaccumfaciens pv. *flaccumfaciens* (*Cff*) is a Gram-positive bacterium and is the causal agent of bacteria wilt of dry beans worldwide (Harveson *et al*., 2015). *Cff* is included in the A2 quarantine list of the European and Mediterranean Plant Protection Organization (EPPO, 2011).

The host range of the pathogen varies among different legumes such as common bean (*Phaseolus vulgaris*) (Urrea & Harveson, 2014), cowpea (*Vigna unguiculata*), mungbean (*Vigna radiata*) (Wood & Easdown, 1990), soya bean (*Glycine max*) (Sammer & Reiher 2012) and pea (*Pisum sativum*) (EPPO 2011; Silva Junior et al. 2012).

Under field conditions, *Cff* can survive on a wide number of nonhost plant species, including alfalfa, maize, eggplant, pepper, sunflower, tomato and wheat (Harveson *et al.*, 2015). Recently, pathogenicity test on common bean plants (*Phaseolus vulgaris*) were conducted with epiphytic *C. flaccumfaciens* strains isolated from symptomless Solanaceous vegetables (Osdaghi *et al*., 2018a). Only a small number of tested strains were no pathogenic on these plants, instead the most of them showed wilt symptoms, exactly such as those caused by *C. flaccumfaciens* pv. *flaccumfaciens (Cff)* (Osdaghi *et al*., 2018a).

Metals and metalloids are natural elements present in soils (Hobman & Crossman., 2014). Bacteria require these compounds for their growth, however, they are toxic for them in high concentrations. (Argudìn *et al.*, 2019). Concentrations in soils vary and as such, bacteria have developed very efficient and different resistance mechanisms over the age (Trevors et al., 1985). In many organisms, the genes controlling metal(loid) resistance are carried on plasmids or other mobile genetic element, which provide the bacteria with a competitive advantage over other organisms when metals are present (Argudìn *et al*. 2019; Trevors *et al*., 1985). Research on metal-*Cff* interactions is still in its early stages of development. Recent study has demonstrated that, unlike the no virulent strains, the Cff strains, which were virulent on common bean are resistance to arsenic compounds (Osdaghi *et al*, 2018b). The association between arsenic resistance and virulence on common bean remains to be elucidated.

In this study, the chemical sensitivity to a wide number of metals and metalloids of three *Cff* strains (P990 strain, 50R strain and *Cff* type strain) was tested through Phenotype MicroArray analysis. In addition, the most significant metals/metalloids were further tested though traditional microbiological plate assays, including also the no pathogenic *C. flaccumfaciens* strain Tom 827 for comparison. At last, a genomic comparative analysis was

conducted in order to detect the genetic determinants of tellurite and arsenic resistance, and that could be putatively related to the differential virulence on bean and other hosts of strains *Cff* P990, *Cff* type strain, and *C. flaccumfaciens* strain Tom827.

6.2 Materials and methods

Bacterial strains, media and growth condition

The *Curtobacterium* spp. used in this study are listed in Table 1. These strains were routinely grown at 26°C as liquid or solid cultures in Luria-Bertani LB (Miller, 1972) medium.

Table 1: List of *C. flaccumfaciens* strains used in this study.

Strain	Host of isolation	Date of isolation	International collection n°	Reference
P990	Bell pepper	2015	ICMP 22053	Osdaghi *et al.* 2018
Tom827	Tomato	2015	ICMP 22084	Osdaghi *et al.* 2018
50R	Common Bean	2014	ICPM 2207	Osdaghi *et al.* 2016
Cff Type	Common Bean	1957	ICMP 2584^{T}	ICMP

T: Type strain

Phenotype Microarray tests

Cff strains were tested by Phenotype Microarray (PM) technology on panels for chemical sensitivity (PM09-PM20). Overall 960 different conditions were tested, among which 100 refer to metals and metalloid compounds (*i.e.* 25 metal/metalloid compounds tested at 4 different concentrations). The complete list of the compounds here assayed can be obtained at http://www.biolog.com/pdf/PM1-PM10.pdf. PM uses tetrazolium violet (TV) reduction as a reporter of metabolic activity and cell viability in aerobic cells (Bochner *et al.*, 2033). At the concentrations here used, TV is a colourless salt, water-soluble, positively charged and thus cell permeable, which after its uptake into the cells functions as an artificial electron acceptor to detect dehydrogenase activities. As a consequence of TV reduction, water-insoluble and purple coloured formazan is irreversibly produced, that can be quantified by using spectrophotometric methods. According to PM protocols, the formation of formazan is recorded every 15 min, to provide quantitative and kinetic information about the response of cells to the compounds assayed (Bochner *et al.*,2001).

Each bacterial strain was grown for 48 h 25°C on Luria Bertani (LB, composition 10 g/L triptone, 5 g/L yeast exctract, 10 g/L NaCl) agar medium. Colonies were picked up with a sterile cotton swab and suspended in 0.8% NaCl water solution. Cell density was adjusted to 81% transmittance (T) on a Biolog turbidimeter. The cellular suspension was diluted ten times in LB liquid medium and 1x dye

G (Biolog), containing TV. PM plates were then sealed with Breath-aesy gas permeable membrane (Sigma- Aldrich), and incubated statically at 25°C in an Omnilog Reader for 32 hours. Kinetic data was analyzed by the Omilog-PM software (release OM_PM_109M) (Biolog). Strains were defined sensitive, moderately tolerant or resistant to each toxic compound on the bases of the trend of their kinetic curves at four different, increasing but unknown concentrations. Strains showing no metabolic activity in presence of the lowest concentration were considered sensitive, strains showing metabolic activity which decrease on the four increasing concentrations were considered moderately tolerant, while strains showing high metabolic activity and similar at any concentration were considered resistant. To identify different levels of tolerance to metal and metalloids in the three *Cff* strains here examined, the differences between the areas of the kinetic curves of the three strains for each metal/metalloid concentration were calculated. Differences higher of 3,000 Arbitrary Omnilog Units (AOU) or lower than -3,000 AOU were considered relevant to identify respectively and higher resistance or higher sensitivity of one strain in respect to the others (Bochner *et al.*, 2001).

Screening for metal and metalloid resistance

According to the PM results here obtained, then the specific responses to different metal and metalloid of *Cff* P990 strain, *Cff* 50R strain, *Cff* type strain, and of *C. flaccumfaciens* Tom827 strain were further evaluated by traditional microbiological assays. Tellurium, silicon and caesium compounds (*i.e.* potassium tellurite [K_2TeO_3], sodium metasilicate [Na_2SiO_4] and caesium chloride [CsCl] were selected and used at different known concentrations (Table 3). The bacterial strains were screening using Luria-Bertani (LB) agar plates supplemented with three different concentration of potassium tellurite (0.3, 0.2 and 0.1 mM), sodium metasilicate (8, 6.5 and 5 mM) and caesium chloride (75, 50, 25 mM). For each strain, LB agar plate without any metal/metalloid supplemented was used as positive control. For each strain, several tenfold dilutions were prepared from a starter suspension (OD_{600}= 2.5) obtained from a fresh culture grown at 26°C for 12h on LB medium. For each dilution, 12 spots of 5µl each were plated on each Petri dish, amended with the tested metals/metalloids

or not. The plates were then incubated at 26°C for 24h, and after that the number of colonies forming units (CFU) was evaluated for each spot.

Comparative metal resistance determinants analysis

Comparative genomics of the *Cff* type strain, *Cff* P990 strain and *C. flaccumfaciens* strain Tom827 were carried out using Roary (Page *et al.,* 2015). The presence of possible metal resistance genes in these three draft genomes was analysed by calling sequences for well-known metal resistance

determinants in other bacterial systems, and then the assigned functions were further checked by BLAST analysis (Altschul *et al.,* 1990).

Data analysis

Statistically significant differences among treatments were calculated by one-way ANOVA with Tukey-Kramer post-test ($p<0.05$) with PAST software (Version 3.17, Øyvind Hammer, Natural History Museum, University of Oslo).

6.3 Results

Phenotype Microarray tests.

PM analysis was applied to evaluate the tolerance of the three *Cff* strains to toxic compound, and in particular to metals and metalloids. Twenty-five metals/metalloid compounds containing 19 different metal/metalloids (Al, Cd, Co, Cr, Cs, Cu, Fe, Li, Mn, Ni, Tl, V, W, Zn, As, B, Sb, Si, Te) were tested at four different unknown concentrations in PM panels (PM11-20). The results obtained showed that all the three strains were sensitive to cadmium, resistant to both sodium metasilicate and cesium chloride, whereas showed a moderately tolerance to all the other tested compounds (Table 2). The three *Cff* strains showed a different tolerance only to three metalloids (As, Sb, and Te) in the form of the four compounds sodium arsenite, sodium arsenate, antimony (III) chloride and potassium tellurite (Figure 1). In particular *Cff* type strain was more sensitive to sodium arsenite, sodium arsenate, antimony (III) chloride than both *Cff* 50R strain and *Cff* P990 strain, whereas *Cff* P990 strain was more sensitive than *Cff* type strain and *Cff* 50R strain to sodium tellurite.

Table 2: Tolerance of *Cff* strains as determined by Phenotype Microarray analysis.

			Tolerance Level		
	CHEMICAL ELEMENTS	CHEMICAL COMPONDS	**Sensitive[A]**	**Tolerant[B]**	**Resistant[C]**
METALS	Al	Aluminium sulfate		χ	
	Cd	Cadmium chloride	χ		
	Co	Cobalt chloride		χ	
	Cr	Potassium chromate		χ	
		Sodium dichromate		χ	
		Chromium Chloride		χ	
	Cs	Cesium chloride			X
	Cu	Cupric chloride		χ	
	Fe	Ferric chloride		χ	
	Li	Lithium chloride		χ	
	Mn	Manganede (II) chloride		χ	
	Ni	Nickel chloride		χ	
	Tl	Thallium (I) acetate		χ	
	V	Sodium metavandanate		χ	
		Sodium orthovandanate		χ	
	W	Sodium tungstate		χ	
	Zn	Zinc chloride		χ	
METALLOIDS	As	Sodium m-arsenite		χ	
		Sodium arsenate		χ	
	B	Boric acid		χ	
		Sodium taborate		χ	
	Sb	Antimony (III) chloride		χ	
	Si	Sodium metasilicate			X
	Te	Potassium tellurite		χ	

[A]SENSITIVE:strains showing no metabolic activity in presence of the lowest concentration were considered sensitive

[B]MODERATELY TOLERANT: strains showing metabolic activity which decrease on the four increasing concentrations were considered moderately tolerant

[C]RESITANT: strains showing high metabolic activity similar on all the four concentrations was considered resistant

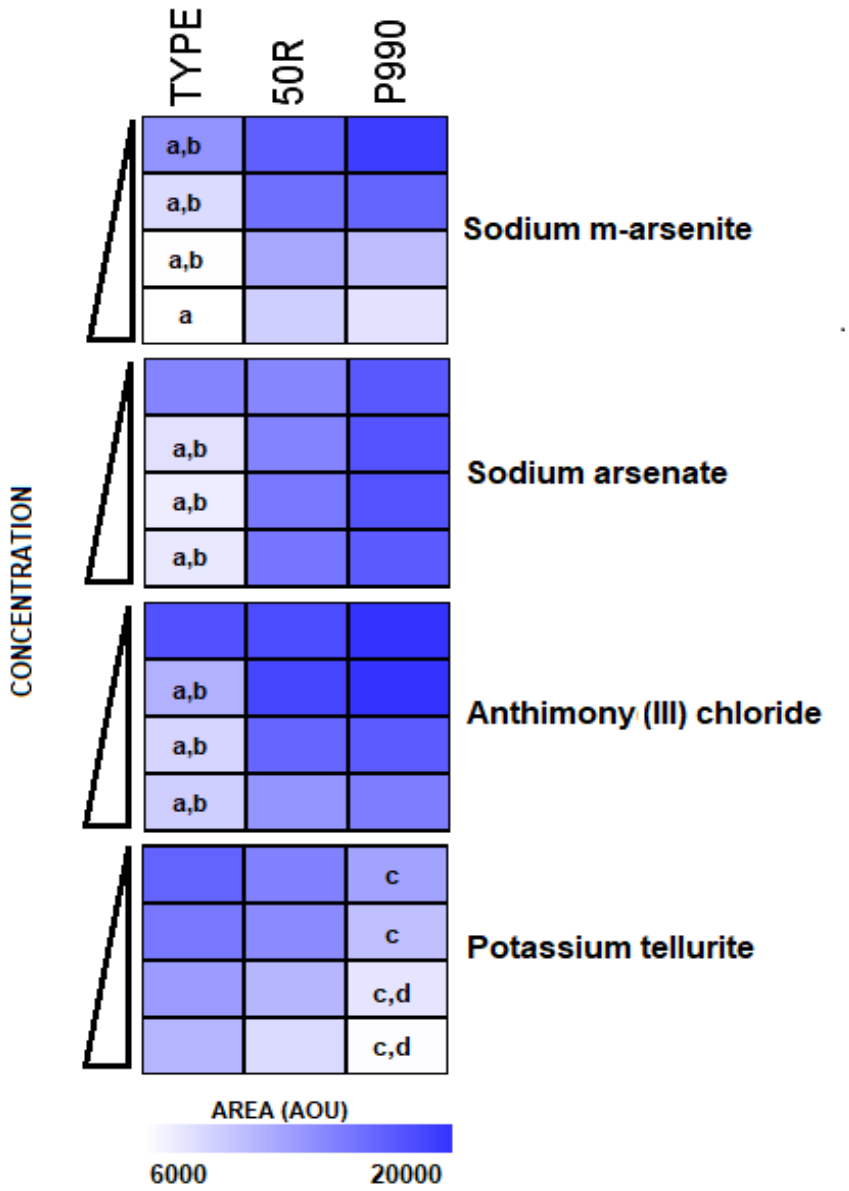

Figure 2: Different tolerance of *C. flaccumfaciens* strains to As, Sb and Te compounds as detected by PM technology. Each toxic compound was tested at four different increasing concentrations. The blue scale represents the area of kinetic curves of the three strains detected in PM experiments. For each concentration of the four toxic compounds the differences between the areas of the three strains were calculated. Differences higher of 3000 AOU or lower than -3000 AOU were considered relevant to identify respectively and higher resistance or an higher sensitivity of one strain in respect to the others (**a**: Type strain more sensitive than 50R, **b**:Type strain was more sensitive than P990, **c**: P990 strain more sensitive than Type strain, **d**: P990 strain more sensitive than 50R).

Screening for metal and metalloid resistance

All the *Cff* strains were shown to be resistant to sodium metasilicate and caesium chloride by PM analysis. When grown on plates supplemented with 5 mM of Na_2SiO_4 they all grew, whereas the CFU values begun to decrease at 6.5 mM and 8 mM concentrations (Table 3). As far as caesium chloride is concerned, the bacterial growth was similar to that of controls when plated on 50 mM and 25 mM CsCl concentration, while it was impaired at 75mM CsCl (Table 3). Results differentiating the four *C. flaccumfaciens* strains here studied were obtained on plate supplemented with potassium tellurite (Table 3). At 0.1 mM and 0.2 mM concentrations, *Cff* 50R strain and *Cff* type strain had a regular growth, comparable to that of the positive control. Conversely, *Cff* P990 strain and *C. flaccumfaciens* strain Tom827 were impaired in their growth at 0.2 mM potassium tellurite. At last, all the *C. flaccumfaciens* strains showed a growth reduced when plated on LB agar supplemented with 0.3 mM K_2TeO_3.

Table 3: Grow rate of *Cff* and *C. flaccumfaciens* strains on different concentrations of caesium chloride (CsCl), sodium metasilicate (Na_2SiO_4) and potassium tellurite (K_2TeO_3)

	Resistance to								
	Caesium Chloride			Sodium Metasilicate			Potassium Tellurite		
	75 mM	**50 mM**	**25 mM**	**8 mM**	**6.5 mM**	**5 mM**	**0.3 mM**	**0.2 mM**	**0.1 mM**
ICPM 2584	10^6-10^7	10^7-10^8	10^7-10^8	10^5-10^6	10^6-10^7	10^6-10^7	10^5	10^6	10^6
50R	10^6-10^7	10^7-10^8	10^7-10^8	10^5-10^6	10^6-10^7	10^6-10^7	10^5	10^6	10^6
P990	10^6-10^7	10^7-10^8	10^7-10^8	10^5-10^6	10^6-10^7	10^6-10^7	10^4	10^5	10^5
Tom827	10^6-10^7	10^7-10^8	10^7-10^8	10^5-10^6	10^6-10^7	10^6-10^7	10^4	10^5	10^5

Comparative metal resistance determinants analysis

The comparative genome analysis of *C. flaccumfaciens* Tom827 strain, *Cff* P990 strain and *Cff* type strain allowed to detect genes putatively involved in arsenic and tellurite resistance (Table 4). The aim was to understand if the virulence of *Cff* on its specific hosts is somehow related to its resistance to some metals which are differently accumulated by different plant species. One *terC* gene was found on the all three draft genomes analysed. Moreover, 6 genes involved in arsenic resistance were detected on all three *C. flaccumfaciens* analysed (Table 4). In particular only one of these genes encodes for a putative arsenic transporter, whereas

the others encode for putative ArsR family transcriptional regulators. In addition, one *arsR* gene occurs only on virulent *Cff* P990 strain and *Cff* type strain and was absent on no virulent *C. flaccumfaciens* Tom287 strain (Table 4). On the contrary, another arsR gene was no detected only on *Cff* type strain (Table 4). Finally, only *Cff* P990 strain shows a set of consecutive genes involved in arsenic resistance, *arsB* gene, *arsC* gene, *arsR* gene and sulfure reductase enzyme. (Table 4, Figure 2)

Table 4: Putative virulence genes found in the *Cff* type strain, *Cff* P900 strain and *C. flaccumfaciens* Tom827 genomes (Based on the annotation results from Prokka1.13.3)

CDS identifiers P990 strain	CDS identifiers Tom827 strain	CDS identifiers Type strain	Annotation
p990_03232	tom827_03239	type.fna_03051	ArsR family transcriptional regulator
p990_03402	tom827_03077	type.fna_03216	ArsR family transcriptional regulator
p990_03213	tom827_03252	type.fna_03036	ArsR family transcriptional regulator
p990_02850	tom827_02826	type.fna_02700	arsenic transporter
p990_02888	tom827_03569	type.fna_02735	ArsR family transcriptional regulator
p990_00289	tom827_00625	type.fna_01400	ArsR family transcriptional regulator
p990_03700		type.fna_03670	ArsR family transcriptional regulator
p990_02301	tom827_02082		ArsR family transcriptional regulator
p990_02305			ArsC asenate reductase
p990_02306			ArsB arsenical efflux pump
p990_02307			Sulfure Reductase
p990_02308			ArsR family transcriptional regulator
p990_00865	tom827_00048		TerC tellurite resistance protein

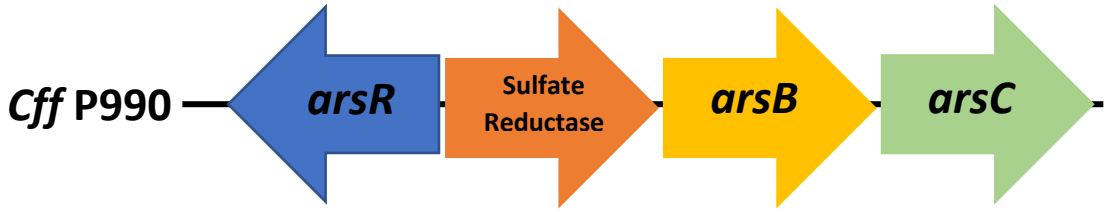

Figure 2: Organization of the genomic region containing *arsRBC* operon. The transcriptional direction of each gene is indicated in blue, orange, yellow and green arrows for *arsR*, sulfate reductase, *arsB* and *arsC* respectively

6.4 Discussion

Phenotype MicroArray analysis (PM) was applied to value the tolerance of *Cff* 50R strain, *Cff* P990 strain and *Cff* type strain to metals and metalloids. All the strains showed tolerance and resistance to a high number of metals and metalloids (Table 2). These data could be interpreted as a result of *Cff* ecological flexibility, which in fact can survive in soil with an ability to persist on plant debris (Silva Junior *et al*., 2012), as well as on alternative hosts (Harveson *et al* 2015, Osdaghi *et al* 2018a). In addition, all the strains were sensitive to cadmium chloride, confirming that Gram positive bacteria are more sensitive to this compound than Gram negative (Babich *et al,* 1977). The PM analysis conducted showed that the *Cff* strains, which are all virulent on beans, are differently tolerant to arsenic, antimony and tellurium compounds (Figure 1). It is well known that resistance to toxic oxyanionic salts of arsenic and antimony depends on the same genetic determinants (Kaur et al.,1992). Moreover, previous study had demonstrated that virulent *Cff* strains are tolerant to arsenic and antimony compounds compared to no virulent strains, ad exception of *Cff* type strain which is moderately tolerant (Osdaghi *et al.*, 2018b).

Considering that the PM analysis confirmed a different tolerance level to arsenic and antimony compounds, resistance analyses were enhanced through the agar plating method, adding the no virulent *C. flaccumfaciens* Tom827 strain, in order to understand if the virulence of *Cff* on its specific hosts is somehow related to metal resistance. The experiments were carried out with all compounds that PM analysis identify as no toxic for *Cff* (i.e. caesium chloride and sodium metasilicate), and with potassium tellurite, since *Cff* strains are differently tolerant to this salt. All the strains, both virulent and no virulent, showed resistance to caesium chloride and sodium metasilicate, proving that none of these compounds are related to the virulence on beans (Table 3).

Moreover, the *Cff* 50R strain and the *Cff* type strain, both isolated from bean, offered higher level tolerance to potassium tellurite than the *Cff* P990 strain and *C. flaccumfaciens* Tom827 strain, isolated from bell pepper and tomato respectively (Table 4). However, it is possible that tellurite resistance is related with Fabaceae plants, as is already known for *Pseudomonas syringae* pv. *pisi*, as well as for most of the *P. syringae* strains virulent on legumes (Taylor, 1999).

The genomes comparative analysis was conducted in order to identify genetic resistance determinant of tellurite and arsenic compounds, which induce phenotypic difference among the strains as demonstrated by PM analysis combined with traditional microbiological plate assays. One tellurite resistance determinant (TerC) (Turkovicova et al., 2016) was detected in the genomes of *Cff* P990 strain, *Cff* type strain and *C. flaccumfaciens* strain, to suggest that genetic determinants not yet identified could explain the phenotypic differences here observed for tellurite resistance. Arsenic defence mechanisms are based on the presence of arsenic resistance operon (*ars*) which codes for a regulatory protein (ArsR), an arsenate ATPase (ArsA), an arsenite permease (ArsB), an enzyme involved in arsenate reduction (ArsC) and an arsenite metallochaperone (ArsD) (Fekih *et al*., 2018. Most of arsenic resistance determinants were found on the all *C. flaccumfaciens* strains here examined (Table 4). These genes are not closely-spaced, therefore we can exclude that constitute an operon, and thus their role probably is not crucial to arsenic resistance (Price *et al*., 2006; Fekih *et al*., 2018). On the contrary, *Cff* P990 strain exhibited a set of closely spaced genes involved in arsenic resistance (i.e. *arsR*, *arsB* and arsC), suggesting that are forming an *arsRBC* operon, as is already referred to *Corynebacterium glutamicum* (Figure 2) (Mateos *et al*., 2006; Ordoñez et al., 2005). Moreover, the sulfur reductase enzyme detected between the *arsR* gene and *ars*B gene, could have a role to carry out the reduction of arsenate to arsenite, as is already known for the Gram-positive bacteria. (Cervantes *et a.,* 1994). Finally, the *Cff* type strain despite of moderately tolerance to arsenic compounds, did not show a set of genes forming an *ars* operon. Thus, probably other mechanisms to uptake and efflux of arsenic compounds could be explain the phenotypic differences of *Cff* type strain, but poorly genomic information about *Curtobacterium* spp. prevent the detection of these presumed arsenic resistance determinants.

In conclusions, Phenotype MicroArray analysis combined with traditional microbiological plate assays have showed that *Cff* strains are tolerant and resistant to high number of metals and metalloids, as results of their ecological flexibility. Moreover, obtained results have suggested that there is a positive correlation between tellurite

resistance and Fabaceae plants. Finally, experiment conducted have confirmed that the virulent strains are tolerant to arsenic compound, and for the first time a putative *arsRBC* of *Cff P990* strain has been identified, whereas arsenic resistant mechanism of *Cff* type strain has yet to be elucidated.

6.5 References

- **Altschul S.F.,** Gish W., Miller W., Myers E.W., Lipman D.J. (1990) Basic local alignment search tool. Journal of Molecular Biology, 215(3):403–410.
- Appl Environ Microbiol. 2005 Oct;71(10):6206-15.
- **Argudín M.A.**, Hoefer A.,Butaye P. (2019).Heavy metal resistance in bacteria from animals Research in Veterinary Science,122, 132-147.
- **Babich H**., Stotizky G. (1977). Sensitivity of Various Bacteria, Including Actinomycetes, and Fungi to Cadmium and the Influence of pH on Sensitivity. Appl Environ Microbiol, 681-695.
- **Bochner, B.** Gadzinski P., Panomitros E. (2001) Phenotype microarrays for high throughput phenotypic testing and assay of gene function. Genome Res., 11, 1246–1255.
- **Cervantes C.,** Ji G., Ramírez J.L., Silver S. (1994) Resistance to arsenic compounds in microorganisms. FEMS Microbiol,15(4):355-67.
- **EPPO**. (2011). Curtobacterium flaccumfaciens pv. flaccumfaciens. Bulletin OEPP/EPPO, 41, 320–328.
- **Fekih I.B.,** Zhang C., Li Y.P., Zhao Y., Alwathnani H.A., Saquib Q., Rensing C., Cervantes C. (2018) Distribution of Arsenic Resistance Genes in Prokaryotes. Front Microbiol, 9(2473).
- **Harveson R.M**., Schwartz H.F., Urrea C.A.; Yonts C.D. (2015). Bacterial Wilt of Dry-Edible Beans in the Central High Plains of the U.S.: Past, Present, and Future. Plant Disease, 99(12), 1665-1677.
- **Hobman J.L**, Crossman L.C. (2014) Bacterial antimicrobial metal ion resistance. Journal of Medical Microbiology 64, 471–497.
- **Kaur P.,** Rosen B.P. (1992). Plasmid encoded resistance to arsenic and antimony. Plasmid, 27(1), 29-40.
- **Mateos L.M.,** Ordóñez E., Letek M., Gil J.A. (2006) *Corynebacterium glutamicum* as a model bacterium for the bioremediation of arsenic. Int Microbiol, 9(3):207-15.
- **Miller H.** Experiments in molecular genetics. Cold Spring Harbor Laboratory Press: New York, 1972.
- **Ordóñez E.,** Letek M., Valbuena N., Gil J.A., Mateos L.M. (2005) Analysis of genes involved in arsenic resistance in *Corynebacterium glutamicum* ATCC 13032. Appl Environ Microbiol 71(10):6206-15.
- **Osdaghi E.,** Taghavi S.M., Calamai S., Biancalani C., Cerboneschi M., Tegli S., Harveson R.M. (2018b). Phenotypic and Molecular-Phylogenetic Analysis Provide Novel Insights into the Diversity of Curtobacterium flaccumfaciens. Phytopathology, 108:1154-1164
- **Osdaghi E**., Taghavia S. M., Hamzehzarghania H., Fazliaraba A., Harvesonb R. M., Tegli S., Lamichhane J. R. (2018a). Epiphytic *Curtobacterium flaccumfacien*s strains isolated from symptomless solanaceous vegetables are pathogenic on leguminous but not on solanaceous plants. Plant Pathology, 67,388–398
- **Page, A. J.,** Cummins C. A., Hunt M., Wong V. K., Reuter S., Holden M. T. G., et al. (2015). Roary: rapid large-scale prokaryote pan genome analysis. *Bioinformatics* 31, 3691–3693.
- **Price M.N**., Arkin A.P., Alm E.J. (2006) The Life-Cycle of Operons. PLoS Genet. 2(6), 96.
- **Sammer U.F.**, Reiher K. (2012) *Curtobacterium flaccumfaciens* pv. *flaccumfaciens* on soybean in Germany – a threat for farming. Journal of Phytopathology 160(6), 314-316.
- **Silva Junior T.A.F**., Negrao D.R., Itako A.T., Maringoni A.C. (2012) Pathogenicity of *Curtobacterium flaccumfaciens* pv. *flaccumfaciens* to several plant species. J Plant Pathol, 94:427–43
- **Silva Junior**T. A. F., Negrão D. R., Itako A. T., Soman, J. M., and Maringoni, A. C. (2012). Survival of *Curtobacterium flaccumfaciens* pv. f*laccumfaciens* in soil and bean crop debris. *J. Plant Pathol.* 94, 331–337. doi: 10.4454/JPP.FA.2012.025

- **Taylor D.E.** (1999) Bacterial tellurite resistance. Trends in microbiology, 7(3), 111-115.
- **Treivors, J.T.,** Oddie, K.M., Belliveau, B.H. (1985) Metal resistance in bacteria. FEMS Microbiol Letters, 32, 39-54.
- **Turkovicova** L., Smidak., Jung G., Turna J., Lubec G., Aradska J. (2016) Proteomic analysis of the TerC interactome: Novel links to tellurite resistance and pathogenicity. Journal of Proteomics,136:167-173].
- **Urrea C.A.,** Harveson R.M. (2014). Identification of sources of bacterial wilt resistance in common beans (*Phaseolus vulgaris* L.). Plant Disease, 98 (7), 973-976
- **Wood B.A.,** Easdown W.J. (1990). A new bacterial disease of mung bean and cowpea for Australia. Australian Plant Pathology, 19 (1), 16-21.

Chapter 7

Conclusion

7.1 Discussion

The control of bacterial diseases of plants still mainly relies on the use of copper compounds (La Torre *et al*. 2018). According to the latest European regulations is now required in all European Union Member countries a drastic reduction in the use of the copper in plant protection against biotic diseases, both in traditional and organic agriculture, as part of a broader review process about pesticides and their residues, started with Directive 91/414 / EEC. In addition, due to the increased globalization and connectedness via world trade, the threat from quarantine, alien and invasive plant pathogenic bacteria is expected to increase, both as entry as well as establishment in those Countries where they were previously absent (Ormsby et al., 2017).

Therefore, it is mandatory to develop highly effective and eco-friendly alternatives to copper in plant protection, against phytopathogenic bacteria both endemic and recently introduced. For these reasons complementary research approach has been adopted, looking for several potential bacterial targets among new pathogenicity and virulence determinants of both Gram-negative and Gram-positive phytopathogenic bacteria, that have never been studied before and that here will be investigated.

Pseudomonas syringae pv. *nerii* is a Gram-negative phytopathogenic bacterium, and it is the causal agent of oleander knot disease. For the strain *Psn23*, some of its virulence and pathogenicity determinants has been detected and investigated. Against some of them, such as its Type Three Secretion System (TTSS), several innovative molecules have been already and succesfully tested (Biancalani *et al.*, 2016). Here another possibily successful target was investigated. Previous studies have revealed that in *Psn23* the *matE/iaaL* operon could be also crucial for simultaneous regulation of intracellular IAA concentration, as well as for its differential modulation during the various stages of infection (Cerboneschi *et al.*,2016). Therefore, we have considered necessary to evaluate the role played by the membrane protein MATE on IAA efflux and homeostasis, as well as on virulence of *Psn23*. To this purpose, in *silico* analysis of *Psn*MATE protein has been conducted, to detect those amino acids supposed to be involved in substrate and ions bonding. Accordingly, several mutants have been produced and then phenotypically characterized. The results obtained allowed the development for *Psn23* of a new model concerning IAA biosynthesis and transport outside the bacterial membrane, accounting the essential role of IAA in the cross-talk between this bacterial pathogen and its host plant, as well as in the establishment and growth of the characteristic hyperplastic symptoms. Accordingly, IAA biosynthesis and efflux are

regulated by the paired activity of *matE* and IAA-related genes: the increase of IAA into the intercellular spaces is strictly associated to a fine tuning of levels of free IAA within the cell, where its concentration has to be lower than those having inhibitory activity on its TTSS. Conjugation and efflux are the two strategies adopted by *Psn23* to modulate intracellular IAA concentration, in order to maintain a ready-to-use amount of this phytohormone for its interaction with plant hosts High concentrations of the IAA active form into apoplast produces an impairment of plant defence system, thus to promote the development of the disease. Being the genes for IAA and MATE widely diffuse in *P. syringae* complex, studies on MATE proteins can be considered pivotal to provide information essential for the development of innovative control molecules and strategies against these bacteria, possibly based on MATE inhibitors from vegetable sources, such as indole-competitors.

The same complementary research approach has been applied to Gram-positive plant pathogenic bacteria, which have been definitely less investigated until now, in spite of their relevant impact in recent times as emerging plant pathogens. *Curtobacterium flaccumfaciens* pv *flaccumfaciens*, the bacterial wilt pathogen of edible dry beans, is becoming an increasingly important treat globally, both from epidemiological and phytosanitary points of view (Osdaghi *et al*, 2015). Phenotypic features, genetic diversity and phylogenetic of *C. flaccumfaciens* strains have been here studied. The results revealed that the strain causing wilt disease on dry beans are distributed into two phylogenetic lineages, yellow-pigmented and red-/orange pigmented strains. However, no-pathogenic strains do not form a separate phylogenetic group and are scattered within in the core population of *Cff* or within other pathovar species. Despite no differences between pathogenic and non-pathogenic strains in their plasmid contents, the results show that those strains pathogenic on dry bean are resistant to arsenic compounds. The Phenotype Microarray analysis conducted on three strains (*Cff* Type strain, *Cff* P990 strain, and *Cff* 50R strain) have showed that all the *Cff* strains are tolerant to most of the tested compounds, according to their largely ubiquitous presence in many different environments. In addition, the most significant metals/metalloids have been further tested, including also the no pathogenic *C. flaccumfaciens* strain Tom 827 for comparison, in order to detect a potential relation between virulence and metal resistance. Obtained results combined with comparative genomes analyses on three strains (*Cff* Type strain, *Cff* P990 strain and *C. flaccumfaciens* Tom827 strain) have confirmed that virulence on beans are related with arsenic resistance, and for the first time a putative *arsRBC* of *Cff P990* strain has been identified, whereas arsenic resistant mechanism of *Cff* type strain, which are moderately tolerant to arsenic compounds, has yet to be elucidated. Moreover,

comparative genomes analysis has detected a genomic island (GIs) containing several serine proteases and one pectate lyase, and which is completely absent on no-virulent *C. flaccumfaciens* Tom 827 strain. It is well known that these genes have a role in virulence on *Clavibacter* spp. and *Xanthomonas* spp., (Hotson *et al*., 2003; Nissinen *et* al., 2009; Hwang *et al,* 2018), therefore we can strongly hypothesise these genes could have a role in plant-pathogen interaction for *Cff.* Moreover, integrase genes and presence of known conjugative genes has suggested that *Cff* acquiring these determinants from other plant pathogenic bacteria by horizontal gene transfer (HGT) events, since *Cff* can occur on most common host plants for *Clavibacter* spp. and *Xanthomonas* spp. (Guglielmini *et al*., 2014; Harveson *et al.,* 2015). In conclusion, the study of phenotypic, phylogenetic and genetic diversity of *C. flaccumfaciens* strains has allowed to provide very interesting information, which will open up exciting new possibilities for the study of this plant pathogen in the future and the development of innovative and preventive control methods. .

7.2 References

- **Biancalani, C.;** Cerboneschi, M.; Tadini-Buoninsegni, F.; Campo, M.; Scardigli, A.; Romani, A.; Tegli, S. (2016) Global analysis of Type Three Secretion system and Quorum Sensing inhibition of Pseudomonas savastanoi by polyphenols extracts from vegetable residues. PloS One
- **Cerboneschi, M.;** Decorosi, F.; Biancalani, C.; Ortenzi, M. V.; Macconi, S.; Giovannetti, L.; Viti, C.; Campanella, B.; Onor, M., Bramanti, E. (2016) Indole-3-acetic acid in plant-pathogenic interactions: a key molecule for in planta bacterial virulence and fitness. Res Microbiol, 167, 774-787.
- **Guglielmini J.**, Néron B., Abby S.S., Garcillán-Barcia M.P., De La Cruz F., Rocha E.P. (2014). Key components of the eight classes of type IV secretion systems involved in bacterial conjugation or protein secretion. Nucleic Acids Research, 42(9):5715-27.
- **Harveson R.M**., Schwartz H.F., Urrea C.A.; Yonts C.D. (2015). Bacterial Wilt of Dry-Edible Beans in the Central High Plains of the U.S.: Past, Present, and Future. Plant Disease, 99(12), 1665-1677.
- **Hotson A.,** Chosed R., Shu H., Orth K., Mudgett M.B. (2003) Xanthomonas type III effector XopD targets SUMO-conjugated proteins in planta. Molecular Microbiology, 50, 377–389.
- **Hwang I.S.,** Hom-Ji Oh E.J., Kim D., Oh C.S. (2018). Multiple plasmid-borne virulence genes of Clavibacter michiganensis ssp. capsici critical for disease development in pepper. New Phytologist, 217: 1177–1189.
- **La Torre A.,** Iovino V. and Caradonia F. (2018). Copper in plant protection: current situation and prospects. Phytopathologia Mediterranea 57, 2, 201−236.
- **Nissinen R.,** Xia Y., Mattinen L., Ishimaru C.A., Knudson D.L., Knudson S.E., Metzler M., Pirhonen M. (2009). The putative secreted serine protease Chp-7 is required for full virulence and induction of a nonhost hypersensitive response by *Clavibacter michiganensis* subsp. *sepedonicus*. Molecular Plant Microbe Interaction. 22(7):809-19.
- **Ormsby M.,** Brenton-Rule E. (2017). A review of global instruments to combat invasive alien species in forestry Biological Invasions 19:3355–3364).
- **Osdaghi E**., Taghavi S.M., Fazliarab A., Elahifard E., Lamichhane J.R. (2015). Characterization, geographic distribution and host range of *Curtobacterium flaccumfaciens*: An emerging bacterial pathogen in Iran. Crop Protection 78, 185:192.